Modern Roundabouts: A Challenge of the Future

Lead Guest Editor: Tomaž Tollazzi
Guest Editors: Raffaele Mauro, Daiva Zilioniene, Irena I. Otković,
and Nikiforos Stamatiadis

Modern Roundabouts: A Challenge of the Future

Modern Roundabouts: A Challenge of the Future

Lead Guest Editor: Tomaž Tollazzi
Guest Editors: Raffaele Mauro, Daiva Zilioniene, Irena I. Otković, and Nikiforos Stamatiadis

Editorial Board

Contents

Editorial

Modern Roundabouts: A Challenge of the Future

Tomaž Tollazzi [ID],[1] **Raffaele Mauro,**[2] **Daiva Žilionienė** [ID],[3]
Irena I. Otković [ID],[4] **and Nikiforos Stamatiadis**[5]

[1]*University of Maribor, Maribor, Slovenia*
[2]*University of Trento, Trento, Italy*
[3]*Vilnius Gediminas Technical University, Department of Roads, Vilnius, Lithuania*
[4]*University J.J. Strossmayer, Faculty of Civil Engineering, Osijek, Croatia*
[5]*University of Kentucky, College of Engineering, Lexington, KY, USA*

Correspondence should be addressed to Tomaž Tollazzi; tomaz.tollazzi@um.si

Throughout the world, research into the various aspects and types of roundabouts has spanned many decades. During this long period the number of vehicles, their sizes, and performance characteristics, including speeds, have radically changed. Similar changes are also noted for the drivers' experiences. These changes have had a strong influence on the evolution of modern roundabouts. The primary aspects of the layout of modern roundabouts in relation to capacity and traffic safety are now known.

However, there are still areas that merit further evaluation and research and they are addressed as part of the aims and the scope of this special issue.

The paper by K. Shaaban and H. Hamad presents a method to analyze driver behavior and estimate the critical gap for three-lane roundabouts. The operations of multilane roundabouts, especially three-lane roundabouts, are unique and more complicated than any other type of roundabouts. Analysis showed that the vast majority of the vehicles accept the gap in groups and the critical gap was estimated accordingly. The study provides a new explanation for the operation at multilane roundabouts.

The paper by R. Lattarulo et al. developed a complete framework of motion planning for automated vehicles while considering different constraints with parametric curves for lateral and longitudinal planners. Parametric Bézier curves are used as the core approach for trajectory design in intersections, roundabouts, and lane change maneuvers. Additionally, a speed planner algorithm is presented using

the same parametric curve approach, considering comfort and safety. The planning method was tested in simulation conditions and with the real platform in automated mode and showed good results.

The paper by O. Giuffrè et al. presented a microsimulation-based approach for roundabout safety performance evaluation and developed a crash prediction model from simulated peak hour conflicts. A generalized linear model framework was used to estimate the prediction model based on field collected crash data for 26 roundabouts. The crash prediction model was based on the assumption that the crashes per year are a function of peak hour conflicts, the ratio of peak hour traffic volume to average daily traffic volume, and the roundabout outer diameter.

The paper by D. Lee et al. investigates gap acceptance behaviors at roundabouts based on field observations during both good weather and rainy conditions. The critical gaps were estimated in 4 conventional roundabouts, and a logit model for gap acceptance using various roundabout variables was developed to investigate gap acceptance maneuvering at roundabouts. Analysis showed that rain conditions influenced the accepted gaps. Drivers need about 10 percent longer gap entry into roundabouts during rainy conditions, and gap acceptance probabilities are 10 to 20 percent lower for the same given gap time during rainy conditions compared to good weather conditions.

The paper by A. V. Goncharenko investigates theoretically the possible directions of some specified methods for

the alternative roundabouts effectiveness on modeling and optimization. The study provides a prototypic approach used upon the issues related to the support of the alternative roundabouts worthiness (vehicle worthiness, riding worthiness, transportation worthiness, etc.). More in particular, the prototypic approach is adopted from the aircraft airworthiness support measures concepts of developed from subjective analysis on the basis of Jaynes' principle in the framework of the calculus of variations theory.

The paper by G. Tesoriere et al. performed an analysis through a comparison of two nonconventional double-lane roundabout schemes defined as elliptical and turbo to define the safest solution considering direct and surrogate parameters. The comparison of their geometry and technical elements was done by VISSIM microsimulator and SSAM tools, assuming that turbo roundabout due to its physical separating traffic lanes in the central circulatory carriageway will enable potentially better traffic safety conditions. This comparative analysis allows for reducing possible security and economic impacts for the community.

The paper by M. Park et al. presents the analyses of the effects of the geometric and traffic flow conditions on traffic accident frequency at roundabouts. This study was contributed to the understanding of which factors realistically affect traffic accident occurrence and random parameters were applied. This study tried to make up for the weakness of the fixed parameters model, which constrains estimated parameters to be fixed across all observations. A total of eight variables were determined to be the main influencing factors on traffic accident frequency and more safe roundabout design, and more efficient roundabout operations are expected based on this study results.

Conflicts of Interest

The editors declare that they have no conflicts of interest regarding the publication of this special issue.

Acknowledgments

Tomaž Tollazzi
Raffaele Mauro
Daiva Žilionienė
Irena I. Otković
Nikiforos Stamatiadis

Review Article

Review of Roundabout Capacity Based on Gap Acceptance

Ruijun Guo, Leilei Liu [iD], and Wanxiang Wang [iD]

School of Traffic and Transportation, Dalian Jiaotong University, Dalian 116028, China

Correspondence should be addressed to Wanxiang Wang; wangwanxiang4@163.com

Circulating vehicles have priority at modern roundabouts. Entrance vehicles can enter the roundabout when there is a time gap larger than the critical gap; otherwise, the vehicles need to wait until there is a large enough gap. The gap acceptance theory was used to analyze the entrance capacity of roundabouts, which can be derived by queuing theory involving two vehicle streams. The paper introduces the main styles of headway distribution, which are named as bunched exponential distribution or M3 distribution. The calculation model of free stream ratio is also introduced. The entrance capacity models can be classified by different entrance vehicle types, which are piecewise function or linear function, or by different critical gap types, which are constant or stochastic function. For each form, the typical capacity expressions are given. The calculation values show a very small difference between these kinds of models. The capacity value based on the critical gap of stochastic function is more realistic and more complex in function style. Some conclusions were derived that drivers' nonhomogeneous and inconsistent character is more realistic than the fixed critical gap and following gap. The calculation results of capacity are similar to the field capacity under the assumption of homogeneity and continuance, with only a minor percent deviation. Finally, the paper points out additional problems and the suggested research in capacity of roundabouts.

1. Introduction

Modern roundabouts have some obvious characteristics such as small diameter of the central island, entrance vehicles yield to circulating vehicles, deviation of entrance vehicles, and split island between entrance and exit. The bottleneck appears at the entrance of the roundabout because vehicles need time to judge whether to enter the roundabout or to wait for another lager gap. Therefore, the research emphasis of modern roundabouts is always the entrance capacity.

Vehicles on the entrance lanes should yield to vehicles on the circulating lanes because of the entrance yield rule. The entrance lanes are regarded as the minor road and the circulating lanes as the major road. The roundabout can be regarded as the typical priority-controlled intersection. The entrance capacity, delay and queue length can be calculated by using the gap acceptance theory. The gap acceptance theory was well developed in Germany [1, 2]. The base theory was proposed by Major, Buckley and Tanner et al. (refer to [3, 4]). The capacity model had

been developed based on different signal timing, different lane numbers, and different vehicle traffic characteristics.

Brilon [5] defined the full capacity as the sum of arrival flow rates when the saturated degree is 1 on the lanes. It is too difficult to find the field status because the arrival flow rate of every entrance is equal to entrance capacity based on the definition. Some research [6, 7] regarded the sum of entrance capacities as the full capacity when an entrance is saturated with the increase of flow rate of all entries by a certain proportion.

Some methods advised 3000 vehicles per hour as the capacity value of a single lane roundabout. Weaving theory was used to describe the traffic characteristics of roundabouts, such as Clayton's method, the equation of DOE (Department of Environment in UK) and Wardrop's method, which was proposed by Transport and Road Research Laboratory (TRRL) in UK.

After the 1970s, Wardrop's method could not be used to calculate the weaving capacity of roundabouts because the entrance yield rule was applied in the field. The regression

method and gap acceptance method were since developed (Ashworth, 1989); [8, 9].

Philbrick proposed the linear regression method (refer to [10]), which is mainly used in England. The exponential regression methods (Brilon and Stuwe, 1993) were based on numerous survey data among the saturated entrance flow rate and conflicting flow rate, geometry, etc.

The linear regression models in England were developed from traditional roundabouts, which had the large-diameter island design and entrance priority. The capacity, such as in the models proposed by Kimber [11], McNell and Smith [12], and Hollis and Semmens et al. [13], was regressed with geometry parameters of roundabouts and the total circulating traffic volume [14] regardless of traffic status of every lane.

In gap acceptance theory, some parameters should be determined including headway distribution of circulating vehicles, the critical gap, and following gap although they are variable with different geometry and traffic conditions of roundabouts. Vehicles enter the roundabout by use of acceptable gaps of circulating flow and the capacity is mainly determined by circulating flow rate and headway distribution.

Some countries such as USA, Germany, Australia, UK, Japan, France, and Russia have built complete capacity methods which are suitable for their own traffic conditions, including Highway Capacity Manual in USA, aaSIDRA, AUSTROADS and NAASRA in Australia, Swedish CAPCAL, SETRA method, and CETUR method in Germany.

The gap acceptance can be regarded as the signal timing process, which was proposed by Achelik and Chung (1994). Both the gap acceptance theory and regression method can be used to calculate the delay and queue length. The gap acceptance models are identical among roundabouts, two-way stop, and all-way stop intersections.

The capacity models and traffic control methods of roundabouts were studied in many countries. Al-Madani [15] collected the data of 13 large roundabouts including circulating and exiting flows, the number of lanes, and lateral position of vehicles in Bahrain. The developed model matched the field data reasonably well and fell well in other methods. Khoo and Tang [16] proposed a control strategy which was effective in reducing system travel time and increasing volume especially during medium to high levels of demand. A case study of a two-lane roundabout in Malaysia was developed in a microscopic simulation environment to study the roundabout system properties and to test the effectiveness of the proposed control strategy. Macioszek (2016) applied the capacity method of HCM 2010 in the field roundabouts in Poland. The calculated values were similar as the experience values.

Biel and Wong [17] proposed the entrance capacity model of circulating multilanes roundabout based on the regression model and HCM model. Under the limited priority condition, Qu et al. [18] calculated the entrance capacity based on Raff's critical gap model and the maximum likelihood method. Yap and Gibson et al. [19] proposed two regression methods and compared various methods based on the survey data of roundabouts in UK. The capacity model of negative exponential distribution showed a coincidence with the

reality than the regression model under both the high flow rate and low flow rate. By using of the Germany capacity programs, Mauro and Branco [20] compared the capacity and delay model between circulating multilane roundabout and Turbo roundabout.

Weaving theory was used to describe the traffic characteristics, including weaving capacity in weaving sections. It is applicable in the traditional roundabouts where the central island is large and entry flow stream has the priority. But the regression method and gap acceptance theory can be used to calculate entrance capacity in modern roundabouts.

Linear regression method is mainly used in England. The entrance capacity is regressed with conflicting flow rate, geometry, etc. regardless of traffic status of every lane. Regression method usually can obtain satisfied results after a large number of data survey of roundabouts under the condition of saturated traffic flow.

Gap acceptance characters are related to traffic conditions of roundabouts including the headway distribution of circulating vehicles, circulating volume, critical gap, and following gap. Queuing theory was used to describe the gap acceptance process and to deduce the capacity equation. Gap acceptance theory and regression method can be used to calculate the delay and queue length too. By choosing the reasonable traffic parameters such as critical gap value or its distribution, gap acceptance theory can obtain the consistent capacity results as the field data. Gap acceptance theory was usually applied in the science research of traffic flow, whereas the regression method was more appropriate in the traffic engineering field.

Based on the gap acceptance theory, the basic assumptions were induced, the headway distributions were introduced, and the relevant parameters were summed up. Most entrance capacity models were classified according to the different critical gap types and the g(t) functions. Their applicable conditions and current application fields were concluded.

2. The Assumptions of Gap Acceptance

The headway is the time interval that elapses between the arrival of the leading vehicle and the following vehicle at the designated test point. Gap is a little different from headway in that gap is the measure of the time between the rear bumper of the first vehicle and the front bumper of the second vehicle, rather than front-to-front time.

Gap acceptance usually happens in unsignalized intersections that are controlled by priority. The entrance vehicles will enter the intersection when there are no vehicles on the major road or wait for the acceptable gap at the stop line. The entrance vehicle will enter the intersection if the gap on the major road is larger than or equal to the critical gap; otherwise the entrance vehicle will decelerate or stop so as to wait for the next gap when it is larger than the critical gap. The critical gap can be regarded as the driver's judgment threshold, which determines whether the entrance vehicle has enough time to enter the intersection safely or not. Drivers' behaviors are different from each other in reality, so the critical gaps of various drivers are different. The critical gap is usually

regarded to follow a certain distribution described by average value and variance.

Passing behavior hardly happened on the circulating lanes of a roundabout. It was supposed that the headway of circulating vehicles followed a certain distribution such as negative exponential distribution, M3 distribution, or Erlang distribution. In addition, some assumptions were given in gap acceptance theory [21–23]:

(1) Gap of vehicles is regarded as headway for ease of data collection.

(2) All gaps of circulating vehicles can be combined into single-lane traffic flow.

(3) Vehicles on the entrance arrive stochastically at the roundabout.

(4) Vehicles on the circulating lanes do not change their running behaviors when vehicles enter into the roundabout.

(5) Drivers on the entrance can recognize the vehicles going to exit roundabout before the conflict spot.

In reality, the above assumptions cannot exactly reflect all the driving operations in a roundabout. More complicated priority types, such as limited priority and priority conversation, reasonably accord with the reality. The interactions among vehicles are more complicated under these conditions.

Some influence factors are important to gap acceptance including queue length on the minor road, traffic volume on the major road, number of lanes on the major road and the minor road, the exiting vehicles, the geometry of entrance lanes, and the velocity of major road vehicles.

3. Traffic Character of Major Flow

Headway is important to analyze the gap acceptance process and calculate capacity and signal timing of intersections. The headway distribution is especially indispensable to traffic flow simulation. The regular headway distributions include negative exponential distribution also named as M1, shifted negative exponential distribution named as M2, and bunched exponential distribution named as M3 distribution. M1 and M2 distribution can be regarded as the special types of M3 distribution. We just give the probability density function and cumulative probability function of M3 distribution which is a dichotomized headway model. Erlang distribution, log-normal distribution, and mixed distribution (refer to [24, 25]) were also usually used in the field.

Critical gap t_c, gap t_f, and minimum headway t_m are also important traffic parameters. They can be constant or stochastic distribution depending on drivers' behavior character. The empirical values were given in HCM and some traffic engineering manuals. There are a lot of methods to calculate t_c.

3.1. M3 Distribution of Major Stream.
Cowan [26] proposed the M3 distribution in which some vehicles run as a fleet and other vehicles run under the free flow status. The probability density function f(t) and cumulative distribution function F(t) are as follows:

$$f(t) = \begin{cases} \alpha\lambda e^{-\lambda(t-t_m)} & t \geq t_m \\ 0 & t < t_m \end{cases} \tag{1}$$

$$F(t) = \begin{cases} 1 - \alpha e^{-\lambda(t-t_m)} & t \geq t_m \\ 0 & t < t_m \end{cases} \tag{2}$$

where q is the flow rate on the major road (veh/s); α is the ratio of free flow; λ is the decay constant (1/s); t_m is the minimum headway. The estimation of λ can be found by using (3) (Troutbeck, 1997).

$$\hat{\lambda} = \frac{\alpha q}{1 - qt_m} \tag{3}$$

The estimated value of t_m is as follows:

$$\hat{t}_m = \min\{t_1, t_2, \cdots, t_n\} \tag{4}$$

Some extremely small values probably arise because individual drivers violate the priority rule. Hidden perils exist in these driving operations and such data is unreasonable. So the average headway of the vehicle fleet should be determined as t_m in the application of (4).

3.2. Calculate the Ratio of Free Flow.
The parameters of M3 distribution are predicted by using least square method. λ can be calculated by the following equation [27]:

$$\lambda = \frac{1}{(1/n)\sum_{i=1}^{n} t_i - \zeta} \tag{5}$$

where ζ is a headway value at which the vehicles are assumed to be free (s). ζ is accepted as 3 or 4 seconds (Troutbeck, 1997; Hagring, 1998). $(1/n)\sum_{i=1}^{n} t_i$ is the average of headways which are greater than ζ.

The ratio of free flow can be estimated to satisfy the condition that the mean headway must be equal to the reciprocal of the flow rate.

Jocabs (1980, refer to [2]) proposed the relation between traffic volume q and the ratio, as follows:

$$\alpha = e^{-kq} \tag{6}$$

A more complicated equation (7) was given in the SIDRA 2.0 and the early model (Akcelik, Chung, 1994):

$$\alpha = e^{-bqt_m} \tag{7}$$

where k and b are constants.

Tanner [28] proposed the linear relation between the ratio of free flow and traffic volume (refer to [4]; Ashworth, 1970):

$$\alpha = 1 - qt_m \tag{8}$$

The analogous relation model was proposed in the Roundabout Manual of AUSTROADS [29]:

$$\alpha = 0.75(1 - qt_m) \tag{9}$$

TABLE 1: Parameter estimation of free flow ratio.

Lanes numbers		1	2	>2
Non-blocking traffic flow	t_m	1.8	0.9	0.6
	$3600/t_m$	2000	4000	6000
	b	0.5	0.3	0.7
	k_d	0.2	0.3	0.3
Circulating flow in roundabout	t_m	2.0	1.0	0.8
	$3600/t_m$	1800	3600	4500
	b	2.5	2.5	2.5
	k_d	2.2	2.2	2.2

TABLE 2: The ratio of free flow using different equation under different flow rates on circulating vehicles.

q(veh/s)	0.05	0.1	0.15	0.2	0.25	0.3	0.35	0.4	0.45
Eq. (7)	0.78	0.61	0.47	0.37	0.29	0.22	0.17	0.14	0.11
Eq. (8)	0.90	0.80	0.70	0.60	0.50	0.40	0.30	0.20	0.10
Eq. (9)	0.68	0.60	0.53	0.45	0.38	0.30	0.23	0.15	0.08
Eq. (10)	0.80	0.65	0.51	0.41	0.31	0.23	0.16	0.10	0.05

The model in SIDRA 2.0 (refer to Akcelik, 2007) can be applied in nonblocking traffic flow, which is deduced from the traffic volume model between the velocity and the flow rate and the headway distribution model:

$$\alpha = \frac{1 - qt_m}{1 - (1 - k_d) qt_m}, \quad \alpha \geq 0.001 \tag{10}$$

where k_d is the bunched delay constant; for convenience, 0.001 is the minimum value of α.

The constants in (7) and (10) are as listed in Table 1.

The ratio of free flow is 0 when $q = 1/t_m$ except in the exponential model.

For the circulating flow in roundabout, $t_m = 2s, b = 2.5, k_d = 2.2$, we can calculate the ratio of free flow under different circulating flow rates as Table 2 and Figure 1. Equations (8) and (9) are linear models. There are relatively small difference value among (7), (9), and (10). The values of (8) are always 0.75 times of (9).

3.3. Critical Gap and following Gap. Calculations of critical gap t_c and following gap t_f are also important in gap acceptance theory. Many methods can be used to calculate the critical gap such as Raff's method, Maximum likelihood method, Siegloch's method, and Ashworth's method [30–35].

The maximum likelihood method used log normal distribution of critical gap. It was used in measuring values for the Highway Capacity Manual. Brilon et al. [30] reached a conclusion that the maximum likelihood and Hewitts's methods provided the more consistent estimates with the least bias. The probability equilibrium method had a significant bias that was dependent on the flow in the priority stream. The modified Raff technique (Troutbeck, 2011) is an acceptable alternative. Guo [36] proposed the theoretical method which can be substituted into the capacity equations containing critical gap variable. The equation had basically identical critical gap with the maximum likelihood method.
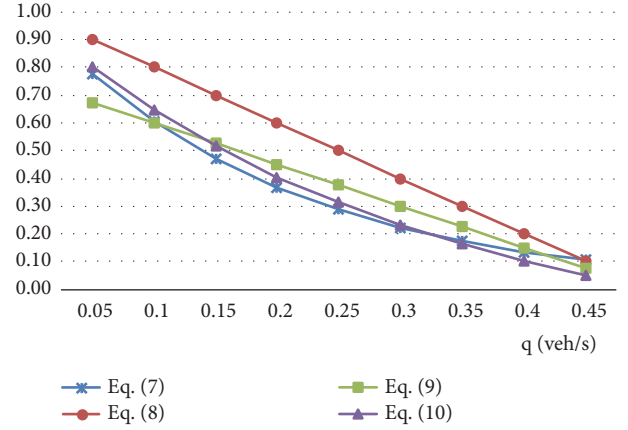
FIGURE 1: The ratio of free flow using different equation ($t_m = 2s, b = 2.5, k_d = 2.2$).

TABLE 3: Critical gap and following gap estimated in HCM 2010 (s).

	Single lane	Left lane in Multi lanes	Right lane in Multi-lanes
t_c	4.8	4.7	4.4
t_f	2.5	2.2	2.2

Brilon [37] found the traditional log normal distribution is not an essential part of the maximum likelihood method. The logistic distribution is easier to handle.

The constant critical gap in HCM 2010 is listed in Table 3 based on the field data of roundabouts in California.

4. Entrance Capacity of a Roundabout

4.1. The Theoretical Model of Entrance Capacity in Priority-Controlled Intersections. Based on gap acceptance theory, the equation of theoretical capacity C of the minor road in unsignalized intersections is as follows (Siegloch, 1973; refer to [2]):

$$C = q \int_0^\infty f(t) g(t) dt \tag{11}$$

where $g(t)$ is the number of vehicles entering the intersection when headways of vehicles on the major road are equal to t. It can be divided into continuous function and piecewise function because the number of vehicles can be expressed as an integer or decimal number.

Siegloch (1973; refer to [2]) proposed the continuous linear function of $g(t)$ as follows:

$$g(t) = \begin{cases} \dfrac{t - t_0}{t_f}, & t > t_0 \\ 0, & t \leq t_0 \end{cases} \tag{12}$$

$$t_0 = t_c - \frac{t_f}{2}$$

where t_f is the following headway; t_0 is the minimum acceptable headway, the intercept in horizontal coordinate of headway. The integration interval is $[t_c, \infty)$ in (11).
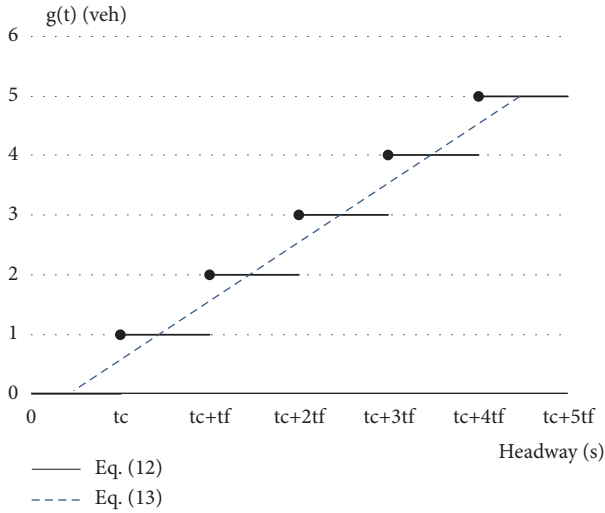
FIGURE 2: The g(t) of continuous function and piecewise function.

When $g(t)$ is a piecewise function, it has an equation as follows (Harders, 1976; refer to [2]):

$$g(t) = nP_n(t), \quad n = 1, 2, \cdots, \infty$$

$$P_n(t) = \begin{cases} 1, & t_c + (n-1)t_f \le t < t_c + nt_f \\ 0, & t < t_c \end{cases} \quad (13)$$

where t_c is the critical gap. The integration interval is $[t_c, \infty)$ in (11).

From Figure 2, the interval of circulating headway which can be accepted is $[t_0, +\infty)$ in continuous $g(t)$ function. The interval of circulating headway which can be accepted is $[t_c, +\infty)$ in piecewise $g(t)$ function.

Equation (11) shows that the capacity is related to the traffic volume on the major road, headway distribution, and $g(t)$ function. The lower limit of integral and $g(t)$ function is dependent on the critical gap.

Capacity model can be divided into two basic types according to critical gap, which can be a constant or stochastic distribution function. On the other side, the capacity model can be divided into two basic types including the continuous function and the piecewise function of $g(t)$ when the critical gap is constant. The basic equations are all based on a single-lane roundabout.

4.2. Entrance Capacity Model When Critical Gap Is Constant

4.2.1. When g(t) Is Piecewise Function.
When the critical gap is constant, the model varies with the headway distribution. As mentioned before, M1, M2, M3, Erlang, log-normal distribution, etc. usually were used to describe the arrival of circulating vehicles. M3 model was mainly recommended because it can be regarded as a general equation of M1, M2, and M3T.

Troutbeck [38] proposed (14) of entrance capacity where the headway on the major road followed M3 distribution

and $g(t)$ is piecewise function. Equation (14) is used in AUSTROADS [29].

$$C = \begin{cases} \dfrac{\alpha q e^{-\lambda(t_c-t_m)}}{1-e^{-\lambda t_f}}, & q > 0 \\ \dfrac{1}{t_f}, & q = 0 \end{cases} \quad (14)$$

The following are the capacity equations in which the distribution parameters are specially determined in M3 distribution. When headway follows M1 distribution, vehicles are under the free flow status and $t_m = 0$ where multiple circulating lanes were usually regarded as single lane. When headway follows M2 distribution, vehicles are under the free flow status and $t_m \ne 0$ in one lane. When headway follows M3T distribution, a dichotomized headway model assumes that a proportion, α, of all vehicles are free and the 1-α bunched vehicles have the same t_m.

(1) M1 Distribution. $\lambda = q$ when $t_m = 0$ and $\alpha = 1$. Buckley et al. ([39], refer to [40]) proposed (15).

$$C = \begin{cases} \dfrac{q e^{-q t_c}}{1-e^{-q t_f}}, & q > 0 \\ \dfrac{1}{t_f}, & q = 0 \end{cases} \quad (15)$$

(2) M2 Distribution. $\lambda = q/(1 - q t_m)$ when $t_m \ne 0$, t_m is a constant, and $\alpha = 1$. Equation (16) can be referred to Luttinen [14] as follows:

$$C = \begin{cases} \dfrac{q e^{-\lambda(t_c-t_m)}}{1-e^{-\lambda t_f}}, & q > 0 \\ \dfrac{1}{t_f}, & q = 0 \end{cases} \quad (16)$$

(3) M3T Distribution. $\lambda = q$ when $t_m \ne 0$, t_m is a constant, and $\alpha = 1 - q t_m$. The equation can be referred to Tanner [28] and Luttein [14].

$$C = \begin{cases} \dfrac{(1 - q t_m) q e^{-\lambda(t_c-t_m)}}{1-e^{-\lambda t_f}}, & q > 0 \\ \dfrac{1}{t_f}, & q = 0 \end{cases} \quad (17)$$

(4) M3 Distribution and Critical Gap Model. When the headway on the major road follows M3 distribution, (18) can be deduced when the function of critical gap [34, 36] is substituted into (14).

$$C = \dfrac{\beta_a q}{1 - e^{-\lambda t_f}} \quad (18)$$

where β_a is total acceptance coefficient, the proportion of the number of accepted gaps to the number of total gaps.

4.2.2. When g(t) Is Continuous Function. The entrance capacity can be expressed as the product of the saturated flow rate s of entrance and the probability larger than the minimum acceptable gap t_0, $P\{t > t_0\}$ (Akcelik, 1998). That is to say, $C = sP\{t > t_0\}$, where $P\{t > t_0\}$ is the probability larger than the minimum acceptable gap t_0.

(1) M1 Model. Siegloch (1973; refer to Wu 1999) proposed (19) in which the headway on the major road followed negative exponent distribution as in (15).

$$C = \frac{e^{-qt_0}}{t_f} \tag{19}$$

Equation (19) was used in HCM 2010, and parameters were set as $t_c = 4.8s$ and $t_f = 2.5s$.

(2) M2 Model. Jacobs (1980, refer to [2]) proposed (20) in which the headway on the major road followed shifted negative exponent distribution as (16).

$$C = \frac{q}{\lambda t_f} e^{-\lambda(t_0 - t_m)} = \frac{1 - qt_m}{t_f} e^{-\lambda(t_0 - t_m)}, \quad t_0 > t_m \tag{20}$$

The equation also can be expressed in similar form as

$$C_p = \frac{e^{-\lambda(t_0 - t_m)}}{t_f(1 + \lambda t_m)}, \quad t_0 > t_m \tag{21}$$

McDonald and Armitage [41] used the above equations as the capacity of roundabouts. They can be compared to signalized intersections where t_f^{-1} is regarded as the saturated flow rate and t_0 is regarded as lost time.

(3) M3 Model. In Cowan's M3 distribution, the minimum acceptable gap is larger than minimum headway, $t_0 > t_m$. The difference between M3 distribution and M2 distribution is the ratio of free flow, α. The potential capacity is as

$$C_p = \frac{q}{t_f}\left[\alpha\lambda\int_{t_0}^{\infty} te^{-\lambda(t-t_m)}dt - t_0 R(t_0)\right]$$
$$= \frac{\alpha q}{\lambda t_f}e^{-\lambda(t_0-t_m)}, \quad t_0 > t_m \tag{22}$$

The M3 model is used in AUSTROADS [29] and SIDRA (Akcelik, 1998). Multilane traffic flow can be regarded as a single-lane traffic flow, and the traffic volume is equal to the sum of all circulating traffic volume.

4.3. Entrance Capacity Model When Critical Gap Follows a Distribution. Different drivers have various critical gaps because the drivers' behaviors or the types of vehicles are different. Ideally, driver behaviors are supposed to be homogeneous and consistent [21, 42]. When a driver is consistent, every driving behavior is identical making the critical gap of the driver a constant. When different drivers are homogeneous, their drive behaviors are similar so they have the same critical gap whether constant or a distribution.

Catchpole and Plank [21] proposed the classification of entrance capacity models, including the constant critical gap and critical gap distribution. The models in Section 4.2 are the first part of Section 4.3.1. Heidemann and Wegmann [4] proposed the models based on a certain distribution of t_c, t_m, t_f and M3 distribution of the circulating stream. Wu's equations [2] were based on Erlang distribution of the circulating headway, whereas Guo's equations [34, 36] were based on M3 distribution of the circulating headway and the exponent function of rejected proportion.

4.3.1. Equations of Catchpole and Plank. Catchpole and Plank [21] proposed the capacity model based on different driver behaviors. When g(t) is piecewise function, the capacity can be expressed as follows.

(1) When the driver behaviors are homogeneous or consistent, that is to say, t_c is a constant, the capacity models are as (14) to (22) mentioned before.

(2) When the driver behaviors are consistent but nonhomogeneous, the capacity is as follows.

$$C = \frac{q(1 - qt_m)e^{qt_m}\mathsf{L}(t_c(q))}{1 - \mathsf{L}(t_f(q))} \tag{23}$$

where $\mathsf{L}(t_c(q))$ is the Laplace transformation of t_c distribution and $\mathsf{L}(t_f(q))$ is the Laplace transformation of t_f.

(3) It can be regarded as a special style of the following number (4) situation when the driver behaviors are homogeneous but inconsistent.

(4) When the driver behaviors are inconsistent and nonhomogeneous, the capacity is as follows.

$$C = \frac{1}{\sum_j(\theta_j/q_j)} = \frac{\alpha q e^{\lambda t_m}}{1 - e^{-\lambda t_f}} \cdot \frac{1}{\sum_j \theta_j/\mathsf{L}(\theta_j(q))} \tag{24}$$

where θ_j is the proportion of the jth kind of entrance vehicle; $\mathsf{L}(\theta_j(q))$ is the Laplace transformation of θ_j.

4.3.2. Equations of Heidemann and Wegmann. Heidemann and Wegmann [4] proposed that the capacity equation of unsignalized intersections follow a certain distribution for t_c, t_m, t_f. Based on M3 distribution of the headway on a major road, the capacity is (25) when $g(t)$ is the piecewise function, and it is (26) when $g(t)$ is the continuous function.

$$C = \frac{\lambda}{1 + \lambda\overline{B}}\frac{\mathsf{L}(t_c'(\lambda))}{1 - \mathsf{L}(t_f(\lambda))}$$
$$= \frac{\lambda}{1 + \lambda\overline{B}}\frac{\mathsf{L}(t_c(\lambda))\mathsf{L}(t_m(-\lambda))}{1 - \mathsf{L}(t_f(\lambda))} \tag{25}$$

$$C = \frac{\lambda}{1 + \lambda \overline{B} \left(1 - L\left(t_f(\lambda)\right)\right) L\left(t_c'(-\lambda)\right)}$$

$$= \frac{\lambda}{1 + \lambda \overline{B} \left(1 - L\left(t_f(\lambda)\right)\right) L\left(t_c(-\lambda)\right) L\left(t_m(\lambda)\right)} \quad (26)$$

where $\overline{B} = \overline{t}_m/\alpha$, $t_c' = t_c - t_m$; $L(t_c'(\lambda))$ is the Laplace transformation of t_c' at λ, $L(t_c'(\lambda)) = L(t_c(\lambda))L(t_m(-\lambda))$; $L(t_f(\lambda))$ is the Laplace transformation of t_f at λ; $L(t_m(-\lambda))$ is the Laplace transformation of t_m at $-\lambda$.

$$C_{bunch} = \alpha q \frac{\left(\lambda\left(\overline{t}_c - \tau_{t_c}\right)/k_{t_c} + 1\right)^{-\alpha_{t_c}} e^{-\lambda \tau_{t_c}} \left(-\lambda\left(\overline{t}_m - \tau_{t_m}\right)/k_{t_m} + 1\right)^{-\alpha_{t_m}} e^{\lambda \tau_{t_m}}}{1 - \left(\lambda\left(\overline{t}_f - \tau_{t_f}\right)/k_{t_f} + 1\right)^{-\alpha_{t_f}} e^{-\lambda \tau_{t_f}}} \quad (28)$$

The capacity is as follows when the drivers are homogeneous.

$$C_{bunch} = \alpha q \frac{\left(-\lambda\left(\overline{t}_c - \tau_{t_c}\right)/k_{t_c} + 1\right)^{\alpha_{t_c}} e^{-\lambda \tau_{t_c}} \left(\lambda\left(\overline{t}_m - \tau_{t_m}\right)/k_{t_m} + 1\right)^{\alpha_{t_m}} e^{\lambda \tau_{t_m}}}{1 - \left(\lambda\left(\overline{t}_f - \tau_{t_f}\right)/k_{t_f} + 1\right)^{-\alpha_{t_f}} e^{-\lambda \tau_{t_f}}} \quad (29)$$

(2) When g(t) Is Continuous Function. Some assumptions have been given that the headway on a major road follows shifted Erlang distribution and t_f follows random distribution. The capacity is as follows when the drivers are nonhomogeneous.

$$C_{bunch} = (1 - q\overline{t}_m) \frac{1}{\overline{t}_f} \left(\frac{\lambda\left(\overline{t}_0 - \tau_{t_0}\right)}{k_{t_0}} + 1\right)^{-\alpha_{t_0}}$$

$$\cdot e^{-\lambda \tau_{t_0}} \left(\frac{-\lambda\left(\overline{t}_m - \tau_{t_m}\right)}{k_{t_m}} + 1\right)^{-\alpha_{t_m}} e^{\lambda \tau_{t_m}} \quad (30)$$

The capacity is as follows when the drivers are homogeneous.

$$C_{bunch} = (1 - q\overline{t}_m) \frac{1}{\overline{t}_f} \left(\frac{-\lambda\left(\overline{t}_0 - \tau_{t_0}\right)}{k_{t_0}} + 1\right)^{\alpha_{t_0}}$$

$$\cdot e^{-\lambda \tau_{t_0}} \left(\frac{\lambda\left(\overline{t}_m - \tau_{t_m}\right)}{k_{t_m}} + 1\right)^{\alpha_{t_m}} e^{\lambda \tau_{t_m}} \quad (31)$$

4.3.4. Guo Equation. The equation of Guo [34, 36] is based on M3 distribution. All the headways of the free flow on the major road have rejected proportions; that is to say, every

4.3.3. Wu Equation. Wu [2] proposed the probability density function when the headway on a major road follows Erlang distribution as follows.

$$f(t_x) = \frac{\gamma}{\left(\alpha_{t_x} - 1\right)!} \left(\gamma t_x\right)^{\alpha_{t_x} - 1} e^{-\gamma t_x} \quad (27)$$

where $\gamma = \alpha_{t_x}/\overline{t}_x$; $\overline{t}_x$ is the average value of t_x; α_{t_x} is the constant in Erlang distribution of t_x.

(1) When g(t) Is a Piecewise Function. It is supposed that the minimum value of t_c is τ_{t_c} and $\tau_{t_c} > \tau_{t_m}$, the minimum value of t_f is $\tau_{t_f} > 0$ and $\tau_{t_f} > 0$, the minimum value of t_m is τ_{t_c} and $\tau_{t_m} > 0$, and t_c, t_m, t_f all follow negative exponent distribution. The capacity is as follows when the drivers are nonhomogeneous.

headway in the interval of (t_m, ∞) on the major road is probably to be accepted. The rejected proportion function is the exponent function and the accepted proportion increases when the headway on the major road increases.

The rejected proportion function $f_{ro}(t)$ is the exponent function as follows.

$$f_{r0}(t) = \begin{cases} e^{-r(t - t_m)}, & t \geq t_m \\ 0, & t < t_m \end{cases} \quad (32)$$

where r is the rejected proportion coefficient.

The capacity can be deduced when g(t) is continuous function as follows.

$$C = \alpha q \left[\frac{r}{(\lambda + r)} + \frac{e^{-\lambda t_f}}{t_f \lambda} - \frac{\lambda e^{-(\lambda + r)t_f}}{t_f (\lambda + r)^2}\right] \quad (33)$$

The capacity can be deduced when g(t) is piecewise function as follows.

$$C = \frac{\alpha q}{(\lambda + r)} \left[\frac{r}{\left(1 - e^{-\lambda t_f}\right)}\right.$$

$$\left. - \frac{\lambda e^{-(\lambda + r)t_f}}{\left[1 - e^{-(\lambda + r)t_f}\right]} \left(\frac{r}{\lambda + r}\right)^{(\lambda + r)/\lambda}\right] \quad (34)$$

4.4. The Capacity of Limited Priority Merge. Under some special situations, gap acceptance theory can be based on different assumptions such as limited priority merge or priority conversion. The driving behavior under limited priority merge [43–46] means that vehicles on the circulating lane need to adjust the gaps for the vehicles entering the intersection.

Another priority style, priority conversion means that vehicles on the entrance are forced to enter into the intersection and the circulating vehicles have to yield for the entrance vehicles. These driving behaviors are more feasible in the field and their equations are more complicated to be applied for calculation.

Troutbeck [45] proposed the following equation of limited priority merge:

$$C = \frac{\alpha f_L q e^{-\lambda(t_c - t_m)}}{1 - e^{-\lambda t_f}}, \quad t_m < t_c < t_f + t_m$$

$$f_L = \frac{1 - e^{-\lambda t_f}}{1 - e^{-\lambda(t_c - t_m)} - \lambda\left(t_c - t_f - t_m\right) e^{-\lambda(t_c - t_m)}}$$

(35)

When $t_c \geq t_f + t_m, f_L = 1$, the vehicles on the major road are not delayed after merging and the system can be modeled as an absolute priority system. It can be referred to Bunker and Troutbeck [46], Troutbeck [44, 45], Troutbeck and Kako [43].

If both t_c and t_f are set up as t_m, all the gaps are t_m after merging. The capacity is as follows:

$$C = \frac{1}{t_m} - q$$

(36)

where $f_L = (1 - e^{-\lambda t_m})/\lambda t_m$ and $C = \alpha q/\lambda t_m$.

5. Comparison of Different Models

When critical gap follows a stochastic distribution, that is to say, a driver might reject a gap which he accepted before or drivers have different critical gaps, this effect results in an increase of capacity comparing with the condition of constant critical gap.

The limited priority merge can have a significant effect on the entry capacity at roundabouts. The limited priority capacity is very close to the empirical results from the UK linear regression method. The capacity prediction based on the limited priority and the UK method are reasonable in general.

It is difficult to compare different models in the field because each model adapts in different road geometrical and traffic conditions. The headway distribution of the circulating vehicles, the ratio of free flow, the type of g(t) function, the critical gap t_c, and other parameters, such as t_f, t_m, vary with different geometrical and traffic conditions, and they affect the calculation value of entrance capacity in roundabouts.

Suppose that the headway of circulating vehicles follow the M3 distribution as (1), the decay constant λ is (3), and the ratio of free flow is (7). Equations (14), (18), (22), (34), and (35) can be compared using the same parameter values
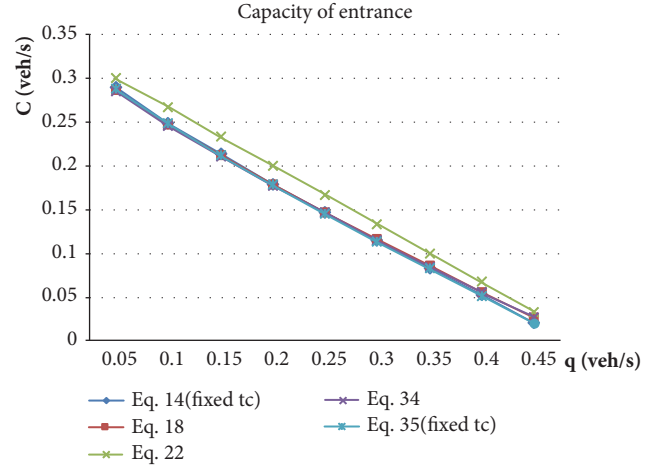
FIGURE 3: Calculation of entrance capacity under different flow rates on circulating vehicles.

where $t_m = 2s$ and $t_f = 3s$. Due to different g(t) functions and calculation models of t_c, some different parameters need to be set in some Equations. In (14) and (35), $t_c = 4.35s$. In (22) and (34), $t_0 = t_m = 2s$. In (18) and (35), $r = 0.365$. The entrance capacity C can be calculated using the five equations under a different flow rate q. The results can be shown in Table 4 and Figure 2.

From Figure 3, it can be concluded that the values of (22) are larger than values of other equations. The values of (14), (18), (34), and (35) are so similar that different curves cannot be clearly recognized. Because the number of vehicles entering the intersection can be considered as a decimal if continuous g(t), (22) with continuous g(t) function will result in a larger value of entrance capacity than the other equations based on the piecewise g(t) function. The influence of different critical gap models on capacity value is limited. The capacity values of (18) and (34) are slightly larger than (14) and (35) when the circulating vehicles are close to the saturated flow rate, where q=0.4 and q=0.45. The capacity values of the four equations are almost equal with each other.

The above capacity models have very small differences of each other regardless of the critical gap type and the g(t) type. Therefore, the simple calculating models based on the constant critical gap and piecewise g(t) function should be recommended in the field.

6. Application Conclusions of Different Models

The capacity models based on gap acceptance theory are analysis methods in which traffic parameters have a certain physical meaning. When the critical gap is constant, the deviation of the capacity model is conveniently used to obtain the equations and calculate the accurate capacity values. Drivers' behavior characteristics are different in different countries. For example, the critical gap of the single-lane roundabout is 4.8s in America; however, it is about 3.5s in China. Drivers' nonhomogeneous and inconsistent character

TABLE 4: Calculation of entrance capacity under different flow rates on circulating vehicles ($t_m = 2s$, $t_f = 3s$).

No.	q(veh/s)	alpha	λ(1/s)	βa	tc(s)	Eq. (14)(fixed tc) (veh/s)	Eq. (18)(veh/s)	Eq. (22)(veh/s)	Eq. (34)(veh/s)	FL in Equ. (35)	Eq. (35)(fixed tc)(veh/s)
1	0.05	0.779	0.043	0.696	4.589	0.289	0.286	0.300	0.285	0.997	0.288
2	0.1	0.607	0.076	0.502	4.489	0.249	0.247	0.267	0.246	0.995	0.248
3	0.15	0.472	0.101	0.370	4.418	0.213	0.212	0.233	0.210	0.994	0.212
4	0.2	0.368	0.123	0.275	4.362	0.179	0.179	0.200	0.177	0.993	0.178
5	0.25	0.287	0.143	0.206	4.311	0.146	0.147	0.167	0.146	0.991	0.145
6	0.3	0.223	0.167	0.153	4.255	0.114	0.116	0.133	0.115	0.990	0.113
7	0.35	0.174	0.203	0.112	4.179	0.083	0.086	0.100	0.084	0.989	0.082
8	0.4	0.135	0.271	0.078	4.050	0.052	0.056	0.067	0.055	0.986	0.051
9	0.45	0.105	0.474	0.046	3.756	0.021	0.027	0.033	0.027	0.982	0.020

is more realistic than the fixed critical gap and following gap. Although the calculation results of capacity are similar as the field capacity under the assumption of homogeneity and continuance, there is only a little percent deviation.

Several widely used models and the parameters can be compared as follows.

(1) The headway was usually regarded as negative exponent distribution. M3 distribution was also paid enough attention [4].

(2) Based on a field traffic survey in Australia [22], the capacity Equation (22) of M3 distribution and continuous g(t) was applied in aaSIDRA (Akcelik et al., 1994, 1997, 1998) in which the following gap and critical gap are varied from the geometry of the roundabout, the flow rate of entrance and circulating lanes. The capacity is related to the circulating flow rate, lane use, OD metric of flow rate, queue on entrance lanes and the ratio of free flow. All the lanes on entrance can be modeled at the same time.

(3) Based on the survey of a limited number of roundabouts in America and in comparison with the experience values of other countries, the capacity equation (15) of M1 distribution and piecewise function g(t) was used in HCM (2000). In the model, the constant parameters of gap acceptance were used which did not vary from the geometry of the roundabout and traffic volume. The calculation results have limitations when the circulating volume increased up to 1200pcu/h for a single-lane roundabout.

(4) The capacity equation (19) of M1 distribution and continuous function g(t) was used in HCM (2010), in which both t_c and t_f were determined and some equations were built based on a different number of entrance lanes and different number of circulating lanes. The calculating process of traffic characteristics was proposed including capacity, delay, level of service, and queue length.

(5) The capacity equation (18) was deduced by directly plugging the critical gap model into the capacity equation (14). Equation (18) has reasonable results in accordance with some classical methods and it has more accurate results under some conditions; for example, the low capacity is closer to the reality than linear regression under low flow rate conditions.

(6) The method based on stochastic critical gap is more realistic with operation in roundabouts, but most of the equations are too complicated to calculate quickly. Simplification is needed to apply in the field.

With the increase of traffic volume, the application of traditional roundabouts becomes more and more difficult. Many roundabouts, especially in China, were dismantled and few roundabouts were newly built. The field capacity becomes very small because many drivers do not obey the priority rule. Traffic jams or even traffic accidents occurred at roundabouts. In reality, signal timing was applied in some roundabouts, in which the inner lanes of the weaving area were designed as left-turn waiting areas. Left-turn vehicles need to watch the signal light two times when passing through the roundabout. The validity needs to be verified further.

Drivers are sensitive to some problems of roundabouts at peak hours, but ignore the advantages at off-peak time, such as safe, environment friendly, suitable to large-volume left turns. To the researchers and engineers in the traffic field, traffic organization and optimization should be the key focus to increase capacity and reliability at peak hours.

Conflicts of Interest

The authors declare that there are no conflicts of interest regarding the publication of this paper.

References

[1] W. Grabe, *Leistungsermittlung von nicht lichtsignalsteuerten Knotenpunkten des Stranverkehrs [Capacity calculation of unsignalized intersections in road traffic]*, Forschungsarbeiten aus dem Strassenwesen, Neue Folge 11, Kirschbaum Verlag, Bielefeld, Germany, 1954.

[2] N. Wu, "A universal procedure for capacity determination at unsignalized (priority-controlled) intersections," *Transportation Research Part B: Methodological*, vol. 35, no. 6, pp. 593–623, 2001.

[3] C. F. Daganzo, "Traffic delay at unsignalized intersections: Clarification of some issues," *Transportation Science*, vol. 11, no. 2, pp. 180–189, 1977.

[4] D. Heidemann and H. Wegmann, "Queueing at unsignalized intersections," *Transportation Research Part B: Methodological*, vol. 31, no. 3, pp. 239–263, 1997.

[5] W. Brilon, "Studies on Roundabouts in Germany: Lessons Learned," in *Proceedings of the The 3rd International Transportation Research Board*, 2010.

[6] W. Wang, H. Gao, W. Li et al., *Capacity Analysis Method of Highway Intersection*, Science Press, 2001.

[7] R. J. Guo, B. L. Lin, and W. X. Wang, "The Iterative Caculation of Full Capacity of Roundabouts," in *Proceedings of the Second International Symposium on Information Science and Engineering*, pp. 570–573, IEEE, Shanghai, China, 2009.

[8] P. K. Jeffrey, N. Gautami, and L. Elefteriadou, "Queuing delay models for single-lane roundaboutst," *Civil Engineering and Environmental Systems*, vol. 22, no. 3, pp. 133–150, 2001.

[9] E. Chevallier and L. Leclercq, "A macroscopic theory for unsignalized intersections," *Transportation Research Part B: Methodological*, vol. 41, no. 10, pp. 1139–1150, 2007.

[10] A. J. Miller, *An Empirical Model for Multilane Road Traffic*, Northwestern University for the U.S. Bureau of Public Roads, 1968.

[11] R. M. Kimber, "Gap-acceptance and empiricism in capacity prediction," *Transportation Science*, vol. 23, no. 2, pp. 100–111, 1989.

[12] D. R. McNeil and J. T. Smith, *A Comparison of Motorist Delays for Different Merging Strategies*, United States Department of Transportation, 1968.

[13] E. M. Hollis, M. C. Semmens, and S. L. Denniss, "ARCADY: A Computer Program to Model Capacities, Queues and Delays at Roundabouts," Transport and Road Research Laboratory 940, TRRL Laboratory Report, Crowthorne, Berkshire, UK, 1980.

[14] R. T. Luttinen, *Capacity and Level of Service at Finnish Unsignalized Intersections*, Finnish Road Administration, 2004.

[15] H. M. N. Al-Madani, "Capacity of large dual and triple-lanes roundabouts during heavy demand conditions," *Arabian Journal for Science and Engineering*, vol. 38, no. 3, pp. 491–505, 2013.

[16] H. L. Khoo and C. Y. Tang, "Roundabout system capacity estimation and control strategy with origin-destination pattern," *Journal of Transportation Engineering*, vol. 142, no. 5, Article ID 04016017, 2016.

[17] J. Bie, H. K. Lo, and S. C. Wong, "Capacity evaluation of multi-lane traffic roundabout," *Journal of Advanced Transportation*, vol. 44, no. 4, pp. 245–255, 2010.

[18] X. Qu, L. Ren, S. Wang, and E. Oh, "Estimation of entry capacity for single-lane modern roundabouts: Case study in Queensland, Australia," *Journal of Transportation Engineering*, vol. 140, no. 7, Article ID 05014002, 2014.

[19] Y. H. Yap, H. M. Gibson, and B. J. Waterson, "Models of roundabout lane capacity," *Journal of Transportation Engineering*, vol. 141, no. 7, Article ID 04015007, 2015.

[20] R. Mauro and F. Branco, "Comparative analysis of compact multilane roundabouts and turbo-roundabouts," *Journal of Transportation Engineering*, vol. 136, no. 4, pp. 316–322, 2010.

[21] E. A. Catchpole and A. W. Plank, "The capacity of a priority intersection," *Transportation Research Part B: Methodological*, vol. 20, no. 6, pp. 441–456, 1986.

[22] O. Hagring, "Effects of OD Flows on Roundabout Entry Capacity," *Transportation Research Circular E-C018: 4th International Symposium on Highway Capacity*, pp. 434–445, 2000.

[23] A. Khattak and P. Jovanis, "Capacity and delay estimation for priority unsignalized intersections: Conceptual and empirical issues," *Transportation Research Board*, pp. 129–137, 1990.

[24] D. Branston, "Models of single lane time headway distributions," *Transportation Science*, vol. 10, no. 2, pp. 125–148, 1976.

[25] China Highway Society, *Manual of Transportation Engineering*, China communication press, Beijing, China, 2001.

[26] R. C. Cowan, "Useful headway models," *Transportation Research*, vol. 9, no. 6, pp. 371–375, 1975.

[27] Ö. C. Yiğiter and S. Tanyel, "Lane by lane analysis of vehicle time headways — Case study of Izmir ring roads in Turkey," *KSCE Journal of Civil Engineering*, vol. 19, no. 5, pp. 1498–1508, 2015.

[28] J. C. Tanner, "The capacity of an uncontrolled intersection," *Biometrika*, vol. 54, no. 3-4, pp. 163–170, 1967.

[29] AUSTROADS, *Roundabouts: Guide to Traffic Engineering Practice*, Association of Australian State Road and Transport Authorities, Sydney, Australia, 1993.

[30] W. Brilon, R. Koenig, and R. J. Troutbeck, "Useful estimation procedures for critical gaps," *Transportation Research Part A: Policy and Practice*, vol. 33, no. 3-4, pp. 161–186, 1999.

[31] Z. Z. Tian, M. Vandehey, B. W. Robinson et al., "Implementing the maximum likelihood methodology to measure a driver's critical gap," *Transportation Research Part A*, vol. 33, pp. 187–197, 1999.

[32] Z. Tian, R. M. Troutbeck, W. Kyte et al., "Further investigation on critical gap and follow-up time," in *Proceedings of the Transportation Research Circular E-C018: 4th International Symposium on Highway Capacity*, 2002.

[33] R. Guo, "Estimating critical gap of roundabouts by different methods," *Transportation of China*, pp. 84–89, 2010.

[34] R. J. Guo, X. J. Wang, and W. X. Wang, "Estimation of critical gap based on Raff's definition," *Computational Intelligence and Neuroscience*, vol. 2014, Article ID 236072, 7 pages, 2014.

[35] R. Guo and Y. Zhao, "Critical gap of a roundabout based on a logit model," in *Proceedings of the Fifth International Conference on Transportation Engineering*, pp. 2597–2603, Dailan, China, 2015.

[36] R. J. Guo and B. L. Lin, "Gap acceptance at priority-controlled intersections," *Journal of Transportation Engineering*, vol. 137, no. 4, pp. 269–276, 2011.

[37] W. Brilon, "Some remarks regarding the estimation of critical gaps," *Transportation Research Record*, vol. 2553, no. 1, pp. 10–19, 2016.

[38] R. J. Troutbeck, "Average delay at an unsignalized intersection with two major streams each having a dichotomized headway distribution," *Transportation Science*, vol. 20, no. 4, pp. 272–286, 1986.

[39] D. J. Buckley, "A semi-poisson model of traffic flow," *Transportation Science*, vol. 2, no. 2, pp. 107–133, 1968.

[40] M. Kyte, W. Kittelson, Z. Z. Tian et al., "Analysis of traffic operations at all-way stop-controlled intersections by simulation," in *Proceedings of the Annual Meeting of Transportation Research Board*, Washington, DC, USA, 1996.

[41] M. McDonald and D. J. Armitage, "The capacity of roundabouts," *Traffic Engineering and Control*, vol. 19, pp. 447–450, 1978.

[42] R. J. Troutbeck and W. Brilon, "Traffic Flow Theory," in *Part 8: Unsignalized Intersection Theory*, Gartner and Messer, Eds., pp. 8:1–8:47, 1997.

[43] R. J. Troutbeck and S. Kako, "Limited priority merge at unsignalized intersections," *Transportation Research Part A: Policy and Practice*, vol. 33, no. 3-4, pp. 291–304, 1999.

[44] R. J. Troutbeck, "The performance of uncontrolled merges using a limited priority process," in *Transportation and Traffic Theory in the 21st Century*, M. A. P. Taylor, Ed., pp. 463–482, Taylor, Australia, 2002.

[45] R. J. Troutbeck, "The capacities of a limited priority merge," Physical Infrastructure Centre Research Report 98-4, Queensland University of Technology, Australia, 1998.

[46] J. Bunker and R. Troutbeck, "Prediction of minor stream delays at a limited priority freeway merge," *Transportation Research Part B: Methodological*, vol. 37, no. 8, pp. 719–735, 2003.

Research Article

Evaluation of Roundabout Safety Performance through Surrogate Safety Measures from Microsimulation

Orazio Giuffrè,[1] Anna Granà ⬤,[1] Maria Luisa Tumminello,[1] Tullio Giuffrè,[2] Salvatore Trubia,[2] Antonino Sferlazza,[3] and Marko Rencelj ⬤[4]

[1]*Department of Civil, Environmental, Aerospace, and Material Engineering, University of Palermo, Viale delle Scienze, Ed 8, 90128 Palermo, Italy*
[2]*Kore University, Cittadella Universitaria, 94100 Enna, Italy*
[3]*Department of Energy, Information Engineering and Mathematical Models, University of Palermo, Viale delle Scienze, Ed 8, 90128 Palermo, Italy*
[4]*University of Maribor, Faculty of Civil Engineering, Transportation Engineering and Architecture, Slovenia*

Correspondence should be addressed to Anna Granà; anna.grana@unipa.it

The paper presents a microsimulation-based approach for roundabout safety performance evaluation. Based on a sample of Slovenian roundabouts, the vehicle trajectories exported from AIMSUN and VISSIM were used to estimate traffic conflicts using the Surrogate Safety Assessment Model (SSAM). AIMSUN and VISSIM were calibrated for single-lane, double-lane and turbo roundabouts using the corresponding empirical capacity function which included critical and follow-up headways estimated through meta-analysis. Based on calibration of the microsimulation models, a crash prediction model from simulated peak hour conflicts for a sample of Slovenian roundabouts was developed. A generalized linear model framework was used to estimate the prediction model based on field collected crash data for 26 existing roundabouts across the country. Peak hour traffic distribution was simulated with AIMSUN, and peak hour conflicts were then estimated with the SSAM applying the filters identified by calibrating AIMSUN and VISSIM. The crash prediction model was based on the assumption that the crashes per year are a function of peak hour conflicts, the ratio of peak hour traffic volume to average daily traffic volume and the roundabout outer diameter. Goodness-of-fit criteria highlighted how well the model fitted the set of observations also better than the SSAM predictive model. The results highlighted that the safety assessment of any road unit may rely on surrogate safety measures, but it strongly depends on microscopic traffic simulation model used.

1. Introduction

The concept of road safety refers to a property of some elements of the real world which are called units: a road segment, an intersection, a vehicle, or a person. According to Hauer [1], a key characteristic of a unit is that it may be involved in crashes and crashes may occur on it. Many research efforts have been devoted to the study of the relationship between crash history and road design/traffic variables using statistical models. Since regression analysis is used to develop crash prediction models, complete and updated crash databases must be available. Differently from statistical approaches to road crash data analysis, traffic

conflict technique allows studying the road situations and observing traffic conflicts [2]. In recent years, the traffic conflict techniques have been incorporated into traffic simulation models, thus providing considerable potential for proactive safety analysis [3]. Simulation-based surrogate safety measures have also been the subject of recent research [4]; they have been applied to evaluate the safety performance of any road unit using simulated vehicle trajectories exported from microscopic traffic simulation models. In this regard, the Surrogate Safety Assessment Model (SSAM) software processes trajectory outputs provided by traffic microsimulation models, identifies traffic conflict events by analysing vehicle-to-vehicle interactions, and categorizes the conflict events by

type; the SSAM evaluates the surrogate safety measures for pairs of vehicles involved in a traffic conflict [5]. A simulation-based approach to assess road safety performance through the surrogate measures of safety will depend largely on the microscopic traffic simulation model which is applied. The trajectory files provided by microsimulation also depend on how the road unit is modelled and simulated. In view of the well-known potentialities of microsimulation software packages and growing attention of transportation engineers in their use, calibration of these models should be carefully considered so as not to compromise their ability to reproduce the real-world traffic conflicts.

Starting from these considerations, this paper describes a microsimulation-based approach for roundabout safety performance evaluation. The specific objective of the research is to show the methodological path used to develop a crash prediction model based on simulated conflicts. For these purposes, estimation of traffic conflicts by the SSAM software is done for each roundabout of the Slovenian sample using trajectory files generated by AIMSUN [6] and VISSIM [7], after calibration of the two types of software. Calibration is done for each type of roundabout (i.e., the single-lane roundabout, double-lane roundabout and turbo roundabout) using the corresponding empirical capacity function which incorporated the critical and follow-up headways estimated by meta-analysis [8]. The simulated vehicle trajectories of the roundabouts of the Slovenian sample were exported from AIMSUN and VISSIM and were used to develop a conflict analysis through the SSAM software. The idea behind the proposed approach for roundabout safety performance evaluation was to estimate the surrogate measures of safety based on a suitable setting of the SSAM filters so that the simulated outputs from AIMSUN and VISSIM had a comparable level [9]. Then, a generalized linear model framework was used to estimate a prediction model based on crash data collected at Slovenian roundabouts. Since technical literature still presents few studies which focus on the relationship between crashes and simulated traffic conflicts especially at roundabouts, there is a gap in the current literature that this paper aims to address.

The main framework of the paper is organized as follows. After a literature review on the area of road safety evaluation based on traffic conflicts, also through microscopic traffic simulation models, the next sections present the crash dataset for the Slovenian sample of roundabouts, the method proposed to calibrate the microscopic traffic simulation models used, and the calculation of surrogate safety measure from microsimulation. Then, the development of a crash prediction model from simulated peak hour conflicts is described for the sample of 26 Slovenian roundabouts, and the results of validation of the proposed model are presented. Conclusions of the research and future developments of the work are explored in the concluding section.

2. Literature Review

Many safety studies using microscopic traffic simulation models rely on surrogate safety measures, which have been introduced to assess the safety performance of roads and

intersections without waiting for a statistically significant number of real crashes to occur [10]. Different measures have been proposed; the most popular for simulation includes time-to-collision, stopping distance index, modified time-to-collision, vehicle speeds, and headways [5]. The surrogate safety measures are based on the identification, classification, and evaluation of conflict events that occur during microsimulation. As introduced above, the Surrogate Safety Assessment Model (SSAM) reads trajectories files exported from microscopic simulation models and calculates the surrogate safety measures. This approach eliminates the subjectivity associated with the conventional conflict analysis technique and makes it possible to assess the safety performance of a road infrastructure under a controlled environment, before a crash occurs. Since a comprehensive review of the state-of-the-art in the area of road safety simulation models is beyond the research objectives, without being exhaustive we remember a recent study that analysed the geometric design of passing lanes and evaluated their optimal length using VISSIM and the SSAM software [11]. The results highlighted not only the fundamental role of geometric design in the safety performance of the 2+1 short passing lane, but also the use of simulated traffic conflicts being a promising approach for road safety performance analysis. Wang et al. [12] used AIMSUN to simulate driver violating behaviours through user-defined add-ons, proposed a method for analysing collision risk of various driver violating behaviours, and examined the impact on motorway safety. The authors also highlighted the lack of violating behaviours in existing software that has made time-to-collision of stopping-sight-distance difficult to evaluate in current simulation environments. Kuang et al. [13] also verified whether or not the incorporation of the driver's perception-reaction time could improve the performance of a surrogate safety measure. To this end, they proposed the modified surrogate indicators by considering the driver's perception-reaction time. Based on collected data on motorways, calibration of the VISSIM by the error tests and trajectory comparison were done; the performances of the modified surrogate indicators were then evaluated using crash data. Huang et al. [14] classified traffic conflicts generated by the SSAM using vehicle trajectories from simulation; they derived reasonable estimates for field measured traffic conflicts at signalized intersections. Essa and Sayed [15] also used the SSAM to estimate surrogate safety measures at signalized intersections in urban area; they investigated the transferability of VISSIM calibrated parameters for safety analysis between different sites. The results confirmed that the use of simulation models to evaluate road safety without proper calibration should be avoided, and more work is needed to confirm that simulated conflicts represent safety measures beyond what can be expected from exposure. Vasconcelos et al. [16] evaluated the potential of the SSAM approach to assess the safety performance at urban intersections and roundabouts. Model validation was accomplished by comparing the number of conflicts obtained with the SSAM both with the number of crashes predicted by analytic models and with conflicts observed on existing intersections. Recently, Pratelli et al. [17] presented a procedure for analysing safety and operational improvements

from conversion of traffic circles to modern roundabouts using AIMSUN and the SSAM software. However, despite the encouraging results, further case studies were needed to validate the proposed method. Despite some limitations related to the nature of the traffic microsimulation models used in the aforementioned researches, the SSAM analysis resulted in a promising approach to assess the safety of new intersection layouts.

A microsimulation-based approach could be also conducted to estimate the safety impact of autonomous vehicles (AVs) on-road traffic, since AV technology has advanced in recent years with some automated features already available in vehicles on the market. Deluka Tibljaš et al. [18] have already analysed safety performances at roundabouts where different numbers of Conventional Vehicles (CVs) and AVs coexist in traffic. The simulations done with VISSIM and the SSAM gave some highlights on how the introduction of AVs could change the operational and safety parameters at roundabouts. Another recent research focuses on the relationship between crashes and conflicts predicted by simulation models. Saleem et al. [3] developed crash prediction models from simulated peak hour conflicts for a group of urban signalized intersections and evaluated their predictive capabilities. Some case studies simulated with VISSIM and Paramics demonstrated the capability of microsimulation for estimating safety performance. Saulino et al. [19] investigated the use of simulated conflicts as possible surrogate safety measures for roundabouts, for which it has proven difficult to relate crashes to geometric characteristics. They applied microsimulation to estimate the number of peak hour conflicts for roundabout entries using a database of US roundabouts. Their results suggested that simulated conflicts can be considered as a surrogate measure for crashes at roundabouts after a proper calibration. Nevertheless, it should be noted that alternative methods have been developed and applied for safety evaluation at roundabouts. It is possible to refer to Pilko et al. [20] for a new analytical approach that used multicriteria and simultaneous multiobjective optimization of geometric design, efficiency, and safety for a sample of Croatian single-lane roundabouts, while Hatami and Aghayan [21] investigated different types of roundabout layouts and analysed the effects of radius and speed variations on the roundabout performance through several scenarios defined in AIMSUN. However, it should be noted that a few studies on the use of surrogate safety measures from microsimulation were based on field data or have calibrated conflicts for a specific road or intersection. Although a large number of practitioners and transportation engineers during the last decade have been using traffic microsimulation in lots of practical applications, technical literature still presents few studies which focus on the relationship between crashes and simulated traffic conflicts especially at roundabouts. Thus, there is a real knowledge gap in the current literature on estimation of surrogate safety measures at roundabouts that needs to be filled.

3. Materials and Methods

3.1. Crash Dataset.
Keeping in mind the purpose of the study, firstly a sample of roundabouts in operation in several municipalities and rural locations in Slovenia was examined. Crash data were obtained from the Police database for a time period of eight years (years 2009–2016). The dataset included information on the date and the time of day when crashes occurred, condition of signs and markings, environmental conditions including pavement and presence of work zones, type and number of involved users, manoeuvres and road the users came from, and values of Annual Average Daily Traffic (AADT) entering each roundabout. Only total crashes happening at each site were considered, for a total number of 162 crashes. The crashes occurring within 30 meters of the roundabout centre were also included. Twenty-six roundabouts were selected as a representative sample for the later analysis. Table 1 summarizes basic information on the selected roundabouts from Police reports, in some cases integrated by Google maps. The sample included 13 four-legged single-lane roundabouts, 5 double-lane roundabouts (of which a five-legged roundabout and a six-legged roundabout, and the other three four-legged roundabouts), and 8 turbo roundabouts (of which five four-legged and three three-legged turbo roundabouts).

The roundabout features directly related to safety and operational performances had been integrated with on-field surveys. The Annual Average Daily Traffic (over the whole observed period) in turbo roundabouts was between 7,000 and 63,400 vehicles per day; it was between 15,812 and 26,050 vehicles per day for the single-lane roundabouts, while it was between 21,307 and 44,318 vehicles per day for the double-lane roundabouts. The analysis encompassed the turbo roundabouts built since 2009 and some of them were made as reconstruction into a turbo roundabout of already constructed intersections; for this reason, just few crashes were recorded. Table 2 summarizes the main statistics of crash, traffic, and geometric data of the roundabout data sample.

3.2. Calibration of Microscopic Traffic Simulation Models.
Before starting the calibration of AIMSUN and VISSIM, a sensitivity analysis was done to determine the model parameters having the best effect on simulated values of steady state capacity as produced by the two software packages. Although literature proposes a wave of methodologies for the calibration of simulation models, there have been no attempts to find general calibration principles based on the collective knowledge and experience [26]. Thus, the model output of entry capacity simulated for every category of roundabout was compared to the most well-known empirical capacity function based on the model proposed by [27]; each category of single-lane roundabout, double-lane roundabout, and turbo roundabout was assumed as representative in terms of geometric design and behavioural parameters of the corresponding roundabouts of the dataset. Each capacity function included behavioural headways that were collected in the field and then combined in meta-analysis by [8]. For each entry lane, the empirical capacity functions based on a meta-analytic estimation of the critical and follow-up headways represented the target values of empirical capacity to which the simulated capacities were

TABLE 1: Information on the roundabouts case studies from Police Reports.

Name	Roundabout (number of entries)	Municipality	Roads approaching the intersection
Randenci 1	single-lane (4)	Randenci	Pananskacesta, Radgonska cesta South, Radgonska cesta East, Radgonska cesta West,
Brezice Intermarket	single-lane (4)	Brezice	Cesta bratov Milavcev, Tovarniškacesta, Cesta Svobode, Cesta bratov Milavcev
Gederovci	single-lane (4)	Gederovci	Gederovci East, Gederovci North, Sodišinci, Gederovci West
Kranj AC	single-lane (4)	Kranj - Senčcur	Kranj - SpodnjiBrnik, E61,Senčcur, Kranjska cesta
KrižPodgorje	single-lane (4)	Križ	Podgorje West, KorenovaCesta, Podgorje North, Podgorje South,
Levec	single-lane (4)	Levec	Krajevna cesta, Ljubijana cesta, Krajevna cesta, Ljubijana cesta,
Velenje	single-lane (4)	Velenje	Kidričeva cesta, Cesta PodParkom, Aškerčeva cesta, Koroška cesta,
Brežice_Trnje	single-lane (4)	Brežice	Cesta Svobode, Trnje, Bizeljskočatež, Dobovska cesta
MoravskeToplice	single-lane (4)	MoravskeToplice	Dolga ulica, Kranjčevaulica, Dolga Ulica, Kranjčevaulica
Rače	single-lane (4)	Rače	UlicaLackoveCete, Cesta Talcev, Ptujska cesta, Rače
Drnovo	single-lane (4)	Drnovo	8273 LeskovecpriKrškem, Drnovo, 8273 LeskovecpriKrškem, Velika Vas Pri Krškem
Ljutomer	single-lane (4)	Ljutomer	Prešernovaulica, Grossmanovaulica, Prešernovaulica, Cesta l. Slovenskega Tabora
Krško	single-lane (4)	Krško	Cesta 4 Julija,Zdolska cesta, Cesta 4 Julija, Prešernova Ulica
Medvode	double (4)	Medvode	Gorenjska cesta, Zbiljska cesta, 211 Medvode, Finžgarjevaulica
Nova Gorica	double (4)	Nova Gorica	Vojkova cesta, LematovaUlica, Kromberška cesta, 103 Nova Gorica
Novo Mesto	double (6)	Novo Mesto	Ljubjanska cesta, Tržiškaulica, Andrijaničeva cesta, Velika Bučnavas
Rožna_Do	double (4)	ValdiroseRožna Dolina	Podmark, 103 Nova Gorica, Vipavska cesta, 103 Nova Gorica
Ravne_Na_K	double (5)	RavnenaKoroškem	Koroška cesta West, Prežihovaulica, Koroška cesta South, Koroška cesta North, Koroška cesta East
Lesnina	turbo (4)	Koper	Ljubjanska cesta North, Ljubjanska cesta South, Ljubjanska cesta West, Ljubjanska cesta East
Stadion,	turbo (4)	Koper	Ljubjanska cesta, Ferrerska cesta, Ljubjanska cesta, Cesta ZorePerrello – Godina,
Planet Tuš	turbo (4)	Koper	Kolodvorska cesta, Ankaranska cesta, Kolodvorska cesta, Ljubjanska cesta
Supernova	turbo (3)	Koper	Ankaranskacesta North, Ankaranskacesta West, Ankaranskacesta East
Luka Koper	turbo (3)	Koper	Ankaranskacesta West, Koper, Ankaranskacesta South
M1	turbo (4)	Maribor	Borovavas, Borovavas, Borovavas, Ilichovaulica,
M2 Lackova	turbo (3)	Maribor	Borovavas, Lackova cesta East, Lackova cesta West
M3	turbo (4)	Maribor	Titova cesta North, Pobreška cesta West, Titova cesta South, Pobreška cesta East

compared; see [28] for the potential that a single (quantitative) meta-analytic estimate provides compared to the results of individual studies on the parameters of interest. Table 3 shows the geometric design and behavioural parameters of every roundabout category used to calibrate AIMSUN and VISSIM.

It should be noted that geometric design of the single-lane roundabout and the double-lane roundabout is consistent with classification of roundabouts worldwide [29, 30]. The geometric design of single-lane roundabout and the double-lane roundabout here considered also complies with the Italian standards [31] of the compact roundabout and

TABLE 2: The main statistics of the roundabout data sample.

Statistics	8-year total crashes	AADT [veh/d]	Outer Diameter [m]	Ring Width [m]	Entry Width [m]	Exit Width [m]
min	0	7,000.00	30.00	4.50	3.90	3.75
mean	6	26,022.02	46.85	7.78	5.10	5.21
median	2	21,980.33	50.00	7.50	4.83	5.12
max	34	63,400.00	89.60	11.00	8.15	7.10

TABLE 3: Geometric design and behavioural parameters of every roundabout category.

Basic Parameter	Single-Lane Roundabout	Double-Lane Roundabout	Turbo Roundabout
outer diameter[m]	39.00	41.00	40.00
ring width [m]	7.00	9.00	4.50^a (4.20^b)
entry-lane width [m]	3.75	3.50	3.50
exit-lane width [m]	4.50	4.50	4.50
T_{ci} [s]	-	$4.159 (3.898, 4.420)^c$	3.60
T_{ce} [s]	$4.274 (4.051; 4.498)^c$	$3.822 (3.562; 4.082)^c$	3.91
T_{fi} [s]	-	$2.853 (2.665, 3.043)^c$	$2.26^d (2.110, 2.411)$
T_{fe}[s]	$3.103 (2.957; 3.248)^c$	$2.717 (2.569, 2.867)^c$	$2.13^d (1.981, 2.287)$

Note: [a]inside lane width; [b]outside lane width; [c]95% confidence interval; [d]on field collected by Fortuijn [22].
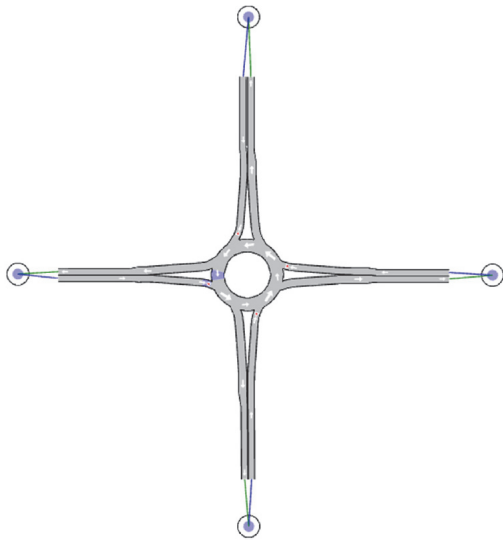
FIGURE 1: The single-lane roundabout model in simulation environment.
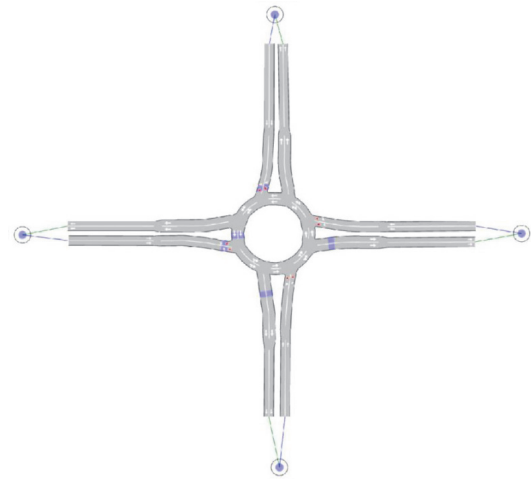
FIGURE 2: The double-lane roundabout model in simulation environment.

FIGURE 3: The turbo roundabout model in simulation environment.

conventional roundabout, respectively. The design features of the double-lane roundabout also correspond to the layout of the typical double-lane roundabout as proposed by [32], Appendix A, Exhibit A-7. The turbo roundabout design met the turbo geometry presented by [25]. Each roundabout typology was then modelled in AIMSUN and VISSIM (see Figures 1–3) in accordance with the geometric parameters in Table 3.

In order to assess each roundabout with the SSAM, the roundabouts were then simulated with desired traffic conditions. Saturated conditions were achieved at entry lanes, so that the maximum number of vehicles entering the roundabout corresponded to the capacity value of each entry lane.

TABLE 4: Default and calibrated values of the model parameters in AIMSUN.

Model Parameter		Roundabout			
		Single-Lane	Double-Lane (Right Lane)	Double-Lane (Left Lane)	Turbo[b]
reaction time [s]	default	0.80 (0.10, 1.50)	0.80 (0.10, 1.50)	0.80 (0.10, 1.50)	0.80 (0.10, 1.50)
	calibrated	0.86 (0.82, 0.86)[a]	0.94 (0.85, 0.95)[a]	0.95 (0.85,0.95)[a]	1.00 (0.10, 1.50)
min headway [s]	default	0.00	0.00	0.00	0.00
	calibrated	1.58 (1.50, 1.70)[a]	1.00 (1.00, 1.50)[a]	1.33 (1.00,1.50)[a]	1.70 (1.00, 1.70)
speed acceptance[c]	default	1.10	1.10	1.10	-
	calibrated	1.00 (1.00, 1.10)[a]	0.95 (0.90, 1.10)[a]	0.97 (0.90,1.10)[a]	-
GEH index [%]	def.	56.25	78.10[d]	78.10[d]	85.00[b,d]
	calibr.	87.50	96.90[d]	93.80[d]	99.00[b,d]

Note: [a]the acceptance range for AIMSUN model parameters is the upper and lower bounds used for GA calibration [23, 24]; [b]the same values of the model parameters were used for each entry lane [25]; [c]the model parameter ranges from a minimum of 0.90 to a maximum of 1.30 as AIMSUN proposes; [d]the same GEH indexes were obtained for each entry lane.

A genetic algorithm-based calibration procedure had been developed by [23, 24] to determine the parameters of AIMSUN for the single-lane and the double-lane roundabouts. In order to calibrate AIMSUN and reproduce realistic traffic on roundabouts, the reaction time, the minimum headway, and the speed acceptance were used as the model parameters. For the turbo roundabout layout under examination, the AIMSUN calibration was made in a previous work [25]; the reaction time and the minimum headway were used as the model parameters. Table 4 exhibits the default and calibrated parameters of the roundabout models built in AIMSUN. Based on [26], the GEH index was used to accept (or reject) the model; GEH_i is expressed as follows:

$$GEH_i = \sqrt{\frac{2(x_i - y_i)^2}{(x_i + y_i)}} \qquad (1)$$

It denotes that a model reproduces the empirical capacity data if the difference between the simulated (x_i) and empirical capacities (y_i) is smaller than 5 in (at least) 85% of the cases. Thus, GEH equal to 100% means that the difference between the simulated and empirical capacities of the entry lanes is smaller than 5 in 100% of the cases. Note that the acceptance range for the AIMSUN model parameters is the upper and lower bounds used for GA calibration [23, 24], while in other cases the acceptance ranges for each parameter are the default ones of the microsimulation model used.

In order to calibrate the roundabouts in VISSIM, the Wiedemann 74 model integrated in PTV VISSIM software (version 10) was selected. The average desired distance between stopped cars, ranging from -1.0 m to +1.0 m (with a standard deviation of 0.3 m), the additive part of desired safety distance, and the multiplicative part of desired safety distance were used as model parameters; for these last two parameters nothing about variation is proposed by VISSIM. Calibration in VISSIM was done manually simulating several replications, adjusting the model parameters and ranging them between successive simulation runs. The optimal setting obtained by the calibration parameters in VISSIM was for each roundabout category as follows.

(i) The Single-Lane Roundabout

average standstill distance: the default value is equal to 2.00 m, while the calibrated value is 5.10 m

additive part of desired safety distance: the default value is equal to 2.00 m, while the calibrated value is 3.60 m

multiplicative part of desired safety distance: the default value is equal to 3.00 m, while the calibrated value is 1.80 m

(ii) The Double-Lane Roundabout (Right Lane)

average standstill distance: the default value is equal to 2.00 m, while the calibrated value is 1.80 m;

additive part of desired safety distance: the default value is equal to 2.00 m, while the calibrated value is 3.05 m

multiplicative part of desired safety distance: the default value is equal to 3.00 m, while the calibrated value is 4.75 m

(iii) The Double-Lane Roundabout (Left Lane)

average standstill distance: the default value is equal to 2.00 m, while the calibrated value is 4.50 m

additive part of desired safety distance: the default value is equal to 2.00 m, while the calibrated value is 5.00 m

multiplicative part of desired safety distance: the default value is equal to 3.00 m, while the calibrated value is 5.00 m

(iv) The Turbo Roundabout (Right Lane and Left Lane)

average standstill distance: the default value is equal to 2.00 m, while the calibrated value is 5.00 m

additive part of desired safety distance: the default value is equal to 2.00 m, while the calibrated value is 3.10 m

TABLE 5: Origin-destination matrix of traffic flow percentages [9].

Case a				
origin-destination	South	East	North	West
South	0	0.33	0.33	0.33
East	0.33	0	0.33	0.33
North	0.33	0.33	0	0.33
West	0.33	0.33	0.33	0
Case b				
origin-destination	South	East	North	West
South	0	0.30	0.05	0.65
East	0.05	0	0.05	0.90
North	0.05	0.65	0	0.30
West	0.05	0.90	0.05	0
Case c				
origin-destination	South	East	North	West
South	0	0.65	0.05	0.30
East	0.05	0	0.05	0.90
North	0.05	0.30	0	0.65
West	0.05	0.90	0.05	0

multiplicative part of desired safety distance: the default value is equal to 3.00 m, while the calibrated value is 1.50 m

Note that the GEH index was below 50% for each roundabout entry lane, when the default values of the model parameters were used; it was greater than 87% when the calibrated values of the model parameters were used. Only, for the left entry lane of the turbo roundabout, the GEH index was below 85%, but only a small number of GEH$_i$ was just over 5; thus, the model was accepted. At last, the entry lane capacities simulated with AIMSUN and VISSIM were compared to the empirical capacity functions before introduced; this was made to verify that the calibrated models in VISSIM were actually comparable to the calibrated models in AIMSUN.

Three origin-destination matrices of traffic flow percentages were simulated for the calibrated models of the roundabouts as they were representative of the most crucial operating conditions observed in the field (in Table 5). In order to guarantee a base for a homogeneous comparison, an iterative procedure based on [29] was implemented to ensure a desired (pre-fixed) saturation ratio at each roundabout entry and to calculate the total entering flows relative to each matrix of traffic flow percentages (in Table 5). For these purposes, we used the capacity formula proposed by [33]; thus, the entering flows with a saturation ratio of 0.60 were calculated. For the roundabouts under examination, based on matrices in Table 5, the corresponding origin-destination matrices were obtained. For each roundabout of the sample the trajectory files were obtained. In order to produce the trajectory data for each roundabout in Table 1, more than 15 replications of simulation were done in both AIMSUN and VISSIM for the calibrated models; the duration in each

replication did not exceed an hour. The 5 simulations that best replicated the origin-destination matrices were then selected.

3.3. Calculation of Surrogate Safety Measures from Microsimulation. The SSAM software analysed vehicle-to-vehicle interactions to identify conflict events and recorded all events happening during the simulation [34]. For each conflict event, the SSAM software calculated the surrogate safety measures recorded in the TRJ.files, separately generated by AMISUN and VISSM, including the following [5]: the minimum time-to-collision, the minimum postencroachment time, the initial deceleration rate, the maximum deceleration rate, the maximum speed, and the maximum speed differential. The default filters of the SSAM were not changed during the initial phase of analysis; they were then changed in order to better compare the results obtained by processing the TRJ.files from AIMSUN and VISSIM. Table 6 shows the mean values of normalised total conflicts given by AIMSUN and VISSIM for the roundabouts under examination and the origin-destination matrices of traffic flow percentages in Table 5. More specifically, the values in Table 6 are the total conflicts by each roundabout and each origin-destination matrix in relation to the total simulated entering flow. Table 6 shows that the normalised total conflicts were smaller for the single-lane roundabouts than the double-lane and turbo roundabouts (in case a and case b) with TRJ.files generated by AIMSUN and the default filters of the SSAM. Again, the normalised total conflicts were higher at the turbo roundabouts than the double-lane roundabouts (in case a and case b) with TRJ.files generated by AIMSUN and the default filters of the SSAM.

However, Table 6 shows differences in the mean values of the normalised total conflicts between the SSAM filter-based total conflicts calculated when the appropriate filter values

Table 6: Normalised total conflicts at roundabouts.

case[a]	Filter	Single-Lane Roundabout		Double-Lane Roundabout		Turbo Roundabout	
		SSAM-AIMSUN[b]	SSAM-VISSIM[c]	SSAM-AIMSUN[b]	SSAM-VISSIM[c]	SSAM-AIMSUN[b]	SSAM-VISSIM[c]
case a	DEFAULT	87.56	69.53	102.70	63.56	127.03	9.21
	FILTER	1.68	1.38	7.79	4.10	1.37	4.30
case b	DEFAULT	76.82	67.25	98.07	49.55	227.80	26.16
	FILTER	0.93	1.03	6.65	11.83	2.48	3.79
case c	DEFAULT	65.53	42.41	81.04	39.98	48.37	28.41
	FILTER	1.42	1.52	6.03	3.69	0.89	4.87

Note: [a]o-d matrixes in Table 5; [b]the mean values of the normalised total conflicts calculated using the TRJ.files generated by AIMSUN both when the default filters of the SSAM were not changed and when the appropriate filters were applied; [c]the mean values of the normalised total conflicts calculated using the TRJ.files generated by VISSIM when the default filters of SSAM were not changed and when the appropriate filters were applied.

were used and the total conflicts calculated with the default filters of SSAM.

In order to identify which settings influenced the results of the SSAM software, a sensitive analysis was then developed. After several trials, the parameter with a greater effect on the SSAM results was the time-to-collision (TTC) [3, 35], the post-encroachment time (PET) [3, 35], and the maximum speed (MaxS) [3]. It should be noted that smaller values of TTC and PET during a traffic conflict correspond to a greater probability of a collision. Moreover, a TTC equal to 0 is, by definition, a collision; in turn, the value of PET, by definition, should be greater than the TTC [5]. The optimal setting, obtained for the aforementioned parameters and the examined cases, was as follows:

(i) TTC: the default value of the maximum TTC is 1.50 s, since a value less than 1.50 s can be considered the maximum threshold of TTC [35]; thus, the maximum threshold of TTC was set equal to 1.50 s

(ii) PET: the default value of the maximum PET is 5.00 s, while the maximum threshold of PET was set equal to 2.50 s except for double-lane roundabouts where a maximum value of PET of 1.90 s was set for the conflicts produced with TRJ.files generated by VISSIM; the last value of the maximum PET was based on what SSAM recorded with the TRJ.files generated by AIMSUN

(iii) the minimum thresholds of TTC and PET were set equal to 0.10 seconds; TTC and PET equal to zero are mere processing errors and were deleted [3]

(iv) MaxS: the minimum threshold values are equal to 1.00 meters per second for the single-lane roundabouts and 1.18 meters per second for the turbo roundabouts; the filter of MaxS was not changed for the double-lane roundabouts

(v) a filter around the intersection area was applied and conflicts falling within 30 meters before each roundabout entry, since VISSIM identified several conflicts very far from the intersection area that had to be excluded

The results of SSAM filter-based total conflicts in Table 6 show a good fit for the frequency of conflicts derived from the two microsimulation models. Indeed, for the traffic cases (in Table 5), the percentage difference of total conflicts calculated with AIMSUN and VISSIM was below 40 per cent. Student's t-test was also carried out to compare the filter-based total conflicts obtained with the SSAM. Figure 4 shows the t-test results for AIMSUN versus VISSIM at roundabouts under examination; see [36] for more in-depth details. The t-test gave non significant results for the single-lane and turbo roundabouts; statistical significance was determined especially at the 0.05 level for the double-lane roundabouts. Based on the above results, traffic conditions and roundabout schemes can have an important effect on roundabout safety: the single-lane roundabout seems less safe than turbo-roundabout in the case b (in Table 5); unlike cases a and b (in Table 5), double-lane roundabouts are less safe than the single-lane and the turbo roundabouts in the case c (in Table 5), where, unlike case b, the percentage of right turns is higher than that of left turns.

4. Fitting a Crash Prediction Models Based on Simulated Conflicts

Once the frequency of conflicts obtained by AIMSUN and VISSIM was made comparable by setting some filters of SSAM as introduced above, and conditions were examined under which a safety analysis could be independent of the software being used; a conflict prediction model was developed using AIMSUN. Differently from conventional crash prediction models where crashes per year are the dependent variable and the average daily traffic is the main independent variable, simulation is typically done at the peak hour level. Thus, AIMSUN-simulated peak hour traffic and then peak hour conflicts were estimated. Ten replications were performed for each roundabout and the resulting TRJ.files generated from AIMSUN were processed with the SSAM software to identify conflicts based on the procedure described in the previous sections. Table 7 summarizes the main statistics for type of conflict and total conflicts of all the roundabouts of the sample in Table 1. However, total conflicts only were considered to fit the model since low conflicts by type resulted except for the rear-end type.

In order to develop a prediction model for total crashes versus total conflicts, peak hour conflicts were modelled

(a)

(b)

(c)
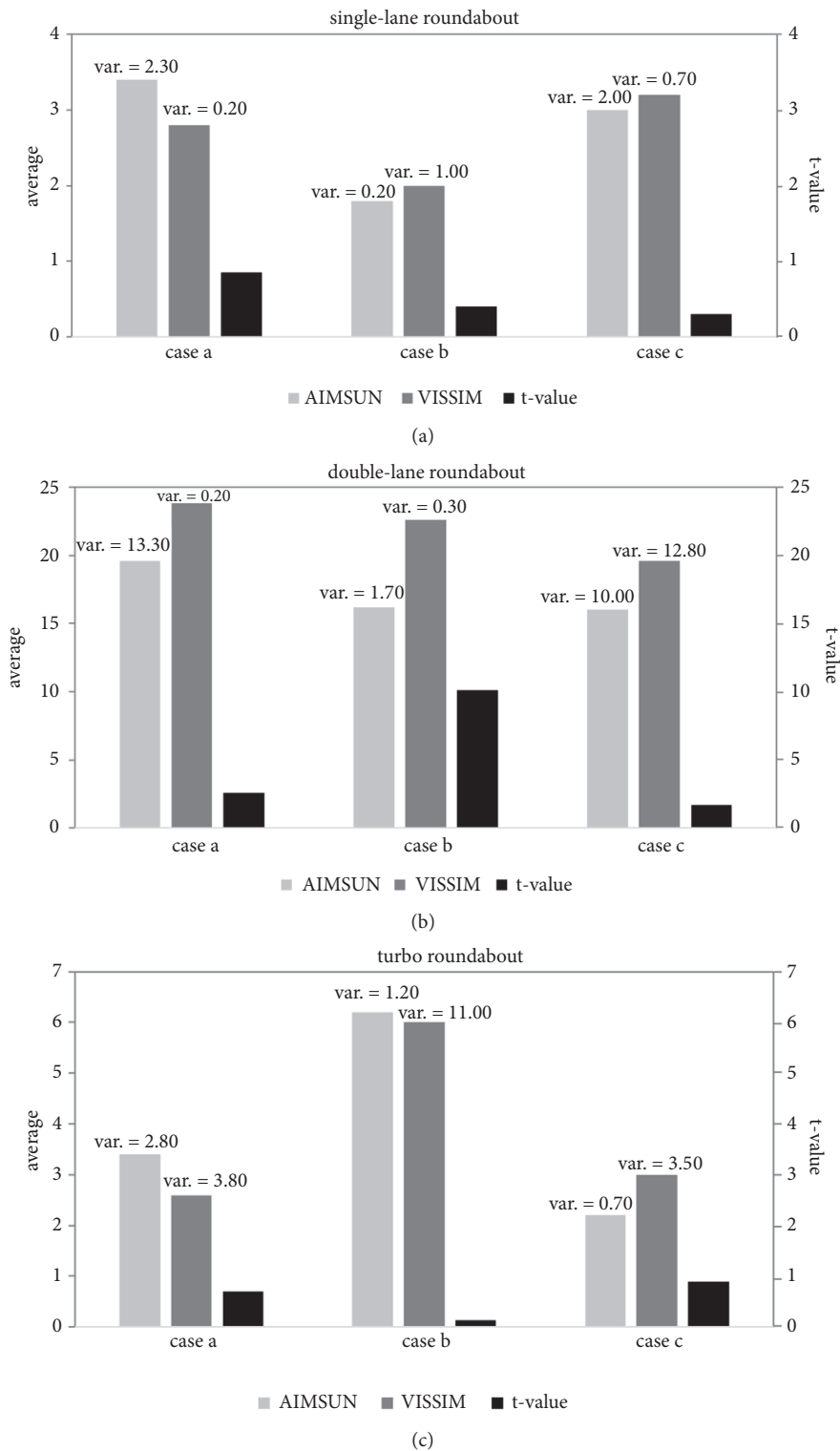
FIGURE 4: t-test results for VISSIM versus AIMSUN at (a) single-lane roundabouts, (b) double-lane roundabouts, and (c) turbo roundabouts. Note: $T_{critical}$ (α=0.05) = 2.31; $T_{critical}$ (α=0.01)= 3.36; average means the mean value of total conflicts in simulation replications; the t-test was not significant for single-lane and turbo roundabouts in cases a, b, and c, while t-test was significant for the double-lane roundabout in cases a and b (at the 0.05 level) and case b (at the 0.01 level).

TABLE 7: Summary of main statistics for type of conflict and total conflict.

Statistics	Type of Conflict			Total Conflicts
	Rear-End	Lane-Change	Crossing	
min	1.00	0.00	0.00	1.00
mean	27.37	8.48	0.19	36.04
median	33.00	5.45	0.00	37.50
max	78.00	57.00	3.00	112.00

against crashes per year (occurring during all hours) by incorporating an extra variable to capture the effect of the ratio of peak hour traffic volume to average daily traffic volume [3]; only the outer diameter was introduced as further covariate of the model, while other covariates did not result significant. It should be noted that a sensitivity analysis was done to test several geometric and traffic features (i.e., entry width, ring width); however, only the variables that were significant were selected as the explanatory variables of the model. Based on state-of-the-art in safety modelling [37], in order to fit the model, a generalized linear model framework was used as available in the statistical package GenStat [38]. Since the data had a variance slightly larger than expected under the assumption of a Poisson distribution (i.e., the variance is equal to the mean), equidispersion assumption was relaxed to avoid model specification errors. It is quite well known that the most common approaches are a quasi-likelihood with Poisson-like assumptions (i.e., the quasi-Poisson from now on) and a Negative Binomial model; these models are derived from the Poisson model and allow the mean to differ from the variance when data exhibit overdispersion [39, 40]. However, in the statistical literature, especially for the regression case, little guidance can be found when the specification of a quasi-Poisson or a Negative Binomial error structure has to be performed [41]. Since, for any given datasets, one can find cases where each model produces a good fit to the data, goodness-of-fit criteria helped us to choose between the two above introduced models.

First, in order to employ the regression technique to relate the actual crash frequency to the AIMSUN-simulated conflict frequency predicted by the SSAM, the functional form of the model was selected. Real-life crashes and conflicts were assumed as discrete random events with a non normal error structure [5]. Consistent with the model forms introduced for the conflict prediction models [3], the power function was here assumed and used to develop the total crash model as follows:

$$E[\mu] = e^{\alpha} \bullet X^{\beta_1} \bullet X^{\beta_2} \bullet X^{\beta_3} \quad (2)$$

where $E[\mu]$ is the expected number of total crashes per year (i.e., the dependent variable), $X_{i(i=1,2,3)}$ are the explanatory variables, and α and $\beta_{i(i=1,2,3)}$ are the regression parameters to be estimated using the maximum-likelihood procedure. The peak hour conflicts (X_1) generated from AIMSUN simulation and the SSAM analysis, the peak hour traffic ratio (X_2), or the ratio of peak hour traffic volume to average daily traffic volume, and the outer diameter (X_3) of the selected roundabouts were selected as the explanatory variables of the model. The peak hour ratio was considered an exploratory variable since it could vary from roundabout to roundabout and depended on the road classification, location, day, date, and time of the peak hour counts. Table 8 shows the parameter estimates with two different distributions in GLM framework. The constant value (α) was not statistically significant for both models, while the estimates of β_1, β_2, and β_3 were statistically significant (at the 5% level and 10% level) in both cases. The table also shows the measures of goodness-of-fit discussed by [42] (1) the mean prediction bias (MPB); a positive (or negative) MPB denotes that a model over predicts (or under predicts) crashes; (2) the mean absolute deviation (MAD) that measures the average dispersion of the model; (3) the mean square prediction error (MSPE) that is used in conjunction with the mean squared error (MSE): an MSPE higher than MSE indicates that the models are overfitting the data and that some of the observed relationships may have been spurious instead of real. Other measures of goodness-of-fit were the mean error (ME) and the mean normalized error (MNE) which are useful when applied separately to measurements at each location instead of to all measurements jointly [26]. Table 8 also shows the GEH index (see (1)), and Pearson product moment correlation coefficient ($r_{Pearson}$) between observed and predicted crashes. As further information about the goodness-of-fit, the method of cumulate residuals (CURE) was applied as dealt with in next section.

5. Results and Discussion

The results in Table 8 show a reasonably good fit for the data; however, the quasi-Poisson model fits the data better than Negative Binomial model and produces a slightly better prediction accuracy: the mean prediction bias (MPB) of the quasi-Poisson model was lower than the NB model, similarly to the mean absolute deviation (MAD) and the mean error (ME). For the quasi-Poisson model the MSPE also was lower than MSE compared with the other model; however, each model did not show signs of overfitting since they had an MSPE value lower than the MSE value and confirmed that no important variables were omitted from the model or the models were misspecified.

Comparisons between models, however, are not always easy; the differences in goodness-of-fit can suggest cases in which models could be improved, but improvements might be difficult to obtain. The GEH index and Pearson coefficient also highlighted how well the models fit the set of observations; however, Pearson coefficients for both

TABLE 8: Parameter estimates for crash models based on AIMSUN simulated conflicts and goodness-of-fit.

Parameter	quasi-Poisson model*			Negative Binomial model*		
	estimate (s.e.)	t	t pr.	estimate (s.e.)	t	t pr.
β_1	0.859 (0.222)	3.88	<.001	1.117 (0.242)	4.62	<.001
β_2	5.77 (1.09)	5.31	<.001	6.38 (1.17)	5.45	<.001
β_3	2.299 (0.533)	4.31	<.001	2.397 (0.578)	4.15	0.003
$MPB = \dfrac{1}{N}\sum_{i=1}^{N}(\widehat{y}_i - y_i)$	- 0.0034	-	-	0.2987	-	-
$MAD = \dfrac{1}{N}\sum_{i=1}^{N}\left|\widehat{y}_i - y_i\right|$	0.4364	-	-	0.5964	-	-
$MSPE = \dfrac{1}{N}\sum_{i=1}^{N}(\widehat{y}_i - y_i)^2$	0.6430	-	-	1.4217	-	-
$MSE = \dfrac{1}{N-dof}\sum_{i=1}^{N}(\widehat{y}_i - y_i)^2$	0.727	-	-	1.607	-	-
$ME = \dfrac{1}{N}\sum_{i=1}^{N}\left|\widehat{y}_i - y_i\right|$	0.0034	-	-	0.2987	-	-
$MNE = \dfrac{1}{N}\sum_{i=1}^{N}\dfrac{\left|\widehat{y}_i - y_i\right|}{\left|y_i\right|}$	0.1613	-	-	0.3299	-	-
$r_{Pearson} = \dfrac{\sum_{i=1}^{N}\left(\widehat{y}_i - \overline{\widehat{y}}\right)\left(y_i - \overline{y}\right)}{\left[\sum_{i=1}^{N}\left(\widehat{y}_i - \overline{\widehat{y}}\right)^2 \sum_{i=1}^{N}\left(y_i - \overline{y}\right)^2\right]}$	0.72	-	-	0.67	-	-
$GEH_i = \sqrt{\dfrac{2\left(x_i - y_i\right)^2}{\left(x_i + y_i\right)}}$	100%	-	-	100%	-	-

Note: N is the data sample size, and $\widehat{y}_i$ is the fitted value of y_i, which is the actual measurement; $\overline{\widehat{y}}$ is the mean value of the fitted values, while $\overline{y}$ is the mean value of the actual measurements; dof stands for degree of freedom; $r_{Pearson}$ stands for Pearson product moment correlation coefficient. (*) Note that in GenStat the dispersion parameter (fixed or estimated) is used when calculating standard errors and standardized residuals. In models with the Poisson and negative binomial, as well as geometric and exponential distributions, the dispersion should be fixed at 1 unless a heterogeneity parameter is to be estimated.

(a) Quasi-Poisson model

(b) Negative Binomial model
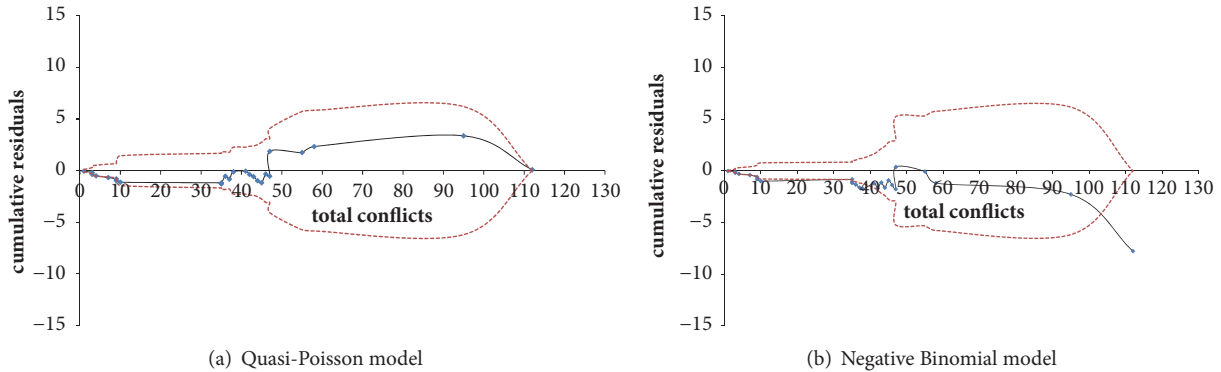
FIGURE 5: CURE plots for total conflicts: (a) quasi-Poisson model; (b) Negative Binomial model.

models showed marginal differences in goodness-of-fit that could be explained by random fluctuations in the observed data, however negligible. As further information about the goodness-of-fit, the method of cumulate residuals (CURE) was applied and CURE plots were developed [1]. The cumulative residuals, defined as the difference between the actual and the fitted values for each observation unit, were arranged in increasing order of the fitted value and computed for each observation unit. Figure 5 shows how well the model under the quasi-Poisson assumption fits the data as a function of a

specific variable of interest; for example, as variable of interest the total conflicts were selected for this comparison. The cumulative residuals on the vertical-axis were plotted against the total conflicts on the horizontal-axis. The indication is that the fit is fairly good especially for the quasi-Poisson model since the cumulative residuals, oscillating around the value of 0, lie between the confidence limits of the standard deviation ($\pm 2\sigma^*$).

Although a horizontal stretch of the CURE plot corresponds to a region of the variable where the estimates can

(a) Quasi-Poisson model
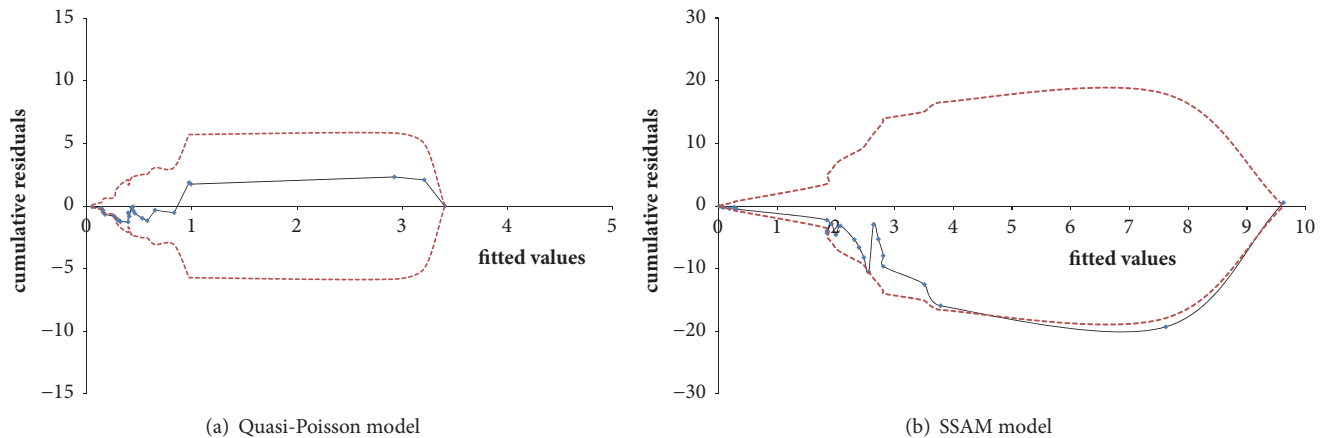
(b) SSAM model

Figure 6: CURE plots for fitted values: a) quasi-Poisson model; b) SSAM model.

be unbiased, the CURE plot (see Figure 5(a)) for the quasi-Poisson model is inside the confidence limits; thus, one can observe that the calibrated model fits the data very well, while for the case of Negative Binomial model a portion of the CURE plot was outside the confidence limits (see Figure 5(b)). In order to assess the overall quality of the model fit [1], the fitted value-based CURE plots were prepared both for the quasi-Poisson model (Figure 6(a)) and for the SSAM model (Figure 6(b)), which is a nonlinear regression model for crashes as a function of total conflicts [5].

In Figure 6 each plot shows how well (or poorly) the model predicts, not for a specific variable but overall, as a function of number of crashes expected on each unit. The CURE plot in Figure 6(a) for the quasi-Poisson model is closer to a random walk around the horizontal-axis than the plot in Figure 6(b) and it is inside the confidence limits. The CURE plot of the SSAM model for total crashes versus total conflicts shows long increasing and decreasing runs corresponding to regions of consistent over- and underestimation [1]. In the last case, the safety performance capability of the SSAM crash–conflict model to predict real-world crashes with actual crash experience at Slovenian roundabouts falls. The occurrence of traffic conflicts also was sensitive to the site configuration and priority rules and other parameters in the microsimulation. This confirms again that the safety assessment of a road entity based on surrogate measures of safety is influenced on microscopic traffic simulation model used.

6. Conclusions

This paper addresses issues on evaluation of roundabout safety performance through surrogate safety measures from microsimulation. Roundabouts were selected since they are becoming increasingly attractive to transportation engineers, and the effectiveness of proper measures and assessment tools for road safety management is still being studied. Based on a sample of Slovenian roundabouts, surrogate safety measures were obtained through microscopic traffic simulation models; then a crash prediction model from simulated peak hour conflicts was developed.

For these purposes, the vehicle trajectories records exported from AIMSUN and VISSIM were used to estimate traffic conflicts through the SSAM. AIMSUN and VISSIM were calibrated for single-lane, double-lane, and turbo roundabouts using the corresponding empirical capacity function which included critical and follow-up headways estimated through meta-analysis. In order to bring the simulated traffic conflicts from VISSIM and AIMSUN to a comparable level, some SSAM filters were set iteratively (i.e., setting lower values of the TTC and PET than the default values, and eliminating the conflicts corresponding to a zero value of TTC and PET). The effect of different traffic scenarios on roundabout safety performance was also tested. It was noted that a different flow distribution provided a different number of conflicts at roundabouts; there was a traffic scenario that provided more (potential) crashes than other scenarios for the same roundabout category.

Once the outputs from the two microsimulation software got to a comparable level, a crash prediction model for the sample of Slovenian roundabouts was developed. Although a large number of practitioners and transportation engineers during the last decade have been using traffic microsimulation in lots of practical applications, technical literature still presents few studies which focus on the relationship between crashes and simulated traffic conflicts especially at roundabouts. This is the gap in the current literature that the paper aimed to address. A generalized linear model framework was used to estimate the prediction model based on traffic and crash data collected in the field at 26 existing roundabouts. Peak hour traffic distribution was simulated with AIMSUN, and peak hour conflicts were then estimated with the SSAM. The model was developed with crashes per year as dependent variable and peak hour conflicts and the ratio of peak hour traffic volume to average daily traffic volume and the outer diameter as independent variables. The CURE plots also showed a good quality of the fit.

Two main conclusions may be derived from the research results that are also useful for professional or other practical issues. The comparison between the surrogate measures of safety based on the simulated trajectories derived from AIMSUN and VISSIM provided insights on how to set

the SSAM settings so that the outputs from AIMSUN and VISSIM reaching a comparable level. The outcome of this first activity represented the starting point to address issues associated with the development of safety prediction models for roundabouts based on surrogate measures of safety. Although the paper does not address a model selection problem (to be solved by a data-driven method), it informs on how intersection safety can be estimated by using simulated conflicts instead of real crash data and other covariates. The coefficient estimates of the crash–conflict model based on real data were statistically significant; however, the model was quite different from the model recommended by the SSAM to identify conflicts from traffic simulation. Nevertheless, it should be noted that the results are based only on a sample of 26 roundabouts within the same country. Thus, future research efforts could be addressed to acquire further roundabout data from other sources in order to improve the statistical link between observational crashes and simulated measures of safety. Further roundabout data, together with other traffic scenarios to be tested, could improve the same reproducibility and accuracy of the simulated output, considering also a better explanation of the actual crashes.

Since the results, within the limits of this study, confirm that surrogate measures of safety strongly depend on microscopic traffic simulation model which is used, they are sufficiently encouraging to continue the line of research.

The results confirmed that the safety assessment of any road entity may rely on surrogate measures of safety, and the simulated conflicts can be used as a promising approach for roundabout safety evaluation. Fundamental design considerations should be also evaluated at a planning level to better understand potential impacts for each roundabout alternative. Designing a roundabout, indeed, requires the optimal balance between safety, operational performance, impacts, and so on, given the constraints for the site under evaluation. Future developments can interest the use of surrogate measures as a sound basis for comparing performances of alternative intersection types. Traffic microsimulation could be a valuable approach to investigate how safety and operational conditions will change when Conventional Vehicles (CVs) and autonomous vehicles (AVs) are coexisting in traffic, since the introduction of on-road autonomous vehicles (AVs) in traffic will inevitably transform the criteria for road network design, traffic modelling, and road safety management. In this view, automated road safety analysis based on reliable safety evaluation tools using surrogate safety measures can be useful to provide prompt safety estimates and to address innovative vehicle and infrastructure developments.

Data Availability

The crash data used to support the findings of this study were obtained from the Police Slovenian database and are available from the corresponding author upon request.

Conflicts of Interest

The authors declare that there are no conflicts of interest regarding the publication of this paper.

References

[1] E. Hauer, *The Art of Regression Modeling in Road Safety*, Springer International Publishing, Berlin Heidelberg, Germany, 2015.

[2] F. H. Amundsen and C. Hyden, "Proceedings from the first workshop on traffic conflicts," Oslo, Norway, 1977.

[3] T. Saleem, B. Persaud, A. Shalaby, and A. Ariza, "Can Microsimulation be used to Estimate Intersection Safety?" *Transportation Research Record*, vol. 2432, no. 1, pp. 142–148, 2018.

[4] A. Tarko, G. Davis, N. Saunier, T. Sayed, and S. Washington, *White Paper Surrogate Measures of Safety*, Transportation Research Board, Washington, DC, USA, 2009, http://citeseerx.ist.psu.edu/viewdoc/download.

[5] D. Gettman, L. Pu, T. Sayed, and S. G. Shelby, "Surrogate safety assessment model and validation: Final report No. FHWA-HRT-08-051," Tech. Rep., Springfield, the National Technical Information Service, Federal Highway Administration, 2008.

[6] "AIMSUN Dynamic Simulator User Manual. Transport Simulation System (TSS) version 8, Barcelona," 2011.

[7] "PTV VISSIM User Manual. PTV Planung Transport Verkehr AG, Karlsruhe," 2017.

[8] O. Giuffrè, A. Granà, and M. L. Tumminello, "Gap-acceptance parameters for roundabouts: a systematic review," *European Transport Research Review*, vol. 8, no. 1, pp. 1–20, 2016.

[9] M. L. Tumminello, *Calibration of Microscopic Traffic Simulation Models for Evaluating Operation and Safety Performance at Roundabouts [PhD. Thesis in Civil, Environmental and Material Engineering]*, University of Palermo, February 2018.

[10] C. Wang and N. Stamatiadis, "Surrogate safety measure for simulation-based conflict study," *Transportation Research Record*, vol. 2386, pp. 72–80, 2013.

[11] S. Cafiso, C. D'Agostino, M. Kieć, and R. Bak, "Safety assessment of passing relief lanes using microsimulation-based conflicts analysis," *Accident Analysis & Prevention*, vol. 116, pp. 94–102, 2017.

[12] J. Wang, Y. Kong, T. Fu, and J. Stipancic, "The impact of vehicle moving violations and freeway traffic flow on crash risk: An application of plugin development for microsimulation," *PLoS ONE*, vol. 12, no. 9, 2017.

[13] Y. Kuang, X. Qu, J. Weng, and A. Etemad-Shahidi, "How does the driver's perception reaction time affect the performances of crash surrogate measures?" *PLoS ONE*, vol. 10, no. 9, Article ID e0138617, 2015.

[14] F. Huang, P. Liu, H. Yu, and W. Wang, "Identifying if VISSIM simulation model and SSAM provide reasonable estimates for field measured traffic conflicts at signalized intersections," *Accident Analysis & Prevention*, vol. 50, pp. 1014–1024, 2013.

[15] M. Essa and T. Sayed, "Transferability of calibrated microsimulation model parameters for safety assessment using simulated conflicts," *Accident Analysis & Prevention*, vol. 84, pp. 41–53, 2015.

[16] L. Vasconcelos, L. Neto, Á. M. Seco, and A. B. Silva, "Validation of the surrogate safety assessment model for assessment of intersection safety," *Transportation Research Record*, vol. 2432, no. 1, pp. 1–9, 2018.

[17] A. Pratelli, P. Sechi, and R. R. Souleyrett, "Upgrading traffic circles to modern roundabouts to improve safety and efficiency – case studies from Italy," *Promet – Traffic & Transportation*, vol. 30, no. 2, pp. 217–229, 2018.

[18] A. Deluka Tibljaš, T. Giuffrè, S. Surdonja, and S. Trubia, "Introduction of autonomous vehicles: roundabouts design and safety performance evaluation," *Sustainability*, vol. 10, no. 4, pp. 1–14, 2018.

[19] G. Saulino, B. Persaud, and M. Bassani, "Calibration and application of crash prediction models for safety assessment of roundabouts based on simulated conflicts," in *Proceedings of the 94th Transportation Research Board Annual Meeting*, Washington DC, USA, 2015.

[20] H. Pilko, S. Mandžuka, and D. Barić, "Urban single-lane roundabouts: A new analytical approach using multi-criteria and simultaneous multi-objective optimization of geometry design, efficiency and safety," *Transportation Research Part C: Emerging Technologies*, vol. 80, pp. 257–271, 2017.

[21] H. Hatami and I. Aghayan, "Traffic efficiency evaluation of elliptical roundabout compared with modern and turbo roundabouts considering traffic signal control," *Promet – Traffic & Transportation*, vol. 29, no. 1, pp. 1–11, 2017.

[22] L. G. H. Fortuijn, "Turbo roundabouts: estimation of capacity," *Transportation Research Record*, vol. 2130, no. 1, pp. 83–92, 2009.

[23] O. Giuffrè, A. Granà, M. L. Tumminello, and A. Sferlazza, "Estimation of Passenger Car Equivalents for single-lane round-abouts using a microsimulation-based procedure," *Expert Systems with Applications*, vol. 79, pp. 333–347, 2017.

[24] O. Giuffrè, A. Granà, M. L. Tumminello, and A. Sferlazza, "Capacity-based calculation of passenger car equivalents using traffic simulation at double-lane roundabouts," *Simulation Modelling Practice and Theory*, vol. 81, pp. 11–30, 2018.

[25] O. Giuffrè, A. Granà, S. Marino, and F. Galatioto, "Microsimulation-based passenger car equivalents for heavy vehicles driving turbo-roundabouts," *Transport*, vol. 31, no. 2, pp. 295–303, 2016.

[26] J. Barceló, *Fundamentals of Traffic Simulation*, Springer International Publishing, London, UK, 2010.

[27] O. Hagring, "A further generalization of Tanner's formula," *Transportation Research Part B: Methodological*, vol. 32, no. 6, pp. 423–429, 1998.

[28] M. Borenstein, L. V. Hedges, J. P. T. Higgins, and H. R. Rothstein, *Introduction to Meta-Analysis*, John Wiley & Sons, Ltd, Chichester, UK, 2009.

[29] R. Mauro, *Calculation of Roundabouts*, Springer International Publishing, Berlin Heidelberg, Germany, 2010.

[30] T. Tollazzi, *Alternative Types of Roundabouts*, vol. 6, Springer International Publishing, New York, NY, USA, 2015.

[31] "Functional and geometric standards for the construction of road intersections" (Italian), Minister of Infrastructure and Transport, 2006.

[32] National Academies of Sciences, Engineering, and Medicine, *Roundabouts: An Informational Guide*, 2nd Edition, The National Academies Press, Washington, DC, USA, 2010.

[33] W. Brilon, N. Wu, and L. Bondzio, "Unsignalized Intersections in Germany. A State of the Art, 1997," in *Proceedings of the 3rd International Symposium on Intersections Without Traffic Signals*, M. Kyte, Ed., University of Idhao, 1997.

[34] D. Gettman and L. Head, "Surrogate safety measures from traffic simulation models," *Transportation Research Record*, vol. 1840, pp. 104–115, 2007.

[35] T. Giuffrè, S. Trubia, A. Canale, and B. Persaud, "Using microsimulation to evaluate safety and operational implications of newer roundabout layouts for European road networks," *Sustainability*, vol. 9, no. 11, pp. 1–13, 2017.

[36] O. Giuffrè, A. Granà, M. L. Tumminello, T. Giuffrè, and S. Trubia, "Surrogate measures of safety at roundabouts in AIMSUN and VISSIM environment," in *Roundabouts as Safe and Modern Solutions in Transport Networks and Systems, LNNS 52*, E. Macioszek et al., Ed., pp. 53–64, 2019.

[37] P. McCullagh and J. A. Nelder, *Generalized Linear Models*, Chapman & Hall, London, UK, 1989.

[38] "GenStat for Windows 17th Edition," VSN International, Hemel Hempstead, UK, 2017.

[39] D. Lord and F. Mannering, "The statistical analysis of crash-frequency data: a review and assessment of methodological alternatives," *Transportation Research Part A: Policy and Practice*, vol. 44, no. 5, pp. 291–305, 2010.

[40] M. Poch and F. Mannering, "Negative binomial analysis of intersection-accident frequencies," *Journal of Transportation Engineering*, vol. 122, no. 2, pp. 105–113, 1996.

[41] J. M. Ver Hoef and P. L. Boveng, "Quasi-poisson vs. negative binomial regression: How should we model overdispersed count data?" *Ecology*, vol. 88, no. 11, pp. 2766–2772, 2007.

[42] J. Oh, C. Lyon, S. Washington, B. Persaud, and J. Bared, "Validation of FHWA crash models for rural intersections: lessons learned," *Transportation Research Record*, vol. 1840, pp. 41–49, 2003.

Research Article

Airworthiness Support Measures Analogy to the Prospective Roundabouts Alternatives: Theoretical Aspects

Andriy Viktorovich Goncharenko [ID]

Aircraft Airworthiness Retaining Department, Academic and Research Aerospace Institute, National Aviation University,
1, Kosmonavta Komarova Avenue, Kyiv 03058, Ukraine

Correspondence should be addressed to Andriy Viktorovich Goncharenko; andygoncharenco@yahoo.com

The goal of this paper is to investigate theoretically the possible directions of some specified methods for the alternative roundabouts effectiveness modeling and optimization. The out-coming criteria have an economical interpretation. Those are the objective functionals of the alternative roundabouts effectiveness as the profit gained in the course of the traffic flow changes in the view of the integral form. This is modeled taking into consideration the transport infrastructure functioning elements such as the traffic flow of a capacity model. It takes into account two major components of the transportation services which are the alternative roundabouts business' incomes and expenses relating to the roundabouts transportation worthiness support. The prototypic approach is that one from the aircraft airworthiness support measures models. Corresponding managerial influences with respect to environmental, safety, utility, and other issues, as well as probable impacts, are modeled with the construction of the relevant under-integral expressions, equations, and appropriate coefficients and parameters of the mathematical models. The achieved theoretical results, on the basis of the Euler-Lagrange equation and accepted assumptions, have been checked for the sufficiency of the objective functional maximum presence at the "point" with the use of the conducted computer simulation. The necessary diagrams are plotted in order to illustrate the theoretical contemplations and speculations, as well as to check the correctness of the applied mathematical derivations and visualize the models' preciseness and abilities. The theoretically constructed mathematical models have a significance of the prognostic values applicability required at the alternative roundabouts effectiveness modeling and optimization ensuring their design progress and evolutions.

1. Introduction

The complexity of the modern roundabouts design, their diversities in designations, and functional, economic, and environmental criteria structures elaboration [1] are predetermining the multialternativeness of the new types of the roundabouts evaluation.

Rational economic activity is the foundation providing the development in all areas and spheres of life [2]. Therefore, theoretical researches with the help of the plausibly developed hypothetical mathematical models are of a great importance [2]; moreover, the usefulness of such models application for the alternative roundabouts effectiveness evaluations is beyond any doubts and it can be traced with the most up-to-date publications [3–15]. The brief literature survey of the presented paper just is highlighting the principal possibilities

of the proposed methods implementations in those areas of science that relate with the multiattribute assessment of road design solutions [3], geometric design of turbo roundabouts [4], or the journal paper [5] dedicated to the turbo roundabouts, design principles, and safety performance, as well as alternativeness [6] and transportation infrastructure [7] aspects.

It is also necessary to underline the importance of the developed here approach for other transportation facilities, like railway [8]; however the methods are aimed at modeling alternative roundabouts effectiveness and in its sense continue the researches of the assessment, analysis, and simulation discussed in references [9–15]. Some of those publications emphasize the evaluation of the environmental and functional benefits of "innovative" roundabouts situational

features, like [11] or the study of the vehicle speed [14] for the design of the roundabouts.

Remarkable in this context is that all the publications either directly or indirectly have dealt or might have dealt with mathematical modeling and simulation in regard to economical parameters.

One of such approaches and corresponding mathematical modeling is the objective of the presented paper.

There are numerous strategies to cope with the problems related with transportation services in general. The diversity of such strategies is stipulated by different types of transportation means, other managerial factors, including financial levers of influence.

For example, in Belgium, as that was reported by the TV news and broadcasted by the mass media, the local subway service becomes free of charge; no one will have to pay in fares, when the on-ground going vehicles' pollutant emission exceeds the accepted allowed limits.

The presented paper theoretical concept is centered upon the issues related with the support of the alternative roundabouts worthiness (vehicle worthiness, riding worthiness, transportation worthiness, etc.). The prototypic approach is adopted from the aircraft airworthiness support measures concepts of [16–20] developed from subjective analysis [21] on the basis of the Jaynes' principle [22–24] in the framework of the calculus of variations theory [25].

2. Mathematical Modeling and Developed Methods

There is an irresistible temptation to model and investigate the process of a roundabout functioning under the prism of its effectiveness. It will depend upon the number of factors; specialists, who have an extensive experience in the field of roundabouts, distinguish the most significant from them [1, 3–15]. It is proposed to consider theoretically the modeling and optimizing of a few, for example, competing roundabouts. The supposed roundabouts worthiness is deemed to be supported in an analogous to airworthiness way [16–20].

2.1. Basic Model. Every aspect of a roundabout functioning is being considered under the prism of multialternativeness, if it deals with someone's choice or individual subjective preferences distribution in regard to the achievable set of alternatives [21], on one hand. And on the other hand, there is a multi-"optionality" phenomenon when the objectively existing options of the ongoing processes are under consideration.

All the issues of a roundabout operation or exploitation relating transportation facilities, network, entire and in particular infrastructure capacity, functional and economical criteria, environmental impacts, safety and precaution means and measures are based upon operational incomes and costs analysis [2].

Profitableness of a roundabout construction along with the roundabout's design, creation, building, and management costs subtracted from the incomes ensures a good reaction of the transportation business upon the challenges of the functioning [1–15].

Herewith, it is proposed a model based upon the principle approach expressed with the following formula:

$$J = \int_{p_0}^{p_1} \left(apcc' - bpc' \right) dp. \tag{1}$$

Here, in equation (1), J is the objectives functional depending upon the variated traffic flow p within the traffic flow's possible range of alterations $[p_0 \ldots p_1]$. The under-integral function of

$$apcc' - bpc' \tag{2}$$

expresses the specific profitableness of the roundabout, reduced per a vehicle in the roundabout's varied traffic flow. In the expressions of (1) and (2), a has a meaning of the proportionality coefficient for the supposed model of the incomes formation, whereas b bears a sense of such a coefficient for the accepted costs model. The function of c takes its own role in the roundabout's operational income versus cost balance formation. For the stated problem setting, it is investigated the model constructed of the expressions of (1) and (2), being also dependent upon the first complete derivative of

$$c' = \frac{dc}{dp} = c'_p. \tag{3}$$

Mathematically, formulated in the view of the equations of (1) – (2), this particularly given problem setting is stated as the simplest problem of the calculus of variations for the objective functionals likewise [25]:

$$J = \int_{p_0}^{p_1} F\left(p, c, c'_p \right) dp, \tag{4}$$

where $F(p, c, c'_p)$ is the under-integral function of the stated problem objective functional (1).

That is,

$$F\left(p, c, c'_p \right) = apcc'_p - bpc'_p. \tag{5}$$

The purpose is to maximize the objective functional (1) on conditions of (2) and (3) by finding such function of c that delivers the wanted maximum of the profit formation; and for the general view integral of (4) there are the necessary conditions for the extremum existence in the view of the well-known Euler-Lagrange equation [25]:

$$\frac{\partial F}{\partial c} - \frac{d}{dp} \left(\frac{\partial F}{\partial c'_p} \right) = 0. \tag{6}$$

2.2. Solution to the Stated Basic Profit Optimization Problem. In previous speculations (1) – (6) framework mentioned above, the sought after solution will be next.

In accordance with the Euler-Lagrange equation (6) [25], in case of (1) – (5)

$$\frac{\partial F}{\partial c} = apc'_p. \tag{7}$$

Then, for the second member of equation (6) that condition yields

$$\frac{\partial F}{\partial c'_p} = apc - bp. \tag{8}$$

Differentiating the partial derivative of the right hand part of equation (8) for the second time with respect to the independent variable p in the complete form derivative it can be obtained that

$$\frac{d}{dp}\left(\frac{\partial F}{\partial c'_p}\right) = \frac{\partial}{\partial p}\left(\frac{\partial F}{\partial c'_p}\right)\frac{dp}{dp} + \frac{\partial}{\partial c}\left(\frac{\partial F}{\partial c'_p}\right)\frac{dc}{dp} \\ + \frac{\partial}{\partial c'_p}\left(\frac{\partial F}{\partial c'_p}\right)c''_p, \tag{9}$$

where

$$\partial c''_p = \frac{d^2 c}{dp^2}. \tag{10}$$

Thus, with taking into account the conditions written with the equations of (9) and (10), for equations (6) and (8) it yields

$$\frac{d}{dp}\left(\frac{\partial F}{\partial c'_p}\right) = ac - b + apc'_p. \tag{11}$$

Here in (11) the complete derivative (9) has got an abridged form since

$$\frac{\partial}{\partial c'_p}\left(\frac{\partial F}{\partial c'_p}\right) \equiv 0. \tag{12}$$

Hence, the second derivative (10) is omitted in the final form of the Euler-Lagrange equation (6); and equation (6) now does not depend upon the second derivative of the sought function, i.e.,

$$\frac{\partial}{\partial c'_p}\left(\frac{\partial F}{\partial c'_p}\right)c''_p \equiv 0. \tag{13}$$

Therefore, substituting the relevant expressions of (7) and (11) for their values into the equation (6), it becomes possible to rewrite it in the view of

$$apc'_p - \left(ac - b + apc'_p\right) = 0. \tag{14}$$

Finally, after cancelling the similar members in equation (14), it yields even not a differential but algebraic equation with respect to the function of c, that determines the considered model structure (1):

$$ac - b = 0. \tag{15}$$

Furthermore, the solution in the view of function c has happened to be not depending upon the independent variable p at all:

$$c = \frac{b}{a}. \tag{16}$$

2.3. Another Model a Roundabout Functioning. It is definitely the simplest model described with expressions of (1) – (5) and yielding the solution in the view of equation (16) obtained through the procedures of (6) – (16) should be checked for the suspected extremum existence since all mathematical constructions and derivations have been performed on the basis of the necessity conditions (6).

Another theoretical development of the model of (1) – (5) applicable for an alternative roundabout functioning is as the following one.

Suppose, there is a nonlinear (raised to a certain power) dependence of the profitableness function (under-integral function) of F upon the traffic flow p. Herein, it is proposed the next up modification (see and compare with the equation of (5)):

$$F\left(p, c, c'_p\right) = ap^n cc'_p - bpc'_p, \tag{17}$$

where n is the power index magnifying the impact of the traffic flow p exerted upon the component of the vehicle contribution in the traffic flow.

The theoretical solution to the objective functional similar to (1) or (4), in the framework of the approach analogous to (6) – (16), results in the other view optimal function.

However, it is obvious, in the proposed model modification expressed with the equation of (17) versus (5), the principle of the wanted solution finding will not differ from the traditional method (6).

2.4. Developed Model Solution. The substitution of the relevant interrelationship of (17) pertaining with the stated problem setting for its value into the objective functional (1) gives for members of equation (6) such formulae.

For the partial derivative with respect to the sought function, likewise (7), the expression will be in accordance with the model equation (17):

$$\frac{\partial F}{\partial c} = ap^n c'_p. \tag{18}$$

For the complete derivative, similar to (9), with respect to the independent variable, the partial derivative with respect to the complete derivative of the sought function with respect to the independent variable, in analogous way to (8), now gets the view of the following equation:

$$\frac{\partial F}{\partial c'_p} = ap^n c - bp. \tag{19}$$

In its turn the complete form derivative (9) in such case yields similar to (11)

$$\frac{d}{dp}\left(\frac{\partial F}{\partial c'_p}\right) = anp^{n-1}c - b + ap^n c'_p. \tag{20}$$

After that collecting corresponding members of equations (18) and (20) into the necessary condition Euler-Lagrange equation (6), there is a possibility to obtain the other equation than (14), i.e.,

$$ap^n c'_p - \left(anp^{n-1}c - b + ap^n c'_p\right) = 0. \tag{21}$$

Again, making obvious transformations, (21) yields the needed result as the following equation:

$$anp^{n-1}c - b = 0. \tag{22}$$

From (22) it inevitably means formula (23):

$$c = \frac{b}{anp^{n-1}} = c(p). \tag{23}$$

This time, unlike in the case resulting with the constant value of (16), the sought solution (23) of the model (17) – (23) is a certain function of the independent variable, traffic flow p: $c(p)$.

2.5. Computer Simulation and Check of the Suspected Solutions Optimality.

As the solutions in the view of equations (16) and (23) are found on just the necessary condition (6) for the extremums existence, it is required to check the solutions for being really optimal subject to the stated problem settings constraints.

The numerical data for the conducted calculation experimentation are as follows. For the basic model described with the procedures of expressions (1) – (16): $a = 2$; $b = 20$ of such Conditional Units (CU) that are correspond to the measurement units of the fractional members of the under-integral function (5) of the objective functional (1). The range of the traffic flow p alteration has been considered from $p_0 = 1$ up to $p_1 = 200$ of CU (possible unit is vehicles per an hour (v/h)). The result of such primitive, so far, experimentation is $c = 10$ CU.

In order to make sure of the optimality of the obtained function $c = 10$ value, it is possible to let the function $c = 10$ some definite variation with the fixed boundaries.

Such effect is modelled with the help of the matrix-vector data description.

The traffic flow matrix at the next three specified points is

$$\mathbf{P} = \begin{bmatrix} p_0^2 & p_0 & 1 \\ \left(\dfrac{p_0 + p_1}{2}\right)^2 & \dfrac{p_0 + p_1}{2} & 1 \\ p_1^2 & p_1 & 1 \end{bmatrix}. \tag{24}$$

The column-vector of the free function values difference is given in the view of

$$\mathbf{C} = \begin{bmatrix} 0 \\ -0.0005 \cdot c_{\text{opt}}\left(\dfrac{p_0 + p_1}{2}\right) \\ 0 \end{bmatrix}, \tag{25}$$

where $c_{\text{opt}}((p_0 + p_1)/2)$ depicts the modeled variated function interrelationships between the alternating traffic flow p in v/h and the function's optimal value of equation (16) $c_{\text{opt}} = 10$ CU in the middle of the accepted range of the traffic flow p variation.

Now, from the matrix-vector equation engaging the equations of (24) and (25)

$$\mathbf{C} = \mathbf{P} \cdot \mathbf{K}, \tag{26}$$

where

$$\mathbf{K} = \begin{bmatrix} a_1 \\ b_1 \\ c_1 \end{bmatrix}, \tag{27}$$

where a_1, b_1, and c_1 are the coefficients, in CU, converting the traffic flow values of the quadratic forms of (24) via (26) with (27) into the free function values of (25).

Solving for (27) it returns

$$\mathbf{K} = \mathbf{P}^{-1} \cdot \mathbf{C}. \tag{28}$$

And for the inverse matrix it yields

$$\mathbf{P}^{-1} = \begin{bmatrix} \dfrac{2}{39{,}601} & -\dfrac{4}{39{,}601} & \dfrac{2}{39{,}601} \\ -\dfrac{601}{39{,}601} & \dfrac{804}{39{,}601} & -\dfrac{203}{39{,}601} \\ \dfrac{40{,}200}{39{,}601} & -\dfrac{800}{39{,}601} & \dfrac{201}{39{,}601} \end{bmatrix}. \tag{29}$$

This gives

$$\mathbf{K} = \begin{bmatrix} a_1 = 5.05 \cdot 10^{-7} \\ b_1 = -1.015 \cdot 10^{-4} \\ c_1 = 1.01 \cdot 10^{-4} \end{bmatrix}. \tag{30}$$

In accordance with the expressions of the procedure of (24) – (30) the free function variations calculated by

$$c_o(p) = a_1 p^2 + b_1 p + c_1 + c_{\text{opt}}(p) \tag{31}$$

for a decreasing function variation and

$$c_O(p) = -\left(a_1 p^2 + b_1 p + c_1\right) + c_{\text{opt}}(p) \tag{32}$$

for an increasing function variation, illustrated in Figure 1, give the results shown in Figures 2 and 3.

In Figure 1 $c_{\text{opt}}(p)$ is standing for the formula (16) extremal value of the optimal function; $c_o(p)$ has been calculated by formula (31) and $c_O(p)$ by formula (32).

In Figure 2 $Z_{\text{opt}}(p)$, $Z_o(p)$, and $Z_O(p)$ are the objective functionals values plotted as a result of the calculations performed by the formula (1) with the variated upper limit of integration for the corresponding determining functions of $c_{\text{opt}}(p)$ by the formula (16): extremal value of the optimal function; $c_o(p)$ by formula (31); $c_O(p)$ by formula (32).

And in Figure 3 the corresponding objective functionals values are plotted for the marginal traffic flow value $p_1 = 200$ v/h.

The nonlinear no constant model (17) – (23) numerical investigation is illustrated in Figures 4–6.

The optimal solution now is being calculated by the extremal formula of (23) and it has been variated in the style of the one described with the expression of (24) – (32).

FIGURE 1: Free function variations for the traffic flow in comparison with the extremal solution (optimal function).

FIGURE 2: Objective functional value.

FIGURE 3: Objective functional value at the final boundary.
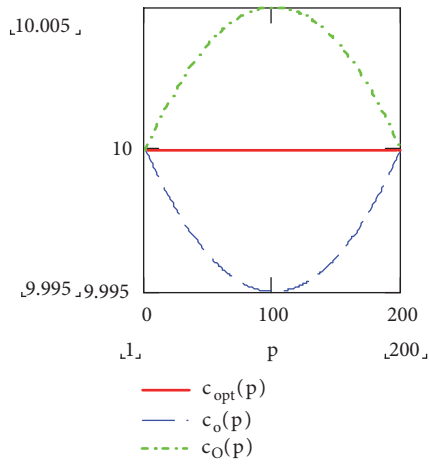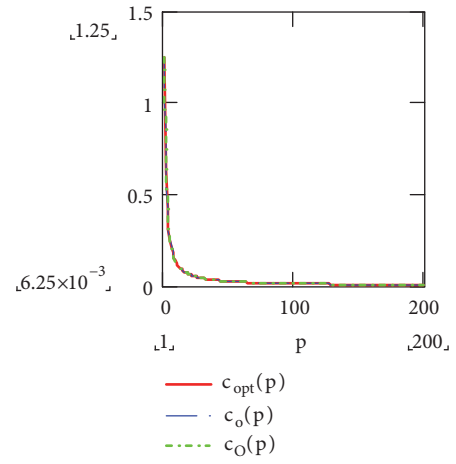

FIGURE 4: Free function variations for the traffic flow in comparison with the extremal solution (optimal function).
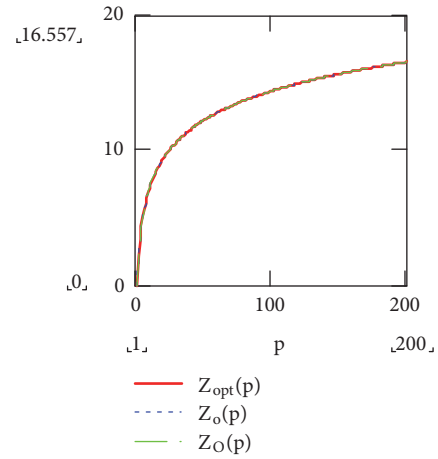
FIGURE 5: Objective functional value.
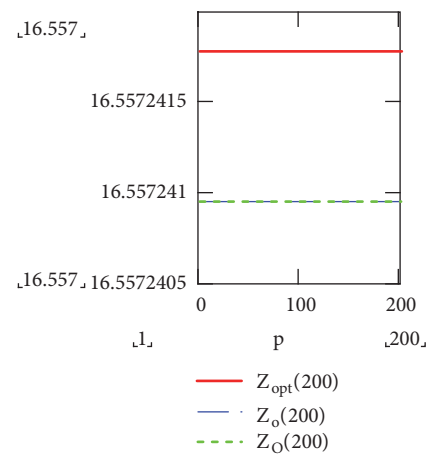
FIGURE 6: Objective functional value at the final boundary.

$c_o(p) =$

	0
0	1.25
1	0.624999876
2	0.416666419
3	0.312499631
4	0.24999951

$c_{opt}(p) =$

	0
0	1.25
1	0.625
2	0.416666667
3	0.3125
4	0.25

$c_O(p) =$

	0
0	1.25
1	0.625000124
2	0.416666914
3	0.312500369
4	0.25000049

$c_o(p) =$

	0
195	$6.377061058 \cdot 10^{-3}$
196	$6.344808309 \cdot 10^{-3}$
197	$6.31288382 \cdot 10^{-3}$
198	$6.28128266 \cdot 10^{-3}$
199	$6.25 \cdot 10^{-3}$

$c_{opt}(p) =$

	0
195	$6.37755102 \cdot 10^{-3}$
196	$6.345177665 \cdot 10^{-3}$
197	$6.313131313 \cdot 10^{-3}$
198	$6.281407035 \cdot 10^{-3}$
199	$6.25 \cdot 10^{-3}$

$c_O(p) =$

	0
195	$6.378040982 \cdot 10^{-3}$
196	$6.345547021 \cdot 10^{-3}$
197	$6.313378807 \cdot 10^{-3}$
198	$6.28153141 \cdot 10^{-3}$
199	$6.25 \cdot 10^{-3}$

FIGURE 7: Initial and final values of the variated determining free function.

The difference is for the accepted in the computerized numerical experimentations vector solution (30), which makes

$$\mathbf{K} = \begin{bmatrix} a_1 = 6.282 \cdot 10^{-10} \\ b_1 = -1.263 \cdot 10^{-7} \\ c_1 = 1.256 \cdot 10^{-7} \end{bmatrix}. \qquad (33)$$

3. Results and Discussion

3.1. Analysis of the Obtained Results. The obtained theoretical results represented with the diagrams shown in Figures 1–6 brightly distinguish the described above two variants of the roundabouts functional strategies.

The maximal value of the objective functional is clearly seen in Figures 2 and 3 for the basic case (1) – (16) simulated with the procedures (24) – (32).

For a more complicated case study (17) – (23) calculated with (24) – (29) and (31) – (33) the effect of the maximization is hardly noticeable (see Figure 5) because of the tiny variations of the determining function values of $c_{opt}(p)$: found with the use of the extremal solution equation (23) (see Figure 4).

Nevertheless, even such negligibly small variations as proposed herewith prove the maximum value deliverance to the objective functional (1) with the under-integral function (17) and corresponding extremal (23) (see Figure 6).

3.2. Discussion. Theoretically, the obtained results are for a rather simple modeling. Nonetheless, the principle is fundamental: the profit is the difference between the incomes and costs of any object (including roundabouts) functioning. And the amount of the profit provides all necessary factors, which are numerous, with their implementation procedures and further outcomes.

The other fact of the simplifications accepted at the modeling is that the problem setting is stated for the fixed boundaries calculus of variations problem.

It is perfectly visible in Figure 1. This approach is applied in the (17) – (23) model too. To make a proof for such statement a couple of the fragmental parts pieces of the calculation tables are presented in Figure 7.

Moreover, all the theoretically considered factors [1–15] have a subjective analysis [21], based upon [22–24], component worth of being studied as a developmental idea of [16–20].

4. Conclusions

The theoretical concepts case study, analyzed in this paper on the alternative roundabouts worthiness in the way analogous to the aircraft airworthiness supporting measures effectiveness research, proves that the described calculus of variations approach allows obtaining the objectively existing optimal values of the operational (functioning) purpose functional with the help of the specially introduced determining functions.

Conditions of multialternativeness for the considered theoretically different types of the roundabouts are embodied with the corresponding parameters of the proposed models. The conditions of uncertainty related with the roundabouts alternatives can be taken into account with the subjective entropy of the individuals' preferences functions optimal distributions.

The preferences functions give the possibility of the considered alternative roundabouts assessment with respect to the preferences entropy uncertainty measure, which should be a part of the further research dedicated to the theory of subjective analysis since it would be useful to find more theoretical results and applicable areas as well as some other effectiveness functions and their variables.

Data Availability

The data used to support the findings of this study are included within the article.

Conflicts of Interest

The author declares that there is no conflict of interests regarding the publication of this paper.

References

[1] T. Tollazzi, G. Tesoriere, M. Guerrieri, and T. Campisi, "Environmental, functional and economic criteria for comparing "target roundabouts" with one- or two-level roundabout intersections," *Transportation Research Part D: Transport and Environment*, vol. 34, pp. 330–344, 2015.

[2] E. Silberberg and W. Suen, *The Structure of Economics. A Mathematical Analysis*, McGraw-Hill Higher Education, 2001.

[3] E. K. Zavadskas, "Multi-attribute assessment of road design solutions by using the COPRAS method," *The Baltic Journal of Road and Bridge Engineering*, vol. 2, no. 4, pp. 195–203, 2007.

[4] T. Džambas, S. Ahac, and V. Dragčević, "Geometric design of turbo roundabouts," *Tehnički vjesnik*, vol. 24, no. 1, pp. 309–318, 2017.

[5] L. G. H. Fortuijn, "Turbo roundabouts: Design principles and safety performance," *Journal of the Transportation Research Board*, vol. 2096, no. 1, pp. 16–24, 2009.

[6] J. C. Engelsman and M. Uken, "Turbo roundabouts as an alternative to two lane roundabouts," in *Proceedings of the 26th Annual Southern African Transport Conference, SATC '07*, pp. 581–589, Pretoria, South Africa, 2007.

[7] Z. Tesoriere, "Infrastructure as interface: Thinking the urban and the high-speed railway station: Italian case-studies," *Spaces & Flows: An International Journal of Urban & Extra Urban Studies*, vol. 3, no. 1, pp. 71–87, 2013.

[8] A. Cazzani, M. Cattani, R. Mauro, and F. Stochino, "A simplified model for railway catenary wire dynamics," *European Journal of Environmental and Civil Engineering*, vol. 21, no. 7-8, pp. 936–959, 2017.

[9] O. Giuffrè, A. Granà, and S. Marino, "Comparing performances of turbo-roundabouts and double-lane roundabouts," *Modern Applied Science*, vol. 6, no. 10, pp. 70–79, 2012.

[10] A. B. Silva, P. Mariano, and J. P. Silva, "Performance Assessment of Turbo-roundabouts in Corridors," *Transportation Research Procedia*, vol. 10, pp. 124–133, 2015.

[11] M. Guerrieri, F. Corriere, B. Lo Casto, and G. Rizzo, "A model for evaluating the environmental and functional benefits of "innovative" roundabouts," *Transportation Research Part D: Transport and Environment*, vol. 39, pp. 1–16, 2015.

[12] L. Vasconcelos, A. Silva, Á. Seco, P. Fernandes, and M. Coelho, "Turboroundabouts: multicriterion assessment of intersection capacity, safety, and emissions," *Transportation Research Record: Journal of the Transportation Research Board*, vol. 2402, pp. 28–37, 2014.

[13] D. Ticali and F. Corriere, "Turbo roundabouts: geometric design parameters and performance analysis," *GSTF Journal on Computing (JoC)*, vol. 2, no. 1, pp. 227–232, 2012.

[14] H. Pilko, D. Brčić, and N. Šubić, "Study of vehicle speed in the design of roundabouts," *Građevinar- Journal of the Croatian Association of Civil Engineers*, vol. 66, no. 5, pp. 407–416, 2014.

[15] J. Chalmovský, J. Štefaňák, L. Miča et al., "Statistical-numerical analysis for pullout tests of ground anchors," *The Baltic Journal of Road and Bridge Engineering*, vol. 12, no. 3, pp. 145–153, 2017.

[16] A. V. Goncharenko, "Aeronautical and aerospace material and structural damages to failures: theoretical concepts," *International Journal of Aerospace Engineering*, vol. 2018, Article ID 4126085, 7 pages, 2018.

[17] A. V. Goncharenko, "Multi-optional hybrid effectiveness functions optimality doctrine for maintenance purposes," in *Proceedings of the 2018 IEEE 14th International Conference on Advanced Trends in Radioelecrtronics, Telecommunications and Computer Engineering (TCSET '18)*, pp. 771–775, IEEE, Lviv-Slavske, Ukraine, 2018.

[18] A. Goncharenko, "Aircraft operation depending upon the uncertainty of maintenance alternatives," *Aviation*, vol. 21, no. 4, pp. 126–131, 2017.

[19] A. V. Goncharenko, "Optimal UAV maintenance periodicity obtained on the multi-optional basis," in *Proceedings of the 2017 IEEE 4th International Conference Actual Problems of Unmanned Aerial Vehicles Developments (APUAVD '17)*, pp. 65–68, IEEE, Kiev, Ukraine, 2017.

[20] A. Goncharenko, "Several models of artificial intelligence elements for airctaft control," in *Proceedings of the 2016 IEEE 4th International Conference on Methods and Systems of Navigation and Motion Control (MSNMC '16)*, pp. 224–227, IEEE, Kiev, Ukraine, 2016.

[21] V. Kasianov, *Subjective Entropy of Preferences. Subjective Analysis: Monograph*, Institute of Aviation, Warsaw, Poland, 2013, http://kasianovv.wixsite.com/entropyofpreferences.

[22] E. T. Jaynes, "Information theory and statistical mechanics," *Physical Review A: Atomic, Molecular and Optical Physics*, vol. 106, pp. 620–630, 1957.

[23] E. T. Jaynes, "Information theory and statistical mechanics II," *Physical Review A: Atomic, Molecular and Optical Physics*, vol. 108, pp. 171–190, 1957.

[24] E. T. Jaynes, "On The Rationale of Maximum-Entropy Methods," *Proceedings of the IEEE*, vol. 70, no. 9, pp. 939–952, 1982.

[25] I. M. Gelfand and S. V. Fomin, *Calculus of Variations*, State Publishing House of Physical and Mathematical Literature, Moscow, Russia, 1961.

Research Article

An Investigation of the Safety Performance of Roundabouts in Korea Based on a Random Parameters Count Model

Minho Park [ID],[1] **Dongmin Lee** [ID],[2] **and Je-Jin Park**[3]

[1]*Ph.D., Transportation & Logistics Research Division, Incheon Institute, Incheon, Republic of Korea*
[2]*Associate Professor, Department of Transportation Engineering, University of Seoul, Seoul, Republic of Korea*
[3]*Ph.D., Transportation Research Division, Research Institute, Korea Expressway Corporation, Gyeonggi-Do, Republic of Korea*

Correspondence should be addressed to Dongmin Lee; dmlee@uos.ac.kr

It is well known that a roundabout is an efficient and safe intersection. However, the safety is generally influenced by the given various conditions. This study analyzed the effects of the geometric and traffic flow conditions on traffic accident frequency at roundabouts, constructed in Korea since 2010. Many previous studies have investigated the efficiency and safety effects of roundabout installation. However, not many studies have analyzed the specific influences of individual geometric elements and traffic flow conditions of roundabouts. Accordingly, this study analyzed the effects of various influencing variables on traffic accident frequency based on a random parameter count model using traffic accident data in 199 roundabouts. Using random parameters that can take into account unobserved heterogeneity, this study tried to make up for the weakness of the fixed parameters model, which constrains estimated parameters to be fixed across all observations. A total of eight variables were determined to be the main influencing factors on traffic accident frequency including the number and width of entry lanes, the presence of pedestrian crossings, the width of the circulatory lanes, the presence of central islands, the radius and number of entry lanes, and traffic volume influence accident frequency. Based on the study results, safer roundabout design and more efficient roundabout operation are expected.

1. Introduction

A (modern) roundabout is a circular intersection in which traffic travels circulating around a central island and the entering traffic must yield to circulating traffic. This roundabout was developed in the United Kingdom to resolve problems associated with traffic circles [1]. Changes of the driving rule to enter the circulatory lanes enabled the success of the modern type of a roundabout. The changed driving rule at a roundabout is that entering traffic must yield to circulating traffic. Through this driving rule change, the operation and safety of roundabouts have improved compared to signalized intersections as well as rotaries.

Some previous studies explained that roundabouts can improve efficiency and safety performance comparing other type of intersections and, more specifically, roundabouts can reduce conflict points at intersections and accident severity significantly [1–6]. However, roundabouts perform better than signalized intersections only for intermediate traffic demands and, for high traffic demands, signalized intersections generally perform better than roundabouts [7]. Furthermore, researches have shown that if existing signalized intersections are changed to roundabouts, the traffic accident frequency and severity can be reduced [8–14].

As other country experience, 484 roundabouts have been built since 2010 in Korea and great safety and efficiency effects have been made. And there were some studies to investigate those effects of roundabout constructions. However, some studies were conducted based on only a simple comparison of accident occurrences between before and after the installation of roundabouts. And there were only few studies to investigate the influence factors for roundabout safety in Korea.

Thus, this study was conducted to analyze the effects of the geometrics of roundabouts and traffic volumes on the traffic accident frequency at the 199 roundabouts in Korea. For this analysis, a random parameters model was used to consider heterogeneity that can occur in the data

Table 1: Number of roundabouts constructed since 2010 in Korea.

Year	2010	2011	2012	2013	2014	2015	2016	2017	Total
# of Roundabouts	87	97	85	96	54	24	18	23	484

Table 2: Accident reduction effects of roundabout construction.

Before/After Roundabouts	Average Annual Crashes				
	Total	Fatality	Severe Injury	Injury	Minor Injury
Before	571	15	258	274	24
After	308	5	118	171	14
%	-46.1%	-66.7%	-54.3%	-37.6%	-41.7%

Source: [15] Korean Roundabout Research Center (http://www.roundabout.or.kr/).

collection and unobserved heterogeneity of traffic accident data instead of a traditional count model. Through the regular count data model for traffic accident frequency used in most of previous studies can be developed based on assumption that influence of each variable is fixed and homogenous. In other words, the influence is not changeable in the data and model development. However, in real, the possibility of heterogeneity in them always exists, and this heterogeneity problem can reduce the contribution and precise of the traffic accident frequency models.

2. Literature Review

2.1. Roundabout Construction Projects in Korea. Even though there have been many suggestions from transportation experts to apply roundabouts in Korea since 2000, the construction of roundabouts began just in 2010. In many other countries, roundabouts have been implemented based on engineers' recommendations regarding alternative designs and operation methods of intersections. However, in Korea, a roundabout application project was conducted by leading federal governments, typically the Presidential Council on National Competitiveness. The roundabout construction projects by the Presidential Council on National Competitiveness were developed and accomplished by several government organizations including the Ministry of Land, Transport, and Maritime Affairs; the Ministry of Public Administration and Security; National Police Agency; and some research institutes [16].

Through this roundabout projects, there have been more than 480 roundabouts constructed in Korea with federal government subsidies since 2010 and it brought many positive impacts on intersection operation and safety. There were more than 80 roundabouts constructed every year between 2010 and 2013; after 2013, the number of roundabouts constructed with federal government subsides decreased every year, as shown in Table 1. However, there were many roundabouts constructed by local government budgets, which are not included in the Table 1. Overall, there have been observed reductions of the total numbers of crashes and fatalities of 46.1% and 66.7%, respectively, as shown in Table 2. This crash reduction of roundabouts in Korea is consistent with international observations, as shown in Table 3. United States is a country that started to apply a roundabout relatively late

but has applied greatly a roundabout in recent. In 1990, there were only two roundabouts in the United Stated; however until 2016, about 3,200 roundabouts have been built and operated [17]. Typically, roundabouts in Minnesota have had over an 80% reduction in fatal and serious injury crashes. A 69% and an 83% reduction in the right angle crash rate and in the left turning crash rate, respectively, at intersections where Single Lane Roundabout have been installed [18]. The safety benefit was analyzed in view of economic saving in Pennsylvania. Through a before-after analysis with data from the fourteen intersections, they concluded that there was $35.6 million saving that include economic costs to society and the impact on driver's quality of life [19].

2.2. Previous Studies Regarding the Influences of Geometric Elements on Roundabout Safety. The safety performance of roundabouts has been mainly discussed based on the influences of geometric elements on roundabout safety including the number of circulatory lanes, inscribed circle diameter, the number of legs, AADT, entry width, angle between legs, splitter island width, and intersection sight distance. In general, the crash frequency increases as the inscribed circle diameter, the amount of vehicles entering the roundabout, and the number of legs to the roundabout increase [12]. Maycock and Hall observed a linear relationship between entry width and entering circulating crashes using statistical modeling [20]. For US roundabouts, it was also found that entry width has a direct relationship with entering-circulating crashes. However, this study concluded that there was no significant relationship between the number of entry lanes and entering-circulating crashes as entry width increases in the United States. Kamla and his coresearchers applied random parameters model to investigate geometric and traffic characteristics on accident frequency at roundabouts in the United Kingdom. They used data from 70 roundabouts. In random-parameter results, some variables were significant in the random parameter model including approach traffic rates, truck percentage, inscribed circle diameter, number of lanes, and presence of traffic signals. However, because only two variables for geometric conditions were included in their study, it is limited to explain influence of various geometric condition factors on traffic accident occurrence [21].

Meanwhile, there are some studies to investigate roundabout geometric characteristics and cycling safety. A VTI

TABLE 3: Mean crash reductions in various countries.

Country	Mean Reductions (%)	
	All Crashes	Injury Crashes
Australia	41-61%	45-87%
France	-	57-78%
Germany	36%	-
Netherlands	47%	-
United Kingdom	-	25-39%
United States	35%	76%

Source: [1] NCHRP Report 672, Roundabouts: An Informational Guide, p 5-16.

study summarized roundabout geometric characteristics influencing on cycling safety based on literature reviews including number of circulatory lanes, entry/exit number of lanes, number of legs and deflection angle, refuge and central island characteristics, and geographic location such as urban and rural areas [22].

There were Korean studies to analyze safety effects of driving environments in roundabouts. Park analyzed the relationship between traffic accident types and geometric conditions on roundabouts from 40 roundabouts, and he developed an accident frequency model using a negative binomial model [23]. Since he used accident data collected from 9 roundabouts in Korea, and 31 roundabouts in other countries, his model did not consider variety of driving environments of different countries. There was another study to investigate the influence of roundabout geometric and traffic conditions on traffic accident frequency. Na and Park developed traffic accident frequency model based on a Zero-Inflated negative binomial modeling method using 94 roundabouts [24]. However in these roundabouts used in the study, some were the (modern typed) roundabouts but others were the rotaries. Therefore the results from this study could not explain the real influence of geometric and traffic conditions in the roundabout. Kim investigated influencing factors of roundabout geometrics on accidents using the Classification and Regression Tree(CART) method [25]. She found that wider circulatory land width caused more accidents in roundabouts. Kim and Choi investigated crash data at roundabouts in order to identify the major factors influencing such events in South Korea [26]. They developed a crash prediction model using a negative binomial distribution with various independent variables including the number of approaches, number of entering lanes, entry width, flare width, number of circulating lanes, and circulating lane width. The data used for modeling in their study were collected from 14 roundabouts in Korea and 31 in other countries. Furthermore, some of 14 roundabouts in the data were operated as a rotary system not a roundabout. Therefore, their study result might be biased and mixed results between a roundabout and rotary as well as between Korea and other countries.

2.3. Previous Studies to Develop Traffic Accident Models Using Common Methods and RRPM. Random parameters modeling for count data such as accident frequencies is a recent development in the traffic safety field. Before applying random parameters, fixed parameters were a common method to model with count data. However, the major limitation of modeling with fixed parameters is that they cannot incorporate segment-specific or time variation effects, and this limitation called as a unobserved heterogeneity problem results in underestimation of the standard errors of coefficients. To find a solution to this unobserved heterogeneity, a count model with random parameters was introduced. Anastasopolus and Mannering used a random parameter negative binomial model to account for heterogeneity that could arise from road geometrics, traffic characteristics, driver behavior, pavement condition, vehicle type, and other unobserved factors [27]. Venkataraman and his coresearchers proposed the use of a random parameter negative binomial model to take into consideration the segment-specific insight into crash frequencies for the analysis of nine years of crash data on interstate highways in Washington, USA [28]. In many other studies [28, 29], the authors determined that some variables vary across observations, and considering random parameters is an alternative solution to solve the unobserved heterogeneity problem.

3. Methods

3.1. Random Parameters Count Model. Generally, count data modeling is used for accident frequency prediction models where the accident frequency is not continuous and is a non-negative integer value in nature. In this regard, Poisson and negative binomial models are the main methods employed to develop prediction models for count data [30]. For the basic framework of the Poisson model, the probability $P(y_i)$ of a roundabout i having y_i accidents is presented in

$$P(y_i) = \frac{\exp(-\lambda_i)\lambda_i^{y_i}}{y_i!} \tag{1}$$

where λ_i is the Poisson parameter for the roundabout i (equal to i's expected number of accidents, $E(y_i)$).

The Poisson model specifies the parameter of the expected number of accidents (λ_i) as a function of independent variables (in this study, geometrics and traffic characteristics) using the log-linear function shown in

$$\lambda_i = \exp(\beta X_i) \tag{2}$$

where X_i refers to a vector of independent variables and $\boldsymbol{\beta}$ is a vector of estimable parameters.

However, the Poisson model may not always be appropriate to analyze the accident frequency because the Poisson distribution constrains the variance and the mean to be equal ($\mathrm{E}(n_i)=\mathrm{Var}(n_i)$). If this constraint is violated, the data can be considered to be under-dispersed ($\mathrm{E}(n_i)>\mathrm{Var}(n_i)$) or overdispersed ($\mathrm{E}(n_i)<\mathrm{Var}(n_i)$), which results in incorrect and inconsistent inferences [27, 31]. In addition, most accident frequency data have been shown to have overdispersed characteristics, for which the Poisson model is not suitable [32, 33].

To account for the possibility of either underdispersion or overdispersion, the negative binomial model is derived by way of an errors structure as follows:

$$\lambda_i = \exp\left(\boldsymbol{\beta X_i} + \varepsilon_i\right) \tag{3}$$

where $\exp(\varepsilon_{ij})$ is a Gamma-distributed error term with mean 1 and variance α.

The addition of this term allows the variance to vary from the mean as follows:

$$\mathrm{Var}\left[n_{ij}\right] = E\left[n_{ij}\right]\left[1 + \alpha E\left[n_{ij}\right]\right] = E\left[n_{ij}\right] + \alpha E\left[n_{ij}\right]^2 \tag{4}$$

Thus, by integrating the error structure, the negative binomial probability density function has the following form:

$$
\begin{aligned}
&P\left(n_{ij} \mid \lambda_{ij}, \alpha\right) \\
&= \frac{\Gamma\left((1/\alpha) + n_{ij}\right)}{\Gamma\left(1/\alpha\right) n_{ij}!} \left(\frac{1/\alpha}{(1/\alpha) + \lambda_{ij}}\right)^{1/\alpha} \left(\frac{\lambda_{ij}}{(1/\alpha) + \lambda_{ij}}\right)^{n_{ij}} \quad (5)
\end{aligned}
$$

where $\Gamma(.)$ refers to a gamma function.

Here, the negative binomial model is an expanded model of the Poisson model as the dispersion parameter (α) is not close to 0, which means that the dispersion parameter is not statistically significantly different than 0.

This is the traditional Poisson and negative binomial model structure, which assumes that parameters are fixed across observations (in this study, the roundabout). To account for heterogeneity that may vary across observations, random parameters in count models can be considered [34]. The estimable parameters are expressed as

$$\beta_i = \beta + \varphi_i \tag{6}$$

where φ_i refers to a randomly distributed term($\lambda_i \mid \varphi_i = \exp(\boldsymbol{\beta}_i\boldsymbol{X}_i)$ in the Poisson model and $\lambda_i \mid \varphi_i = \exp(\boldsymbol{\beta}_i\boldsymbol{X}_i+\varepsilon_i)$ in the negative binomial regression model for each roundabout i.

In addition, normal, log-normal, uniform, and other functional forms can be considered as potential density functions for random parameter estimations. The log likelihood with this random parameter can be written as follows:

$$\mathrm{LL} = \sum_{\forall i} \ln \int_{\varphi_i} \mathrm{g}\left(\varphi_i\right) P\left(n_i \mid \varphi_i\right) d\varphi_i \tag{7}$$

where $\mathrm{g}(\bullet)$ refers to the probability density function of φ_i.

Because the numerical integration of the count model with a random parameter distribution is computationally cumbersome, a simulation-based maximum likelihood method is used to maximize the simulated log-likelihood function. To estimate empirical parameters, Halton designed a potential method that was shown to provide a more efficient distribution of draws for numerical integration than random draws [35, 36]

With estimated coefficients of the parameter, the true effect of each independent variable on the dependent variable can be estimated by elasticity and a marginal effect based on the characteristics of the variable. Elasticity is the percentage change in every accident frequency due to a one percent change in the independent variable as follows:

$$E_{x_{ik}}^{\lambda_i} = \frac{\partial \lambda_i}{\lambda_i} \times \frac{x_{ik}}{\partial x_{ik}} \tag{8}$$

Equation (8) shows the elasticity of accident frequency with respect to the kth independent variable for section i.

The elasticity shown in (8) is only valid for continuous variables that do not take on a dummy variable. Another way to interpret the effect of an independent variable is the marginal effect, which reflects the effect of a "one unit" change of an independent variable on the dependent variable, calculated as the partial derivative $\partial \lambda_i/\partial x_{ik}$. It is similar to the elasticity mentioned above except estimating the effect of a change on the dependent variable with 1% change in X on the dependent variable(Y). It measures the effect of a "one unit" change in X on the dependent variable. In addition, although marginal effects are generated by each roundabouts, averages over the roundabout population will be presented.

4. Study Results

4.1. Data Description. A total of 199 roundabouts were utilized to construct the traffic accident frequency model that can be applied with the random parameters count model. The main variables used to develop the model were, region types(urban and rural area), type of intersection (three-way, four-way, or five-way), the curvature radius for each entry lane, the number of lanes, width of the entry lane to the roundabouts, lane width at the exit lane, presence of pedestrian crosswalks, distance between the yield line and pedestrian crosswalk, presence of a central island, presence of a vertical grade, channelization, traffic volumes, inscribed circle diameter, diameter of the central island, number of circulatory lanes, and width of circulatory lanes. All data regarding the geometric elements were obtained through field surveys. Data from the Traffic Accident Analysis System (TAAS) operated by the Korea Road Traffic Authority was utilized to collect the total number of traffic accidents from 2013 to 2015 and traffic volumes in the roundabout design stage.

Table 4 explains the descriptions of the key variables used in building the model via a random parameters negative binomial. The collected data show that urban areas (68%) have more roundabouts than rural areas (32%), and the most common roundabout type is the 4-legged roundabout (51%),

TABLE 4: Descriptive statistics of the variables.

Variable Description	Mean	Standard Deviation	Min.	Max
Region (urban: 1; rural: 0)	0.683	0.466	0	1
3-legged roundabout	0.357	0.480	0	1
4-legged roundabout	0.513	0.501	0	1
5-legged roundabout	0.131	0.338	0	1
Average radius of the entry lane (m)	20.872	12.121	5.5	98.75
Lane number of the entry/exit lane	1.170	0.395	1	3.2
Average lane width of the entry lane (m)	4.319	1.022	3	10.9
Average lane width of the exit lane (m)	4.556	1.068	2	10.1
Pedestrian crosswalk (yes: 1; otherwise: 0)	0.769	0.423	0	1
Distance between the stop line and pedestrian crosswalk	9.26	6.62	0	21
Central island (yes: 1; otherwise: 0)	0.950	0.219	0	1
Vertical grade (yes: 1; otherwise: 0)	0.412	0.493	0	1
Exclusive right turn lane (yes: 1; otherwise: 0)	0.231	0.423	0	1
Number of accidents per year	2.553	4.384	0	37
Logarithm of AADT	9.123	8.852	4.60	10.54
Diameter of the roundabout (m)	31.148	8.335	9	80
Diameter of the central island (m)	17.380	6.150	3	40
Number of circulatory lanes in the roundabout	1.116	0.336	1	3
Width of the circulatory lanes in roundabouts (m)	5.151	0.564	3.8	7

followed by 3-legged (36%) and 5-legged (13%) roundabouts. The curvature radius for each entry lane is 21 meter on average, the number of entry lanes is 1.2 lanes, the width of the entry lanes is 4.3 meter, and the width of the exit lanes is 4.6 m. A pedestrian crosswalk is installed in 77% of roundabouts, and a central island is installed in most roundabouts (95%). In total, 41% of the roundabouts contained a vertical grade, and an exclusive right turn lane to separate traffic volume is included at 23% of the roundabouts. The average number of traffic accidents is 2.5 annually, and the average of AADTs is 9,200 vehicle per year. The mean diameter of the roundabouts is 31 meter, and the mean diameter of the central islands is 17 meter. The average number of circulatory lanes in the roundabouts is one, and the average width of the circulatory lanes in the roundabouts is 5 meter. Using those variables, the factors that influence traffic accidents at roundabouts and their effects were analyzed in this study.

4.2. Model Development. Models of the traffic accident frequencies at roundabouts were developed using the random parameters negative binomial model, as shown in Table 5. The parameters in statistical models can work as fixed parameters or random parameters based on their basic characteristics. The statistical model showed improvement over the baseline fixed parameters negative binomial model, with an improvement in likelihood from -1,123.89 to -382.82. The overdispersion parameter is statistically significant, which

indicates that the negative binomial model is more suitable than the Poisson model.

Whether a used parameter is random or fixed can be determined by the derived standard deviation for each parameter. In the case that the standard of deviation of the parameter density is statistically significant under 95% confidence level, the corresponding parameter is random. On the other hand, if the standard deviation of parameter density is not statistically significant, the parameter is considered fixed across the population. Through the analysis, a total of eight parameters was found to be statistically significant under 95% confidence level with regard to traffic accident frequency at roundabouts. Among them, four variables including the traffic volume, the average lane width of the entry lane, the presence of a central island, and the width of the circulatory lanes were fixed, while the other four variables including the radius of the entry lane, the number of approach/exit lanes, the presence of a crosswalk, and the presence of a vertical grade were determined to be random. For variables with random parameters, various distribution forms, normal, lognormal, uniform, and other distributions, were considered, but the normal distribution showed the highest statistical significance. Table 6 presents marginal effects and elasticity values, which explain the degree of the effect on traffic accident frequency for each parameter.

The interpretation of the parameters' effects on accident frequencies at roundabout begins with the analysis of fixed

TABLE 5: Estimation results of roundabout accident frequencies in Korea.

Variable	Constant Parameter		Random Parameter				
	Mean	t-statistic	Distribution	Mean	t-statistic	Standard Deviation	t-statistic
Constant	-1.82	-1.41		n.a			
Exposure							
Logarithm of AADT	0.23	2.51		n.a			
Geometrics							
Average width of entry lane (m)	0.16	1.96		n.a			
Presence of Central island	1.00	2.29		n.a			
Width of circle lanes(m)	-0.29	-1.93		n.a			
Radius of entry lanes(m)	n.a		normal	-0.04	-4.94	0.02	5.13
number of entry lanes	n.a		normal	0.14	3.34	0.07	4.4
Presence of Pedestrian crosswalk	n.a		normal	0.65	2.61	0.17	1.98
Vertical grade	n.a		normal	-0.63	-3.49	0.62	4.26
Scale Parameter for overdispersion	1.58	4.7					
Number of observations				199			
Log likelihood at convergence of RPNB model				-382.82			
Log likelihood with constant only				-1,123.89			

n.a: not applicable.

TABLE 6: Average marginal effects and elasticities for random parameter negative binomial models.

Variable	Marginal effect	Elasticity
Logarithm of AADT	0.34	0.23
Width of entry/exit lanes	0.24	0.70
Central island (yes: 1; otherwise: 0)	1.49	0.63
Width of the circle lanes in the roundabout (m)	-0.44	-1.54
Radius of the entry lanes (m)	-0.06	-0.87
Number of approach/exit lanes	0.21	0.16
Pedestrian crosswalk (yes: 1; otherwise: 0)	0.97	0.48
Vertical grade (yes: 1; otherwise: 0)	-0.93	-0.88

parameters. As can be seen in the estimation results, four variables were found to have fixed parameters. First, the logarithm of the AADT variable is positive, and it means that, as the AADT increases, the number of traffic accidents increases. This is a consistent result with other previous studies in which traffic accidents increase as the exposure rate increases. In terms of the elasticity viewpoint, an increase in traffic volume by 1% increases traffic accidents by 0.23%. The average width of the entry lane had a positive impact on crash frequency. This result implies that the vehicle speed usually increases with a wide lane, and the traffic accidents can occur more frequently at roundabouts due to difficulty of yield to circulating vehicles. To reduce the accident frequency and severity, geometry to force slow speed for entry vehicles should be considered. A central island is the generally raised area in the center of a roundabout around which traffic circulates, and it affects the increasing traffic accident frequency. A central island can be an obstacle to drivers due

to inexperienced driving skills and out of control vehicles due to too high speed. The last variable as a fixed parameter is the width of the circulatory lanes in the roundabout. This variable affects the decrease of vehicle accidents. Wider circulatory lanes make too high speed on circulatory lanes, and this too high speed causes traffic accident with entry vehicles due to aggressive gap acceptance decision at entry lanes.

Meanwhile, variables that have random parameters are as follows: the radius of entry lanes, the number of entry lanes, the presence of pedestrian crosswalk, and vertical grade. The radius of the entry lane affects the decrease in likelihood of traffic accidents. The radius of the approach lane has a normally distributed random parameter with a mean of -0.04 and a standard deviation of 0.02. Given these distributional parameters, 97.72% of roundabouts show a decrease in accident frequencies and 2.28% of roundabouts show an increase in accident frequencies as the radius of the approach lane increases. As a result, proper design combination of the radius and width of the entry lane mentioned above is needed for increasing safety.

The number of approach and exit lanes affects traffic accidents positively with a normal distribution having a mean of 0.14 and a standard deviation of 0.07. This result indicates that, as the number of approach and exit lanes increases, the traffic accident frequency also increases at most roundabouts. Since the number of lanes is correlated with exposure rates like traffic volume, the likelihood of vehicle crashes increases with the number of lanes. Also, if the number of entry and exit lanes are more, more conflict points exist. In terms of the marginal effect, a one-lane increase in approach and exit lanes would increase the mean number of accidents by 0.21, as reflected in the marginal effect values shown in Table 6. Pedestrian crosswalks influence the occurrence of vehicle crashes. The derived mean of 0.65 and standard deviation of 0.17 show that, under a normal distribution, most roundabouts experienced an increasing number of crashes.

The last variable that has a random parameter is vertical grade, with a mean of -0.63 and a standard deviation of 0.62 with a normal distribution. This result reveals that 84.5% of roundabouts with a vertical grade experienced accident frequency reduction, and 15.5% of roundabouts without a vertical grade show an increase in accident frequency. This result could be because the vertical grade increases safety by influencing vehicle speed and driver's caution.

5. Conclusions

This study determined the effects of geometrics and traffic flow conditions on traffic accident frequency at roundabouts in Korea. Although many roundabouts have been installed in recent years in Korea, most studies have been focused on the general effects of roundabouts in view of efficiency and safety. Furthermore, some studies have been conducted in safety viewpoints based on a simple comparison of accident occurrences before and after installation of roundabouts. However, for safer design and operation of roundabouts, it is important to know which elements have positive or negative effects on traffic accident frequency. This study contributes to understanding which factors realistically affect

traffic accident occurrence. In particular, this study applies random parameters, thereby taking considering unobserved heterogeneity across roundabouts, which was not explained properly in previous studies.

The estimation results showed that eight parameters that significantly affect vehicle crashes can be derived. Among them, traffic volume, average lane width of the entry lane, central island, and width of the circle lane were found to be fixed effects, which means that they produce the same effect on all roundabout. The other four parameters including the radius of the entry lane, the number of approach and exit lanes, the presence of a pedestrian crosswalk, and the vertical grade were found to be random effects, which means that they affect traffic accidents differently depending on the roundabout. The traffic volume, average width of the entry lane, presence of a central island, number of approach and exit lanes, and presence of a pedestrian crosswalk are regarded as variables that increase vehicle crashes, while the other variables are regarded as factors that reduce vehicle crashes.

This study contribute to identifying elements that significantly affect traffic accidents and to applying a random parameter count model to consider unobserved effects in the variable. However, this study has some limitations. Although in this study, a random parameter negative binomial model was applied to understand the relationship between traffic accident frequency at roundabouts recently installed in Korea and geometries for the first time, more in-depth analyses are needed for further understanding. Also, an appropriate offset, which is a distance between a stop line and a pedestrian crosswalk, needs to be calculated in relation to the installation of crosswalks. If a crosswalk is too close to the roundabout, it can be beneficial for pedestrians by reducing walking distance. However, it can result in more conflict with drivers who want to enter the roundabout, which can be a threat to safety. In contrast, if a crosswalk is installed too far from the roundabout, pedestrians have to walk farther than necessary such that jaywalking can occur frequently, which threatens the safety of pedestrians. Accordingly, it is necessary to find the right distance of a crosswalk from the stop line of a roundabout to satisfy the needs of drivers and pedestrians even current Korea roundabout design guideline recommends that there should be more than six meter offset for pedestrian safety.

Another limitation of this study is a matter of universality for database and analysis results. The all data used in this study was from Korea roundabouts, and because Korea is in the early stage of the roundabout application, there have been many safety and operation problems that does not occur in other countries. Therefore, for more universal results, safety improvement change by time series should be kept studying in the future.

Data Availability

The data used to support the findings of this study are available from the corresponding author upon request.

Conflicts of Interest

The authors declare that they have no conflicts of interest.

References

[1] L. Rodegerdts, J. C. Bansen, J. Tiesler et al., *NCHRP Report 672: Roundabouts: An informational guide*, Transportation Research Board, Wash, USA, 2010.

[2] *Highways Agency: Geometric Design of Roundabouts, Design Manual of Roads and Bridges*, London, UK, 16/07 edition, 2007.

[3] C. C. Schoon and J. Van Minnen, "Accidents on Roundabouts: Second Study into the Road Hazard Presented by Roundabouts, Particularly with Regard to Cyclists and Moped Riders. R-93-16," Tech. Rep., SWOV Institute for Road Safety Research in the Netherlands, 1993.

[4] F. Alphand, U. Noelle, and B. Guichet, *Roundabouts and Road Safety: State of the Art in France, Intersections without Traffic Signals*, Springer Verlan, Germany, 1991.

[5] *Safety of Roundabouts in Urban and Suburban Areas*, Centre d'Etude des Transports Urbains, Paris, 1992.

[6] G. Jacquemart, *Modern Rounabout Practice in the United States*, Transportation Research Board, Wash, USA, 1998.

[7] P. Ranjitkar, A. Shahin, and F. Shirwali, "Evaluating operational performance of intersections using SIDRA," *Open Transportation Journal*, vol. 8, no. 1, pp. 50–61, 2014.

[8] B. Guichet, "Roundabouts in France: Development, Safety, Design, and Capacity," in *Proceeding of the Third International Symposium on Intersections without Traffic Signals*, University of Idaho, Moscow, Idaho, Portland, Oregon, 1997.

[9] J. G. Bared and K. Kenndy, "Safety Impacts of Modern Roundabouts," in *ITE Safety Toolbox*, Institute of Transportation Engineers, 1999.

[10] R. A. Retting, B. N. Persaud, P. E. Garder, and D. Lord, "Crash and injury reduction following installation of roundabouts in the United States," *American Journal of Public Health*, vol. 91, no. 4, pp. 628–631, 2001.

[11] R. Elvik, "Assessing the validity of road safety evaluation studies by analysing causal chains," *Accident Analysis & Prevention*, vol. 35, no. 5, pp. 741–748, 2003.

[12] L. Rodegerdts, M. E. Blogg, E. Wemple et al., "NCHRP Report 572," Roundabout in the United States, Transportation Research Board of the National Academics, Wash, USA.

[13] E. Vlahos, A. Polus, D. Lacombe, P. Ranjitkar, A. Faghri, and B. R. III. Fortunato, "Evaluating the conversion of all-way stop-controlled intersections into roundabouts," *Transportation Research Record*, no. 2078, pp. 80–89, 2008.

[14] H. Isebrands, "Crash analysis of roundabouts at high-speed rural intersections," *Transportation Research Record*, no. 2096, pp. 1–7, 2009.

[15] "Korean Roundabout Research Center," http://www.roundabout.or.kr/.

[16] "A Study on Vitalizing Roundabouts, Ministry of Land, Infrastructure and Transport in Korea, 2011".

[17] J. Badgley, J. L. Condon, Rainville., and D. Li, *FHWA Research and Technology Evaluation: Roundabout Research*, 2018.

[18] D. Leuer, "A Study of the Traffic Safety at Roundabouts in Minnesota, 2017".

[19] S. Coffey, S. Park, and N. Zoccoli, "Roundabout Safety Analysis in the Context of Time Series: Case Study in the State of Pennsylvania," in *Proceedings of the International Conference on Transportation and Development 2016: Projects and Practices for Prosperity*, pp. 907–919, USA, June 2016.

[20] G. Maycock and R. D. Hall, "Accidents at 4-Arm Roundabouts," Report LR1120, Transport and Road Research Laboratory, Crowthorne, Berkshire, UK, 1984.

[21] J. Kamla, T. Parry, and A. Dawson, "Roundabout accident prediction model random-parameter negative binomial approach," *Transportation Research Record: Journal of the Transportation Research Board*, vol. 2585, pp. 11–19, 2016.

[22] A. P. Silvano and L. Astrid, "Traffic Safety for Cyclists in Roundabouts: Geometry, Traffic, and Priority rules (A Literature Review)," VTI Report 31A-2017, 2017.

[23] J. Park, *Review of the Potential Applicability of Modern Roundabouts Based on Safety and Operational Performance Analysis*, University of Seoul, Korea, 2010.

[24] H. Na and B. Park, "Accident Models of Circular Intersection by Cause Using ZAM," *Journal of the Korean Society of Road Engineers*, vol. 14, no. 2, pp. 101–108, 2012.

[25] Y. Kim, *The Analysis of a Factor of the Accident at a Roundabout Considering as the Driver's peculiarities*, Myongji University.

[26] S. Kim and J. Choi, "Safety analysis of roundabout designs based on geometric and speed characteristics," *KSCE Journal of Civil Engineering*, vol. 17, no. 6, pp. 1446–1454, 2013.

[27] P. C. Anastasopoulos and F. L. Mannering, "A note on modeling vehicle accident frequencies with random-parameters count models," *Accident Analysis & Prevention*, vol. 41, no. 1, pp. 153–159, 2009.

[28] N. S. Venkataraman, G. F. Ulfarsson, V. Shankar, J. Oh, and M. Park, "Model of Relationship Between Interstate Crash Occurrence and Geometrics - Exploratory Insights from Random Parameter Negative Binomial Approach," *Transportation Research Record: Journal of the Transportation Research Board*, vol. 2236, pp. 41–48, 2011.

[29] M. H. Park, "Relationship between interstate highway accidents and heterogeneous geometrics by random parameter negative binomial model—a case of Interstate Highway in Washington State, USA," *Journal of the Korean Society of Civil Engineers*, vol. 33, no. 6, pp. 2437–2445, 2013.

[30] S. P. Washington, M. G. Karlaftis, and F. L. Mannering, *Statistical and Econometric Methods for Transportation Data Analysis*, Chapman & Hall, Boca Raton, Fla, USA, 2003.

[31] A. C. Cameron and P. K. Trivedi, *Regression Analysis of Count Data*, vol. 53 of *Econometric Society Monographs*, Cambridge University Press, Cambridge, UK, 2nd edition, 2013.

[32] S.-P. Miaou and H. Lum, "Modeling vehicle accidents and highway geometric design relationships," *Accident Analysis & Prevention*, vol. 25, no. 6, pp. 689–709, 1993.

[33] V. Shankar, F. Mannering, and W. Barfield, "Effect of roadway geometrics and environmental factors on rural freeway accident frequencies," *Accident Analysis & Prevention*, vol. 27, no. 3, pp. 371–389, 1995.

[34] W. Green, *Limdep, ver. 9.0. Econometric Software Inc*, Plainview, NY, USA, 2007.

[35] K. Train, *Halton Sequences for Mixed Logit*, Department of Economics, University of California, Berkeley, Calif, USA, 1999.

[36] J. C. Milton, V. N. Shankar, and F. L. Mannering, "Highway accident severities and the mixed logit model: an exploratory empirical analysis," *Accident Analysis & Prevention*, vol. 40, no. 1, pp. 260–266, 2008.

Research Article

The Surrogate Safety Appraisal of the Unconventional Elliptical and Turbo Roundabouts

Giovanni Tesoriere,[1] Tiziana Campisi [iD],[1] Antonino Canale,[1] and Tedi Zgrablić[2]

[1]*Faculty of Engineering and Architecture, University of Enna Kore, Italy*
[2]*Faculty of Engineering and Architecture, University of Maribor, Slovenia*

Correspondence should be addressed to Tiziana Campisi; tiziana.campisi@unikore.it

Double-lane roundabouts have been created in many European countries over the past few centuries and are now characterized by an unsafe geometric development and by a low sustainability capacity or level. In this regard, new double-lane geometries have been implemented to overcome to these critical points. This article shows a comparison of two nonconventional double-lane roundabout schemes defined as elliptical and turbo. Considering this research on the unsafe and congested conditions for each road schemes at grade, the microsimulation approach allows comparing schemes of intersections not yet realized in order to be able to evaluate the critical issues. A symmetric traffic distribution and an identical vehicle mix for both design solutions are considered. The research was conducted considering two different double-lane roundabout-turbo roundabout and the elliptical roundabout. By comparing their geometry and technical elements, this article assumes that turbo roundabout due to its physical separating traffic lanes in the central circulatory carriageway will enable potentially better traffic safety conditions. This article has the following main goal: a comparison of traffic safety using VISSIM microsimulator and SSAM tools. The results can provide to show safety level on investigated scenario considering level of service (LOS) and also the possibility of obtaining time to collision (TTC) and postencroachment time (PET) through the use of surrogate parameters obtained by SSAM tool. In fact, the surrogate safety parameters allows evaluating the possible collision scenarios between them, according to the trajectories of the single vehicles. This assessment is useful in order to be able to evaluate by the local authorities which of the examined schemes can provide greater negativity in the construction and operation phase. Therefore this comparative analysis allows reducing, in the preliminary phase, possible security impacts and also economic ones for the community.

1. Introduction

Today, the different road intersections are increasingly developing. In general, the road intersections in roundabout allow a substantial reduction of the points of conflict between vehicles and vehicles with pedestrians compared to the traditional intersections with precedence or with traffic lights. Proper planning of the roundabout is necessary to reduce the percentage of deaths and injuries on the roads of each countries.

The research was conducted considering two different double-lane roundabouts titled elliptical and turbo. The following paragraphs show a geometric description of the intersections and a detailed analysis of the steps that led to the comparison of the two geometries in safety terms through the use of the VISSIM microsimulator [1] and the dedicated SSAM tool [2].

There was the first phase of selection of the geometries to be analyzed, the traffic scenarios with relative distribution of the vehicle typologies and after the calibration of the model of the microsimulator in order to make the most reliable results. Finally, they were processed in terms of surrogate safety through a dedicated tool.

The comparison of the results shows how to vary the flows and geometries of unconventional satin road intersection you can have more or fewer distributions of certain types of collisions between vehicles along the geometry. In fact, the evaluation and also the comparison of supposed collision

are investigated considering surrogate parameters. Surrogate parameters represent a summary assessment in terms of safety, by placing a double-lane rotary comparison on the central circulatory carriageway.

The hypotheses on which this research is based are related to the definition of the surrogate safety of nonconventional roundabout geometries. Specifically, attention was focused on the comparison of two widespread schemes in Europe, in order to be able to investigate in advance which of these, with the same outflow conditions, be better in terms of service level and therefore road safety.

2. Double-Lane Roundabout Geometry

The geometries chosen for the comparison are of a satin type and are referred to as turbo and elliptical roundabout, respectively. Both have in the case examined a double lane in the central circulatory carriageway. At the end of the 90s, in the Netherlands it is following the design and construction of the turbo-type roundabouts. Scheme of stories has evolved over the years by presenting the preselection of the manoeuvres along the arms and therefore they are vehicles of not manoeuvring abrupt or wrong.

The limitation of the manoeuvres was made possible not only by the preselection along the lanes of the arms but also by the presence of curbs or signs of separation between the manoeuvres along the main ring. From here there has been an increase in safety with a reduction in the number of deaths and injuries along these intersecting geometries. Fortuijn was the first to study and design the turbo-type intersections at grade [3].

Unlike the turbo roundabout, the elliptic schemes are not defined by separated lanes of the circulatory ring. Sometimes there are not even the preselection lanes along one or more arms of the intersection.

Several studies have been conducted in recent years on the assessment of the potential of unconventional roundabout in terms of safety and environmental impact, evaluating both the single and double lane on the central ring in different traffic flow conditions like those described by [5, 6].

The evolution of turbo-type rotary geometries has in recent years been carried out in parallel with the development of public and private transport systems in terms of both eco-mobility and traffic decongestion systems with the reduction of the automatic system in favour of collective passengers transport [7].

The elliptical roundabout is a form of a classical double-lane roundabouts with the emphasis that it is not a proper circular shape, but its geometry corresponds to a closed curve-ellipse. This form of double-lane roundabout is characterized by two semiaxes (R and 2R). Usually the higher semiaxis (2R) is located in the main traffic direction while the lower semi-axis is located in the secondary traffic direction. This form of elliptical roundabout is most often applied in areas where, due to spatial conditions, a classical circular roundabout cannot be performed and where there is more traffic at the main traffic direction. Mainly in the world it is not so much represented, but according to [8], elliptical roundabout is widely used in Iran. Figure 1 represents, respectively, the two geometries examined, considering the main and secondary traffic directions. Both road geometries are not signalized; therefore the precedence of vehicles circulating on the ring has been estimated with respect to those that are introduced by the arms in the various directions, respectively.

3. Calibration of Microscopic Traffic Simulator: Methods and Application

Microsimulation approach and microanalytic simulation are linked to a category of analytical tools that perform highly detailed analysis of activities such as highway traffic flowing through road networks. Traffic microsimulation models generally is defined considering a large number of parameters that must be calibrated before the prediction of applied model.

In this paragraph, the details of the traffic microsimulator used and the tool dedicated to the assessment of road safety have been reported. The definitions of the parameters and the calibration of the models followed the processing of the data and the comparison of the two geometries.

3.1. Microsimulation Tool Description. The modelling phase of the compared roundabouts was made by first considering the geometric parameters and the main and secondary traffic directions. It was carried out considering some hypotheses related to the models on which the VISSIM software developed by PTV is based.

The parameters mentioned above mainly include the characteristics of the vehicle, the composition of the traffic flow in terms of percentages of heavy or other light vehicles, the distribution of the speed of desire, the traffic flows, and some behavioural parameters linked to the style of driving and the driver's psychophysical status [9].

The simulated model considers a random generation in the distribution along the vehicle queues in terms of both composition and volume. It also considers that the priority of the fastest moving vehicle may decrease when it reaches and perceives the presence of a slower vehicle in front.

The basic concept of this model is that the driver of a faster moving vehicle starts to decrease own speed as he reaches his individual perception threshold to a slower moving vehicle. Vehicles would be randomly generated as per the given volume and composition.

In order to be able to evaluate surrogate security parameters using the SSAM specific tool, it is first necessary to generate a layout from VISSIM and through specific files in "trj" format possible to trace the trajectories of individual vehicles and therefore to the propensity that they have to enter in fact that the SSAM tool analyzes vehicle interactions to identify events and catalogue all the events found.

For each such event, SSAM also calculates several surrogate safety measures, including the following:

 (i) Minimum time to collision (TTC)

 (ii) Minimum postencroachment (PET).

The simulation of traffic through the VISSIM software initially considers the definition of traffic flows and their
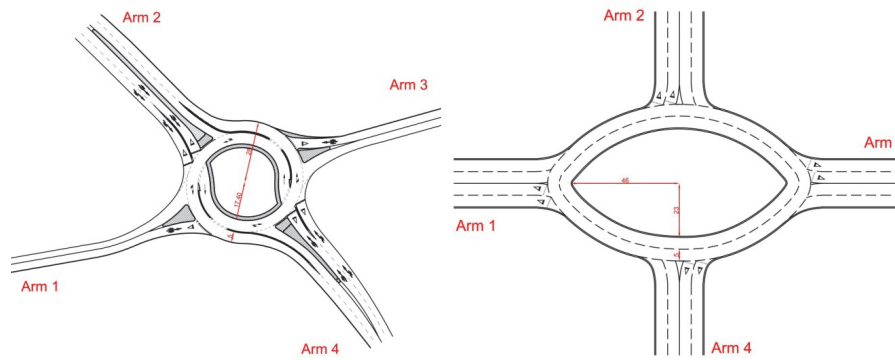
Figure 1: Details of turbo (left) and elliptical (right) geometry.

distribution along the intersection arms through the creation of special O/D matrices. In the rotary intersections, the deflection curves created by the motion of the vehicles depend on the geometry of the roundabout itself and in particular on the size of the central island. Another important geometric parameter is the determination of the input radius of the branches on the circulatory ring. They depend on both the capacity and the safety of the examined scheme. The aforesaid parameter is related to the width of entry, the width of the carriageway on the circulatory ring, and the geometry of the central island. These parameters affect the travel speed of the vehicle and therefore the driving comfort and road safety.

Federal Highway Administration (FHWA) Roundabout Guidebook [10] was considered to select roundabout design parameters. After designing all of the roundabouts in VISSIM for both geometries and conditions, traffic loads were assigned. In this study, the actuated traffic control was used in roundabouts. In addition, the right-of-way control was considered for not signalized roundabouts that were given priority to circulating flow. This controlling system allowed roundabouts to perform better than uncontrolled systems. Each roundabout was designed considering double lane on circulatory carriageway.

The following assumptions were considered for this study are linked to urban areas conditions. The analyzed geometries are characterized by a speed value of about 50 km/h on circulatory carriageway while the access speeds from each arm are assumed to be less than 35 km/h. In elliptical roundabouts, large radius is twice the small radius.

The exact disposition of the data and the traffic flows have been calibrated through the origins of origin and are examined in the next paragraphs.

In general, it is possible to resort to traffic microsimulation instruments if, in a preventive manner and for small areas, the possible introduction of different geometrical schemes is to be analyzed and can be compared from both the point of views of safety-related issues (i.e., precedence, percentage of thinking vehicles, and weak road users) in relation to impacts of various kinds such as the environment [11].

This research investigates on two unconventional geometrical layouts (elliptical and turbo roundabouts). They are

very recent or just theoretic, and it is often not possible to perform an observational evaluation by collecting crash and operational data.

The microsimulation software tool VISSIM (Version 9) [1] was used to simulate operations at the roundabouts. This software can be used to generate all types of outputs simultaneously (safety, traffic performance, and capacity), allowing a more complete and comprehensive picture of the combined effects in making comparisons of various roundabout design scenarios.

The VISSIM output, in particular files linked to trajectories details, was imported into the Surrogate Safety Assessment Model (SSAM) [2], a software application designed to consider vehicle trajectory data output from microscopic traffic simulation models to derive proximal measures such as conflicts, based on thresholds for either time to collision (TTC) or postencroachment time (PET).

The estimated conflicts were then applied in crash-conflict models for roundabouts developed in other research to compare the roundabout designs on the basis of expected crashes.

The approach of using proximal safety indicators such as conflicts has been suggested as an alternative to the use of crash data, especially where the facility being evaluated does not exist and thus does not have a crash record.

It is possible to consider the frequency of conflicts and the severity measures through the use of intersection conflict index in agreement with Sayed and Zein [12].

This suggests the possibility of using significantly shorter study periods to establish statistically reliable results. The fundamental parameters beyond those previously described are related to the capacity of the analyzed geometry, to the estimated or hypothesized traffic volume and to their relationship. The comparison of the results took place considering the geometries shown in the Table 1.

According to Hatami and Aghayan [8], it is possible to admit that the elliptic roundabouts have now become an unconventional type of roundabout.

The geometry of the aforesaid roundabout leads to a reduction of the positive effects especially with the increase of the radius: in fact, there is a roundabout an elliptic not semaphore, like that object of study, to an increase of the

TABLE 1: Details of double-lane roundabouts simulated.

Number of lanes	Types of roundabout	Speed limits[km/h]	Traffic light	Central island radii[m]	Total Traffic Volume[veh/h]	Max Capacity
Two lanes	Turbo	50	Absence	Main radius R=56m	3040veh/h	3480veh/h
Two lanes	Elliptical	50	Absence	Main radius R=56m Secondary radius r=23m	2400veh/h	3000veh/h

criticalities both in terms of capacity and of delay. Against the increase of the speed in it involves a positive effect both on the capacity and on the delay.

The Surrogate Safety Assessment Model (SSAM) is a specific tool created by Federal Highway Administration focused on identification, automatically classification of the presence of potential conflicts generated by the trajectories of vehicles circulating on road schemes. The tool also has integrated statistical analysis functions for the frequency and severity of conflicts that can help in the design of traffic safety structures. The following paragraphs describe the calibration steps of the model and report the relative results of the unidentified roundabout, providing the results with the help of the VISSIM software and the SSAM tool.

3.2. Surrogate Safety Tool SSAM. The name of SSAM tool is the acronym of Surrogate Safety Assessment Model. It has many parameters to configure that allow the user to visualize the analysis and customize the analysis results. Some of these data would be best imported from the simulation application(s) itself (e.g., "import traffic-stream data") using a common file format related to trajectories generated by microsimulator software.

Generally the data required to adequately analyze the traffic situation includes the following:

(i) Network geometry (i.e., number of lanes in each direction, turning pockets, and driveways)

(ii) Traffic-stream data (volume of traffic in each direction, change in the volumes over the simulation period)

(iii) Definition of signalized or not signalized intersection with specific priority of each arms or circulatory carriageway

(iv) Driver behaviour data (i.e., aggressiveness distribution and gap-acceptance criteria).

The evaluation of surrogate parameters allows an evaluation of the safety of the schemes analyzed, providing a greater propensity of the intersection to generate different types of conflict points.

3.3. Calibration Process to Microsimulation Tool. Calibration is the adjustment process to set model parameters and to improve the model's ability to reproduce local driver behaviour and traffic performance characteristics.

It is impossible for the researcher to have knowledge of the number of repetitions to be calibrated in advance, but it is possible to use an estimate of how many times it is necessary

TABLE 2: Minimum number of repetitions needed to obtain the desired confidence interval.

Desired Range (CI/S)	Desired Confidence	Minimum Repetitions
0,5	99%	130
0,5	95%	83
0,5	90%	64
1,0	99%	36
1,0	95%	23
1,0	90%	18
1,5	99%	18
1,5	95%	12
1,5	90%	9
2,0	99%	12
2,0	95%	8
2,0	90%	6

to calibrate the parameter and/or models investigated to obtain a statistically valid result. The required minimum number of model repetitions is computed using the following equation:

$$CI_{1-\alpha\%} = 2 * \frac{t_{(1-\alpha/2),N-1}s}{\sqrt{N}} \qquad (1)$$

where

CI(1-α)% = (1-α)% is confidence interval for the true mean, where alpha equals the probability of the true mean not lying within the confidence interval

t(1-α/2), N-1 is Student's t-statistic for the probability of a two-sided error summing to alpha with N-1 degrees of freedom, where N equals the number of repetitions

s is standard deviation of the model results.

Table 2 shows the link among above equation, the minimum number of repetitions for various desired confidence intervals, and desired degrees of confidence according to [2].

3.4. Calibration Targets. The model calibration process provides the best possible match between model performance estimates and real measurements.

However, there is a limit to the amount of time and effort that anyone can make to eliminate the error in the model, since the high repetition of the process often does not result in greater accuracy of the data.

Table 3 shows the criteria and calibration measures considering specific vehicle flow intervals adopted by DOT [13].

TABLE 3: Wisconsin DOT freeway model calibration criteria.

Criteria and Measures	Traffic Flow range	Calibration Acceptance Targets
Individual Link Flows		
Within 15%	700veh/h<Flow<2700veh/h	>85%of cases
Within 100veh/h	Flow<700veh/h	>85%of cases
Within 400veh/h	Flow>2700veh/h	>85%of cases
Sum of All Link Flows	**Within 5%of sum of all link counts**	
GEH statistic<5 for Individual link Flow	**>85%of cases**	
GEH statistic<5 for all link Flow		GEH<4 for sum of all link counts
Travel times, Model Versus Observed		
Journay Time, Network Within 15%(or 1min if higher)		>85%of cases
Visual Adults		
Individual Link Speeds-visually Acceptable Speed-Flow relationship		To analyst's satisfaction
Bottlenecks		
Visually Acceptable Queuing		To analyst's satisfaction

TABLE 4: GEH value obtained in accordance with [4].

Roundabout schemes with 2 lanes on circulatory carriageway					
	Double lane	Turbo	Flower	Target	Elliptical
GEH on right lane	87,5	87,5	87,5	87,5	87,5
GEH on left lane	100	87,5	87,5	87,5	87,5

TABLE 5: O/D matrix selected to simulation.

O/D	Arm1	Arm 2	Arm 3	Arm 4
Arm1	0	0.15	0.7	0.15
Arm2	0.15	0	0.15	0.7
Arm3	0.7	0.15	0	0.15
Arm4	0.15	0.7	0.15	0

The calibration of the software model used is based on the model defined Wiedemann 74 used by PTV VISSIM (version 9) to simulate in a reliable and realistic way the traffic of vehicles inside unconventional roundabouts.

The car-following model was considered to be satisfactorily calibrated when the two curves overlap.

To further explore the model's validity, the Geoffrey E. Havers (GEH) statistic index (1,2) was used as the criterion for accepting the template.

The formula for the "GEHi Statistic" is

$$\text{GEHi} = \frac{\sqrt{2\left(M - C\right)^2}}{M + C} \quad (2)$$

And

$$\text{GEH} = \frac{\sum_{i=1}^{n} \text{GEHi}}{n} \quad (3)$$

GEH index is a global indicator widely used for the validation of traffic simulation models, especially when only aggregate values such as traffic flow counts in time-based detection stations and input capacity are available [14].

The GEH index value is the average over "n"; it was considered equal to 9, simulations of the index for each simulation i, as shown in Table 4.

3.5. Traffic Flow Conditions. Microsimulation approach is helpful to simulate different hypothesis of traffic operations changing schemes and different traffic conditions. The authors investigated the safety results of the two analyzed road schemes considering the 80% of the maximum value of traffic flow, corresponding to each roundabout capacity.

The simulation of the geometries described above was carried out by evaluating a ratio between Volume and Capacity of each single intersection equal to 0.8, thus equal to 80% of the maximum capacity of each scheme in a double lane examined.

In general, the performances of the road geometry are measured through its level of service while the safety measures can consider surrogate parameters such us the time to collision (TTC). This parameter is obtained considering the trajectories of the individual vehicles and the potential conflicts. Through the TTC it is possible to provide interesting information in advance, suggesting that the new layouts should be considered where justified by considerations on costs and benefits. The VISSIM output includes vehicle trajectory files that were then imported into the Surrogate Safety Assessment Model-SSAM, a software application designed to perform analysis of vehicle trajectory data output from microscopic traffic simulation models to derive proximal measures such as conflicts, based on time to collision (TTC) or postencroachment time (PET). The estimated conflicts were then applied considering conflict models already analyzed by other sources of literature. The approach of using proximal safety indicators such as conflicts has been suggested as an alternative to the use of crash data, especially where the facility being evaluated does not exist and thus does not have a crash record. In particular the flow values used are equal to 80% of the saturation flux of each of the two rotary geometries. In particular, reference was made to a symmetric O/D matrix for both roundabouts and shown as on Table 5.

The analyzed traffic mix refers to observed traffic distributions and consists of the following percentages: 70%of LPV
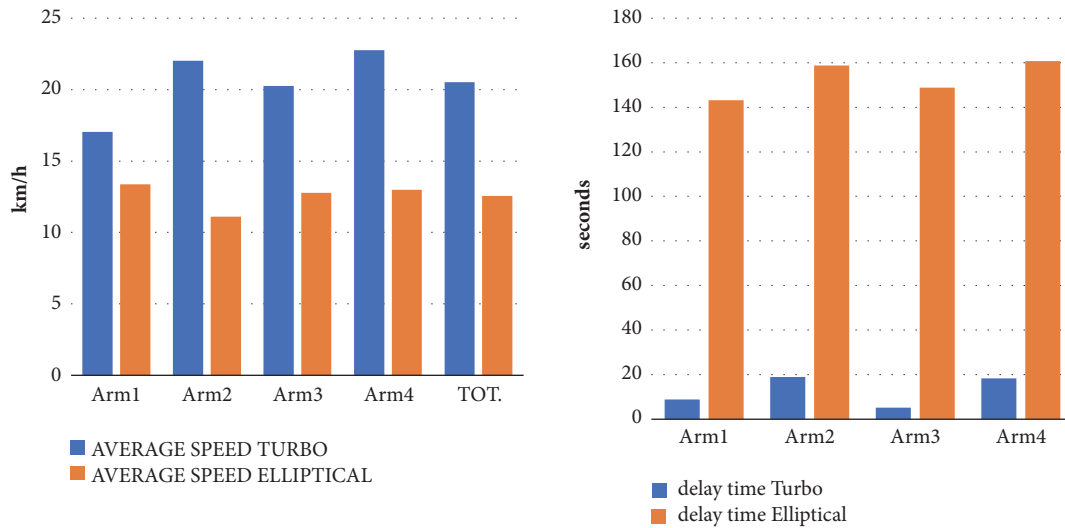
Figure 2: Comparison of average speed and delay time for investigated road scheme on saturated conditions.

(Light Passenger Vehicle), 20%of HPV (Heavy Passenger Vehicle, 5%of Buses and the same percentage is dedicated to Motorcycles. The comparison of the geometries was carried out by evaluating the parameters characterizing the LOS service level of the road intersections and in particular it was estimated: maximum and average length of the queues, average delay, average speed, and number of STOPs. In order to make the two geometries comparable, reference is made to normalized values.

4. Elliptical and Turbo Roundabout Operational Safety Results

Two schemes with two-lane circulatory ring were presented in this work. The choice of one or the other scheme depends on several factors. In general, an elliptical roundabout is a good choice when constraints such as precedence, existing road alignments, buildings, and/or wetlands affect the shape. As regards the turbo roundabout scheme, the separation of directional flows must be underlined through specific vertical signs or curbs [15].

In general, the physical separation of traffic lanes is interrupted only at entry points in the internal circulating carriageway. Since the weaving on the roundabout is no longer possible, drivers should be assisted by clear signage and lane signage.

4.1. Comparison of VISSIM Results. The simulation carried out with the VISSIM software, made it possible to compare the intersections described above through the evaluation of parameters relating to the service level of an infrastructure. In particular, the length of the queues, delays and the stops number were evaluated. These parameters make it possible to evaluate how much a road geometric scheme has, for a given vehicular flow, the propensity to be subject to congestion phenomena and therefore to a low level of service. This status implies the possible collapse of the mobility of the vehicles inside it. Graphs on Figure 2 shows a sharp difference in the delay values along the two geometries with a very high possibility of congestion in the case of the elliptic roundabout compared to the turbo type.

The graph therefore shows a higher average speed along the turbo-rotary because the preselection of the manoeuvres does not compromise the travel speed of the entire roundabout. It shows a total average speed value of about 20-23km/h for the turbo-type roundabout and about a reduced value of 40% for the elliptical roundabout. Likewise, it assumes almost zero or reduced delay values in the turbo-type intersection, while elevating values for the elliptical.

As far as the number of stops is concerned, there is a greater value in the arms B and D of the turbo roundabout, while they are practically of equal value along the elliptical roundabout in accordance with Figure 3. This phenomenon provides an increase in congestion and possible impacts in the aforementioned points.

An operational analysis is conducted to determine if the turbo roundabout will accommodate projected traffic volumes at an acceptable level of service (LOS). Roundabout LOS is measured in control delay consistent with the elliptical roundabout.

It is also fundamental to be able to understand the service level of the analyzed intersections, to evaluate the LOS parameter overall and/or for each arm. As can be seen from the graph shown in Figure 4, the value of LOS afferent to the elliptical roundabout remains almost constant along the arms for the traffic conditions previously discussed. In particular, the LOS=F=6 shows a bad condition of internal movement of this scheme in the roundabout, suggesting a widespread congestion of vehicular traffic to the flow analyzed. On the contrary, as regards the turbo-type roundabout, there is a more acceptable value of LOS, especially in arms 1 and 3 where the accumulated delays and the phenomenon of congestion seem to decrease by about 40% compared to two arms, 2 and 4.
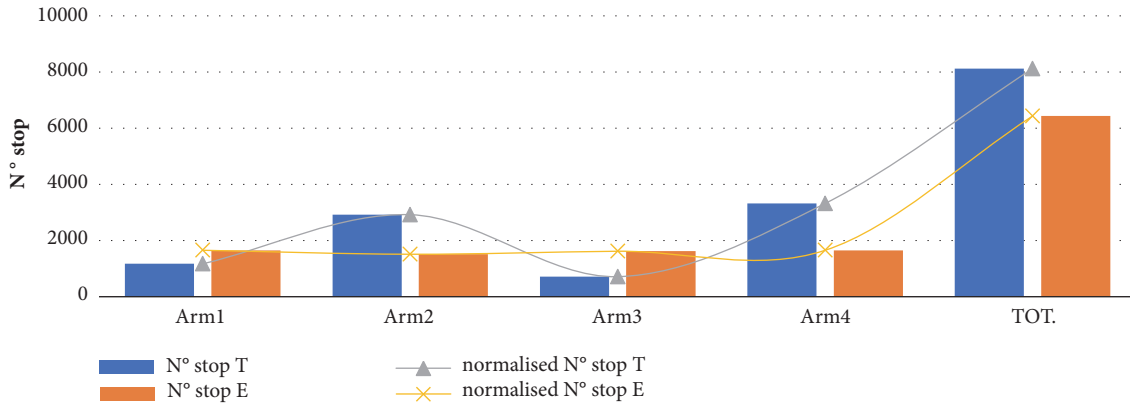
FIGURE 3: Comparison of number of stop related to turbo and elliptical scheme on congested conditions.
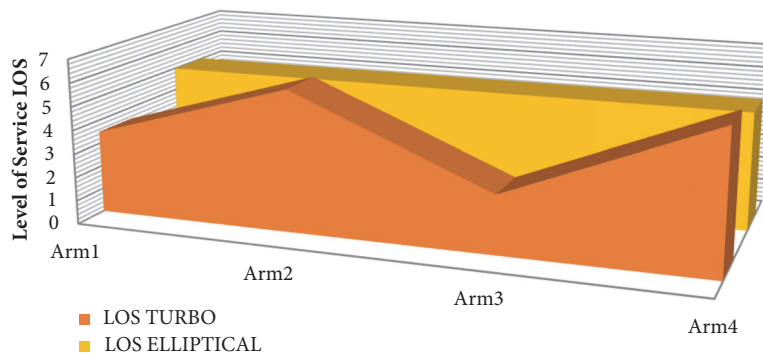
FIGURE 4: Level of service of investigated road schemes at grade.

The greater extension of the diameter along the main direction Arm1_Arm3 of the elliptical roundabout shows through the layouts produced by the microsimulator on Figure 5 a free flow condition near the circulatory carriageway while there is a greater thickening of vehicles along the arms for both the examined configurations. The lack of separation of the lanes on the main ring generates more collisions in the elliptical roundabout as explained in Figure 5.

4.2. Comparison of SSAM Results. TTC and PET are both indicators of proneness to establish a vehicle collision.

The probability of a conflict occurring is greater than the value of these parameters is lower [15]. The research was founded on specific range for both safety parameters in order to establish the possibility of defining a potential conflict, considering 0.1 s < TTC <1.5 s and 0.5 s < PET < 2.5 s. Among the data associated with each conflict is a MinTTC variable, which is the simulation time where the minimum TTC value for that conflict was observed [16]. That variable was used to filter out all conflicts that occurred during the simulation time. Two comparative safety evaluations were conducted based on different measures like described on Figure 6:

(i) The estimated conflicts from SSAM: this is done for entry flows of 0.8 V/C (absolute and normalized per 1000 vehicles) and for 2400 veh/h and 3040veh/h.

(ii) Estimated crashes are based on applying estimated conflicts (for entry flows of 0.8 V/C and for 3040 veh/h) in crash-conflict models; as can be seen from Figure 6, it assists a maximum PET value for both the turbo and elliptic type scheme below the value of 5. The average value, on the contrary, of results for the elliptic configuration is about 30% of the value average relative to the turbo. In terms of PET, there is a clear variability between the two geometries in terms of both maximum value and average value. In particular, the maximum value of the elliptical roundabout reaches a value equal to 5 determining an increase in the possible conflicts within it. Figure 6 shows the distribution of TTC and PET values considering turbo and elliptical scheme. In terms of average values it is possible to consider the high value of TTC for turbo and the same history for PET value.

We can notice a greater distribution in the arms, especially in the main direction with regard to the turbo-type roundabout, while an increase in yellow at the rotary crown couplings as regards the elliptical roundabout, equally distributed along the two directions. Equal distribution in the elliptic is denoted with regard to the conflicts shown in blue which instead are lower in the roundabout of the turbo type and bordering only in part of the lanes dedicated to the manoeuvre of turning to the right. Table 6 shows the comparison of the points
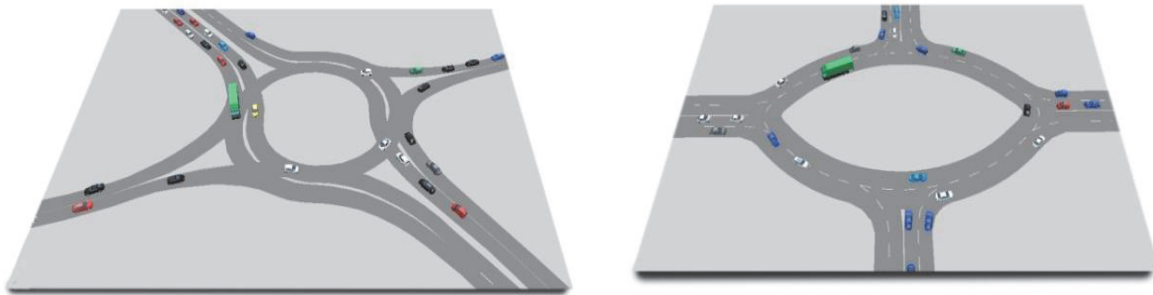
Figure 5: Microsimulator layout.
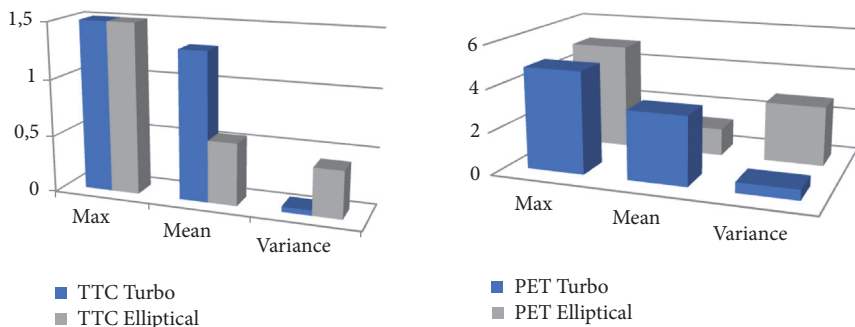
Figure 6: Surrogate safety parameters comparison: TTC and PET.

Table 6: Collision type distribution.

Intersection scheme	Collision Type		
	crossing	rear end	lane change
Turbo	7	12021	145
Total conflict point 12173			
Elliptical	453	8002	3073
Total conflict point 11528			

of conflict for the various manoeuvres on the two types of intersections investigated.

Through the graphic representation of the values mentioned in Table 6 along the geometry, it is better to see Figure 7 in the arms of direct turning of the turbo the types of conflict called rear end while in the elliptical roundabout the same types of conflict are thickened inside the rotary crown near the access arms.

In the elliptical roundabout, also in Figure 7, there is a concentration of the conflicts of the wool change type at the coupling between the circulatory carriageway and the entry arms.

5. Conclusions

This research investigated two alternatives type of double-lane roundabout, turbo and elliptical, in order to define the safest solution considering direct and surrogate parameters.

To date, mutual comparisons in terms of surrogate safety between these two schemes are not discussed in the sector literature but can be compared to other roundabout geometries and or in terms of capacity-delay/geometrical parameters.

The work highlights the potential for estimating road safety through the replacement solution. Therefore the research work carried out wanted to highlight the negativity of one or the other scheme in order not only to compare two but to provide more comprehensive data that can be incorporated into the comparison of more geometries and also to help to technicians or local authorities during the preliminary selection phase of infrastructure projects.

The assessment of the critical aspects related to road safety and to the possible collision of vehicles has been addressed through the use of traffic microsimulation and a dedicated tool.

The hypotheses analyzed consider the presence of a double lane on the ring that if it does not have the curb of separation between them, it allows a greater percentage of collisions due to the lane change manoeuvres along the central ring. In fact the preselection of the manoeuvring lane along the turbo entry arm limits the collision formations for lane change. The evaluation of safety surrogate parameters such as TTC and PET allows analyzing in a preliminary phase the criticalities found in particular geometries and providing the bases to local authorities in order to choose, with the same geometry as a satin, which can generate the maximum reliable value of collisions even in critical conditions of saturation.

Finally, it should be noted that the presence of more points of collision within the circulatory ring can make traffic

Legend	
Graphical representation	Conflict type
Blue dots	Lane-change
Yellow dots	Rear-end
Red dots	Crossing
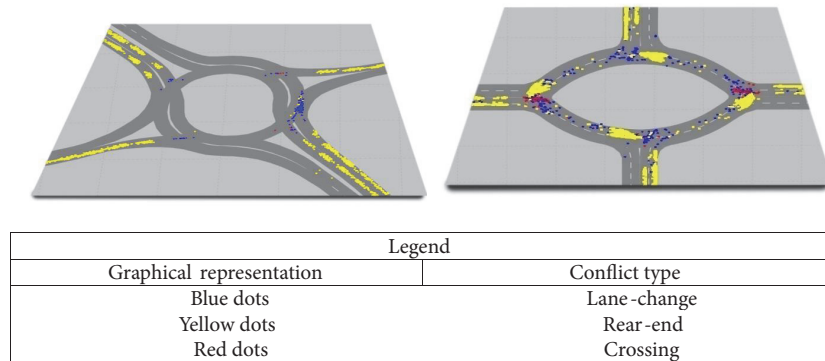
FIGURE 7: Layout related to the types of collisions made by SSAM in the two roundabouts examined.

less easy, especially if more lanes are invaded. These reasons are to evaluate in advance preventive scenarios and possible alternatives and solutions to the problems in progress.

6. Limitations and Future Development

This research is focused on the first phase of comparison in terms of safety of turbo and elliptical roundabout geometries in critical conditions of vehicular outflow with symmetrical distribution along the main and secondary directions. Future developments will be conducted varying not only transport matrices but also percentages of heavy vehicles.

Data Availability

The authors declare themselves available to provide input and output data of the present research work.

Disclosure

This research work is not a public or private expense for its elaboration. No research project of the Kore University of Enna, Italy, and the University of Maribor, Slovenia, has financed this work.

Conflicts of Interest

The authors declare that there are no conflicts of interest regarding the publication of this paper.

References

[1] J. Archer and I. Kosonen, "The Potential of Micro-Simulation Modelling in Relation to Traffic Safety Assessment," in *Proceedings of the ESS Conference*, Hamburg, Germany, 2000.

[2] T. Campisi, G. Tesoriere, and A. Canale, "Microsimulation approach for BRT system: The case study of urban turbo roundabout," in *Proceedings of the International Conference of Computational Methods in Sciences and Engineering 2017, ICCMSE 2017*, Greece, April 2017.

[3] H. Chin and S. Quek, "Measurement of Traffic Conflicts," *Safety Science*, vol. 26, pp. 169–185, 1997.

[4] R. Souleyrette and J. Hochstein, *Development of a Conflict Analysis Methodology Using SSAM; Final Report*, Center for Transportation Research and Education, Iowa State University, Ames, IA, USA, 2012.

[5] O. Feldman, "The GEH measure and quality of the highway assignment models," in *Proceedings of the European Transport Conference*, Glasgow, UK, 2012.

[6] L. G. H. Fortuijn, "Turbo roundabouts: Design principles and safety performance," *Transportation Research Record: Journal of the Transportation Research Board*, no. 2096, pp. 16–24, 2009.

[7] D. Gettman, L. Pu, T. Sayed, and S. Shelby, "Surrogate safety assessment model and validation," FHWA-HRT-08-051, 2008.

[8] T. Giuffrè, S. Trubia, A. Canale, and B. Persaud, "Using microsimulation to evaluate safety and operational implications of newer roundabout layouts for European Road networks," *Sustainability*, vol. 9, no. 11, 2017.

[9] R. Guide, "Wisconsin Department of Transportation," 2006.

[10] H. Hatami and I. Aghayan, "Traffic efficiency evaluation of elliptical roundabout compared with modern and turbo roundabouts considering traffic signal control," *Promet – Traffic & Transportation*, vol. 29, no. 1, pp. 1–11, 2017.

[11] F. Huang, P. Liu, H. Yu, and W. Wang, "Identifying if VISSIM simulation model and SSAM provide reasonable estimates for field measured traffic conflicts at signalized intersections," *Accident Analysis & Prevention*, vol. 50, pp. 1014–1024, 2013.

[12] PTV-Vision, VISSIM 5.30-05 user manual, 2011.

[13] L. Rodegerdts, "Roundabouts: An informational guide," *Transportation Research Board*, vol. 672, 2010.

[14] T. Sayed and S. Zein, "Traffic conflict standards for intersections," *Transportation Planning and Technology*, vol. 22, pp. 309–323, 1999.

[15] T. Tollazzi, R. Mauro, M. Guerrieri, and M. Renčelj, "Comparative analysis of four new alternative types of roundabouts: "Turbo", "flower", "target" and "four-flyover" roundabout," *Periodica Polytechnica Civil Engineering*, vol. 60, no. 1, pp. 51–60, 2016.

[16] T. Tollazzi, G. Tesoriere, M. Guerrieri, and T. Campisi, "Environmental, functional and economic criteria for comparing "target roundabouts" with one- or two-level roundabout intersections," *Transportation Research Part D: Transport and Environment*, vol. 34, pp. 330–344, 2015.

Research Article

Urban Motion Planning Framework Based on N-Bézier Curves Considering Comfort and Safety

Ray Lattarulo [iD],[1] **Leonardo González,**[2] **Enrique Martí,**[1] **José Matute** [iD],[1] **Mauricio Marcano** [iD],[1] **and Joshue Pérez**[1]

[1]*Department of Automotive, Industry and Transportation Division, Tecnalia Research and Innovation, 48160 Derio, Vizcaya, Spain*
[2]*Department of Cyber-Security, ICT Division, Tecnalia Research and Innovation, 48160 Derio, Vizcaya, Spain*

Correspondence should be addressed to Ray Lattarulo; rayalejandro.lattarulo@tecnalia.com

In last decades, great technology advances have been done related to the automotive sector, especially in Advanced Driver Assistance Systems (ADAS) developed to improve mobility in terms of comfort and safety during driving process; hence, automated driving is presented as an evolution of those systems in the present and upcoming years. The aim of this work is to present a complete framework of motion planning for automated vehicles, considering different constraints with parametric curves for lateral and longitudinal planners. Parametric Bézier curves are used as the core approach for trajectory design in intersections, roundabouts, and lane change maneuvers. Additionally, a speed planner algorithm is presented using the same parametric curve approach, considering comfort and safety. A simulation environment is used for testing the planning method in urban conditions. Finally, tests with the real platform in automated mode have been performed showing goods results.

1. Introduction

Every year 1.2 million people die in road related accidents. The NHTSA conducted a study concluding that 94% of accidents are due to human errors, where a great amount of these crashes (33%) is related to wrong decisions during driving process [1]. In 2009, 2.4% of fatalities in the United States were related to a common problem for drivers, i.e., drowsiness [2]. Considering these points, automated driving technology promises a great reduction in crash incidents, adding efficiency in fuel consumption, reduction of parking spaces (ride-sharing), and inclusion of elderly and people with disabilities [3].

In last decades, a considerable amount of institutions, research centers, and companies is seeking to improve this technology faster [4], to make automated driving a reality in public roads as soon as possible [5]. Lateral and longitudinal controllers [6–8], as well as perception (sensors) [9, 10] and communications [11], are some of the topics mostly studied.

There are some other topics; those have received less attention than the ones named before, i.e., vehicle decision

algorithm. This area is one of the most challenging topics in automated driving because it must deal with a great number of task, as generation of smooth trajectories [12], speed profiles based on fuel consumption and comfort [13], obstacles avoidance [14], and even doing coordination among other participants to execute a maneuver [15].

Some methods explored in automated vehicle decision are in [16]; the authors have studied a novel method for autonomous vehicles decision task. They considered dynamic maneuvers satisfying traffic norms and road limitations based on a data-driven vehicle dynamic model and an optimization process using curve arcs. Other authors have explored methods based on generation of multiple curves, i.e., clothoids, setting a possible group of tentacles (possible trajectories) to be tracked by the vehicle, and the optimal solution is obtained using a Markov Decision Process (MDP) [17]. Other approaches are related to Partially Observable Markov Decision Process (POMDP) for generation of high level decision policies (following the lane, lane change, parking, etc.) [18]. Rapidly exploring Random Tree (RRT) is another method currently used for trajectory planning; some authors as [19]

are testing the integration of RRT and visual driver behavior in driving to improve the decision process. The problem is that those methods have been developed to support specific scenarios considering a bunch of specific conditions; sometimes they did not even consider online deployment [20].

Other authors, as [21], are tackling the problem considering the importance of dealing with the general case of driving (especially in urban scenarios). The idea is handling situations that goes from, for example, cruise control to being able of respecting traffic lights or signs, among other things. The problem with this approach was that the authors only considered the longitudinal part of the vehicle's decision. On the other hand, [22, 23] have presented works about general methods for trajectory generation considering intersections and roundabouts, but the speed profile generation was considered later on [24].

In [25] a method combining parametric curves of Bézier is presented; the goal is to deal with the general case of trajectory planning (in urban environments), combining this with a speed profile generation based on Model Predictive Control. The problem with the approach is, basically, considerably more difficult for using two different techniques to resolve the planning problem (they are not unified).

In such a way, this work presents a unified motion planning framework (trajectory planning and speed profile) based on 4th and 5th degree parametric Bézier curves. It specially focuses on urban scenarios and their geometrical design. It leans on the construction of two-dimensional curves for both (lateral and longitudinal) planning methods, simplifying the possible designing parameters to the most considerable ones without degrading the curve capacities. The work specially focuses on giving a tool-set for trajectory designing under typical scenarios as intersections and lane changes and to a more specific and complex scenario as roundabouts. This, last scenario is especially interesting for its set of possible parameters and conditions; it is relevant to consider that the roundabout complexity has not been sufficiently studied for other authors in the past [26].

Finally, the contribution will be organize as follows: Section 2 has the detailed explanation of three urban scenarios considered: intersections, roundabout, and lane changes (the rest can be modeled as straight line or arcs). A definition of relevant Bézier curve properties is carried on, then a global planning approach is developed to satisfy some requirements of the local planning approach (reducing the total amount of map points); these concepts will be followed by the trajectory and speed planning approach. Section 3 presents the general components used in the software architecture (all modules considered for simulation and real vehicle tests). In the following, it presented an urban test case based on simulation (Section 4) and a real case of study (Section 5); both specially focus on roundabout considerations. Finally, Section 6 contains the conclusions of this article summarizing the contributions and future works.

2. Motion Planning Framework

This section explains all the information related to the trajectory planning approach based on real-time parametric

4th and 5th degree Bézier curves. The approach's core will be focused on using these curves in path planning generation for urban scenarios (intersections, roundabouts, and lane changing) and speed planning for comfortable and safe behaviors. This approach is not limited to urban scenarios, although it is the main target of this work.

The planning framework explanation will be divided into three parts: (i) global planning using a global map (based on a point to define the structure of intersections, lane change or roundabouts) describing the route with reduced amount of points, (ii) local planning approach based on Bézier and specially focus on intersections, lane changes, and roundabouts (the straight and arc segment can be resolved as sequences of points), and (iii) the speed planning approach based on the same type of curves.

2.1. N-Bézier Curve Basis. Bézier is a type of parametric curve, which has been commonly used for computer graphics, animations, and path generation in robotics [27]. In general, they are good for real-time implementation, and the computational cost of designing them is lower than clothoids and splines curves [28]. Bézier curves are described by

$$\mathbf{B}\left(t \mid n, P_0, \ldots, P_n\right) = \sum_{i=0}^{n} b_i \mathbf{P}_i, \quad b_i = \binom{n}{i} t^i \left(1 - t\right)^{n-i} \quad (1)$$

where $\{b_i \in \mathbb{R}\}$ is the Bernstein polynomial, $\{\mathbf{P}_i \in \mathbb{R}^2\}$ are the control points used to generate the curve, $\{n \in \mathbb{N}^+\}$ is the Bézier order, and $\{t \in \mathbb{R}, t = [0, 1]\}$ is the parameter for curve construction.

These curves have several properties relevant for the purpose of the current work:

(i) The starting point of the Bézier curve corresponds with control point $\mathbf{P}_0$, and the ending point corresponds with $\mathbf{P}_n$.

(ii) The first point tangent vector (at $t = 0$) will be given by $\overrightarrow{P_0 P_1}$ and the last point tangent vector (at t = 1) will be given by $\overrightarrow{P_{n-1} P_n}$.

(iii) The curve will lie into the convex hull formed by the control points.

(iv) Bézier curves are continuous geometrically and in curvature $\{C^n$ & $G^n, \forall n \in \mathbb{N}^+\}$, and this continuity can be preserved in joints of two different curves.

(v) Bézier curves are symmetric, and the generated curve for $t : 0 \longrightarrow 1$ is equal to the one for $t : 1 \longrightarrow 0$.

This work uses 4th and 5th grade Bézier curves (some considerations with 3rd degree will be done). Higher order curves are not considered because they do not have additional benefits within current approach but increase the complexity [29].

Rewriting the general Bézier equation (see (1)) a more compact representation is obtained:

$$\mathbf{B}(t) = \mathbf{K}_0 + \mathbf{K}_1 t + \mathbf{K}_2 t^2 + \cdots + \mathbf{K}_n t^n \quad (2)$$

where each $\mathbf{K}_i$ will be a function of the control points (fixed position) and curve order. The values of $\mathbf{K}_i$ coefficients are

Table 1: Compact Bézier polynomial Coefficients "C".

| C | Bézier curve order | | |
	3rd Order	4th Order	5th Order
$\mathbf{K}_0$	$\mathbf{P}_0$	$\mathbf{P}_0$	$\mathbf{P}_0$
$\mathbf{K}_1$	$-3\mathbf{P}_0 + 3\mathbf{P}_1$	$-4\mathbf{P}_0 + 4\mathbf{P}_1$	$-5\mathbf{P}_0 + 5\mathbf{P}_1$
$\mathbf{K}_2$	$3\mathbf{P}_0 - 6\mathbf{P}_1 + 3\mathbf{P}_2$	$6\mathbf{P}_0 - 12\mathbf{P}_1 + 6\mathbf{P}_2$	$10\mathbf{P}_0 - 20\mathbf{P}_1 + 10\mathbf{P}_2$
$\mathbf{K}_3$	$-\mathbf{P}_0 + 3\mathbf{P}_1 - 3\mathbf{P}_2 + \mathbf{P}_3$	$-4\mathbf{P}_0 + 12\mathbf{P}_1 - 12\mathbf{P}_2 + 4\mathbf{P}_3$	$-10\mathbf{P}_0 + 30\mathbf{P}_1 - 30\mathbf{P}_2 + 10\mathbf{P}_3$
$\mathbf{K}_4$	–	$\mathbf{P}_0 - 4\mathbf{P}_1 + 6\mathbf{P}_2 - 4\mathbf{P}_3 + \mathbf{P}_4$	$5\mathbf{P}_0 - 20\mathbf{P}_1 + 30\mathbf{P}_2 - 20\mathbf{P}_3 + 5\mathbf{P}_4$
$\mathbf{K}_5$	–	–	$-\mathbf{P}_0 + 5\mathbf{P}_1 - 10\mathbf{P}_2 + 10\mathbf{P}_3 - 5\mathbf{P}_4 + \mathbf{P}_5$

given in Table 1. $\mathbf{K}_1$ and $\mathbf{K}_2$ determine curvature at starting and ending points of the curve, this property is going to be used repeatedly on explanations. Using the information from 3rd to 5th degree Bézier, $\mathbf{K}_1$ and $\mathbf{K}_2$ are defined as follows:

$$\mathbf{K}_1 = n\overrightarrow{v_1}$$

$$\mathbf{K}_2 = \frac{n(n-1)}{2}\left(\overrightarrow{v_2} - \overrightarrow{v_1}\right)$$

(3)

where $\overrightarrow{v_1} = \mathbf{P}_1 - \mathbf{P}_0$ and $\overrightarrow{v_2} = \mathbf{P}_2 - \mathbf{P}_1$ are introduced and n is the degree of the curve.

In general terms the curvature in $\mathbb{R}^2$ is defined as [30]

$$k(t) = \frac{\dot{B}_x(t)\ddot{B}_y(t) - \ddot{B}_x(t)\dot{B}_y(t)}{\sqrt{\left(\dot{B}_x(t)^2 + \dot{B}_y(t)^2\right)^3}} = \frac{\dot{\mathbf{B}}(t) \times \ddot{\mathbf{B}}(t)}{\left\|\dot{\mathbf{B}}(t)\right\|^3}$$

(4)

and in this case, function B is the Bézier equation. Evaluating at $t = 0$, it is obtained:

$$k(t = 0) = 2\frac{\mathbf{K}_1 \times \mathbf{K}_2}{\|\mathbf{K}_1\|^3} = \frac{(n-1)}{n}\frac{\overrightarrow{v_1} \times \overrightarrow{v_2}}{\|\overrightarrow{v_1}\|^3}$$

(5)

The previous equation explicitly shows that if the three starting points in a curve are colinear, generated Bézier curve will have zero curvature at its starting point ($k(t = 0) = 0$); this can be extended to the three ending points due to symmetry. This property is useful for designing the intersections and lane changes, and for the entrance and exit part of the roundabout.

2.2. Global Planning Environment Used for the Approach.

In this work, global planning is used as base route to apply the local planning approach using Bézier. A simple map containing a point to define intersections, roundabouts, or lane changes (point with "x" in Figures 1, 2 and 3) is the input of the global method, decreasing the amount of points and keeping geometric qualities of road.

2.2.1. Intersections.

Figure 1 depicts the description of an intersection using a single point (junction of 2 or more
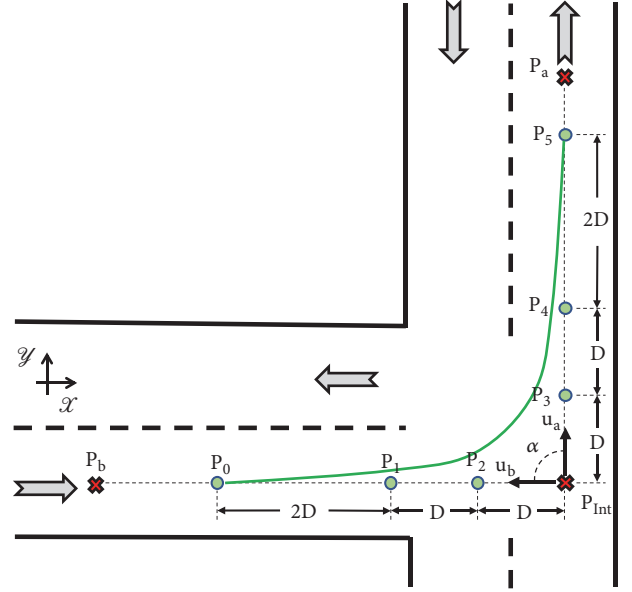
Figure 1: Trajectory planning on intersection.

straight paths). The unitary vectors defining the road (in intersection case) are given by

$$\overrightarrow{u_b} = \frac{\mathbf{P}_b - \mathbf{P}_i}{\|\mathbf{P}_b - \mathbf{P}_i\|}$$

$$\overrightarrow{u_a} = \frac{\mathbf{P}_a - \mathbf{P}_i}{\|\mathbf{P}_a - \mathbf{P}_i\|}$$

(6)

where $\overrightarrow{u_a}$ is an unitary vector that goes from intersection $\mathbf{P}_i$ to past global point $\mathbf{P}_b$ and $\overrightarrow{u_b}$ is other unitary vector formed with the next global points $\mathbf{P}_a$ and $\mathbf{P}_i$. It is relevant to see that the angle α (Figure 1) can be different from 90°, modeling a great variety of intersections. The parameter D will be used later in local planning and for the definition of $\mathbf{P}_i$.

2.2.2. Lane Changes.

In this case, the approach considers straight segments during the maneuver (Figure 2). The vectors for path description defined in (6) can be used for lane change and they have the following relation:

$$\overrightarrow{u_b} = -\overrightarrow{u_a}$$

(7)

FIGURE 2: Trajectory planning on lane change.

FIGURE 3: Trajectory planning on roundabouts.

Additionally, in this type of curve a new point $\mathbf{P}'_{LC}$ is introduced to handle the maneuver in local planning. This point is defined by

$$\mathbf{P}'_{LC} = \mathbf{P}_{LC} + w \begin{bmatrix} \cos\left(\tan^{-1}\left(\dfrac{u_{a_y}}{u_{a_x}}\right) \pm \dfrac{\pi}{2}\right) \\ \sin\left(\tan^{-1}\left(\dfrac{u_{a_y}}{u_{a_x}}\right) \pm \dfrac{\pi}{2}\right) \end{bmatrix} \quad (8)$$

where w is the road width and $\overrightarrow{u_a}$ is the vector presented in (7). The symbol $\pm$ is negative when the lane change is done to the right side and positive to the left side.

2.2.3. Roundabouts.
Figure 3 shows the definition of a roundabout using a simple point. It uses roundabout center point $\mathbf{P}_r$, its radius R, entrance angle a_i, and exit angle a_o. Using these parameters, the roundabouts can be modeled with an approximated circular shape.

Roundabout entrance and exit points are defined by

$$\mathbf{P}_e = \mathbf{P}_r + R \begin{bmatrix} \cos\left(\tan^{-1}\left(\dfrac{u_{b_y}}{u_{b_x}}\right) \pm a_i\right) \\ \sin\left(\tan^{-1}\left(\dfrac{u_{b_y}}{u_{b_x}}\right) \pm a_i\right) \end{bmatrix}$$

$$\mathbf{P}_{ex} = \mathbf{P}_r + R \begin{bmatrix} \cos\left(\tan^{-1}\left(\dfrac{u_{a_y}}{u_{a_x}}\right) \mp a_o\right) \\ \sin\left(\tan^{-1}\left(\dfrac{u_{a_y}}{u_{a_x}}\right) \mp a_o\right) \end{bmatrix} \quad (9)$$

where $\mathbf{P}_e$ is roundabout entrance coordinates, $\mathbf{P}_{ex}$ is roundabout exit coordinates, values of $\overrightarrow{u_a}$ and $\overrightarrow{u_b}$ are defined by (6), but the intersection point $\mathbf{P}_i$ is substituted by roundabout points $\mathbf{P}_{ex}$ and $\mathbf{P}_e$, respectively. In these equations, the upper sign is used when traffic is defined counter clockwise and lower one for clockwise traffic [31].

In addition to these two points, n_r points will be included (points with square shape in Figure 3) defining the route inside the roundabout. Following this procedure, the total amount of points substituting basic center point $\mathbf{P}_r$ will be given by $n_r + 2$.

2.3. Local Planning Method Based on Curvature.
The main contribution of the current paper is in the generation of smooth and continued curvature trajectories by definition in automatic vehicles. The principal goal is urban scenarios, but it is not limited to them; hence the section will be divided into three scenarios: intersections, roundabout, and lane changes.

2.3.1. Intersections.
Figure 1 shows an intersection defined using a single point. This configuration reduces the amount of point in map but demands a trajectory method to connect the two straight segments smoothly. Bézier curves of 5th order will be used to solved this problem.

As it is shown in (5), three Bézier control points (from $\mathbf{P}_0$ to $\mathbf{P}_2$) set over the same line will ensure curvature zero in the starting point of the curve $\{K(t = 0) = 0 : P_{y_{0,1,2}} = mP_{x_{0,1,2}} + b\}$; this means that the segment starts as a straight path. The same equation can be used to define curvature 0 in the ending part of the curve ($t = 1$) with control points $\mathbf{P}_n$ to $\mathbf{P}_{n-2}$ (symmetry criteria).

Using this definition is inferred that the minimum Bézier order that can be used in an intersection is 4th (5 control points), but in this case control point $\mathbf{P}_2$ will be set in the position of the intersection point $\mathbf{P}_i$. Hence, the 5th order is picked as a solution without the addition of many control points and less restrictive than 4th order. The position of the control points is shown in Table 2 where the vectors $\overrightarrow{u_b}$ and $\overrightarrow{u_a}$ are given by (6).

The distance of control points has been set to ensure that maximum curvature of Bézier curve is reached in middle point of the trajectory, in order to know if peak curvature is under the vehicle's mechanical limits. Figure 4 shows the normalized curvature $K/K_{\max}$ (curvature of the generated segment divided by the maximum curvature value) with respect to normalized trajectory distance $d/d_{\max}$ (total

TABLE 2: Bézier control points for lateral and longitudinal approach for intersections "Int", roundabout entrance "RE", roundabout exit "Rex", lane change maneuver "LC", and speed planning.

Planning		Control points n-order Bézier					
		P_0	P_1	P_2	P_3	P_4	P_5
Lateral	Int	$4D\vec{u_b} + \mathbf{P}_i$	$2D\vec{u_b} + \mathbf{P}_i$	$D\vec{u_b} + \mathbf{P}_i$	$D\vec{u_a} + \mathbf{P}_i$	$2D\vec{u_a} + \mathbf{P}_i$	$4D\vec{u_a} + \mathbf{P}_i$
	RE	$\frac{3D}{2}\vec{u_e} + \mathbf{P}_e$	$\frac{D}{2}\vec{u_e} + \mathbf{P}_e$	$\mathbf{P}_e$	$D_{P_3}\vec{u_{P_4}} + \mathbf{P}_4$	$\mathbf{P}_r + R\vec{u_{\theta_e}}$ *	-
	REx	$\mathbf{P}_r + R\vec{u_{\theta_{ex}}}$ **	$D_{P_1}\vec{u_{P_0}} + \mathbf{P}_0$	$\mathbf{P}_{ex}$	$\frac{D}{2}\vec{u_{ex}} + \mathbf{P}_{ex}$	$\frac{3D}{2}\vec{u_{ex}} + \mathbf{P}_{ex}$	-
	LC	$\frac{5\vec{u_b}D}{2} + \mathbf{P}_{LC}$	$\frac{3\vec{u_b}D}{2} + \mathbf{P}_{LC}$	$\frac{\vec{u_b}D}{2} + \mathbf{P}_{LC}$	$\frac{\vec{u_a}D}{2} + \mathbf{P}'_{LC}$	$\frac{3\vec{u_a}D}{2} + \mathbf{P}'_{LC}$	$\frac{5\vec{u_a}D}{2} + \mathbf{P}'_{LC}$
Longitudinal	Speed	$\begin{bmatrix} s_0 \\ v_0 \end{bmatrix}$	$\begin{bmatrix} s_0 + D \\ v_0 \end{bmatrix}$	$\begin{bmatrix} s_0 + 2D \\ v_0 \end{bmatrix}$	$\begin{bmatrix} s_0 + 3D \\ v_0 + W \end{bmatrix}$	$\begin{bmatrix} s_0 + 4D \\ v_0 + W \end{bmatrix}$	$\begin{bmatrix} s_0 + 5D \\ v_0 + W \end{bmatrix}$

* $\theta_e = \tan^{-1}((P_{e_y} - P_{r_y})/(P_{e_x} - P_{r_x}))$, $\vec{u_{\theta_e}} = \begin{bmatrix} \cos(\theta_e + D/R) & \sin(\theta_e + D/R) \end{bmatrix}$

** $\theta_{ex} = \tan^{-1}((P_{ex_y} - P_{r_y})/(P_{ex_x} - P_{r_x}))$, $\vec{u_{\theta_{ex}}} = \begin{bmatrix} \cos(\theta_{ex} - D/R) & \sin(\theta_{ex} - D/R) \end{bmatrix}$
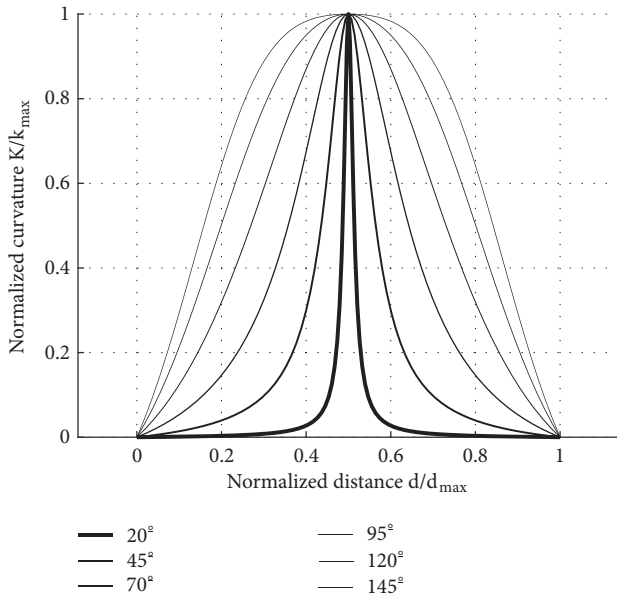

FIGURE 4: Curvature analysis for different intersection angles.

distance of the generated segment divided by the maximum one), considering angles between straight segments α from 20 degrees to 145 degrees.

With the purpose of finding the position of maximum curvature, it is applied derivative to (4):

$$\frac{d}{dt}K(t) = \frac{(\dot{\mathbf{B}} \times \ddot{\mathbf{B}})(\dot{\mathbf{B}} \cdot \dot{\mathbf{B}}) - 3(\dot{\mathbf{B}} \times \ddot{\mathbf{B}})(\dot{\mathbf{B}} \cdot \ddot{\mathbf{B}})}{\|\dot{\mathbf{B}}\|^5} \quad (10)$$

evaluating the derivative of Bézier curve in $t = 0.5$:

$$\dot{\mathbf{B}}(t = 0.5) = \frac{15}{4}D(\vec{u_2} - \vec{u_1})$$
$$\ddot{\mathbf{B}}(t = 0.5) = 10D(\vec{u_2} + \vec{u_1}) \quad (11)$$
$$\dddot{\mathbf{B}}(t = 0.5) = 0$$

where D is the design parameter for trajectory and $\vec{u_{1,2}}$ are unitary vectors defined by (3). From this set of equations it is obtained that $\dot{\mathbf{B}} \times \ddot{\mathbf{B}} = \dot{\mathbf{B}} \cdot \ddot{\mathbf{B}} = 0$ resulting in curvature equal to 0 in $t = 0.5$ (maximum value).

2.3.2. Roundabouts. Figure 3 shows the roundabout using simple point description. In such a way, roundabouts are modeled using two Bézier curves, each one is used to connect the straight road with the inner part, and the roundabout middle part is modeled as a circle with constant radius. The criteria used for design roundabouts trajectory have three considerations:

(i) The curvature at entrance in $t = 0$ or at exit in $t = 1$ points must be 0 (straight paths).

(ii) Generated segments at the entrance and exit of roundabout must fit its inner part with a curvature equal to the inverse of the radius.

(iii) Bézier joining point angle must be the same of the circle arc angle (continuous trajectory).

In order to follow the aforementioned criteria, 3 colinear control points are designed to ensure the first consideration; another 2 points are selected to form a tangent segment to the circle, which assures curvature and direction continuity (second and third criteria) along the roundabout (three colineal points will generate curvature 0 and not R^{-1}). Hence, a Bézier curve 4th order is used to ensure curvature zero in straight path side and different of 0 in the inner roundabout side for entrance and exit segments (Figure 3).

Table 2 shows the control points used for trajectory generation at entrance (RE) and exit (REx) of roundabouts. Control points from $\mathbf{P}_0$ to $\mathbf{P}_2$ in the case of entrance ($\mathbf{P}_2$ to $\mathbf{P}_4$ for exit) are designed using similar criteria as in intersections, with D as a designing parameter. The points $\mathbf{P}_4$ at entrance or $\mathbf{P}_0$ at exit are selected using the distance D in the arc of the circle from entrance or exit depending on the case.

(a) Generated trajectories
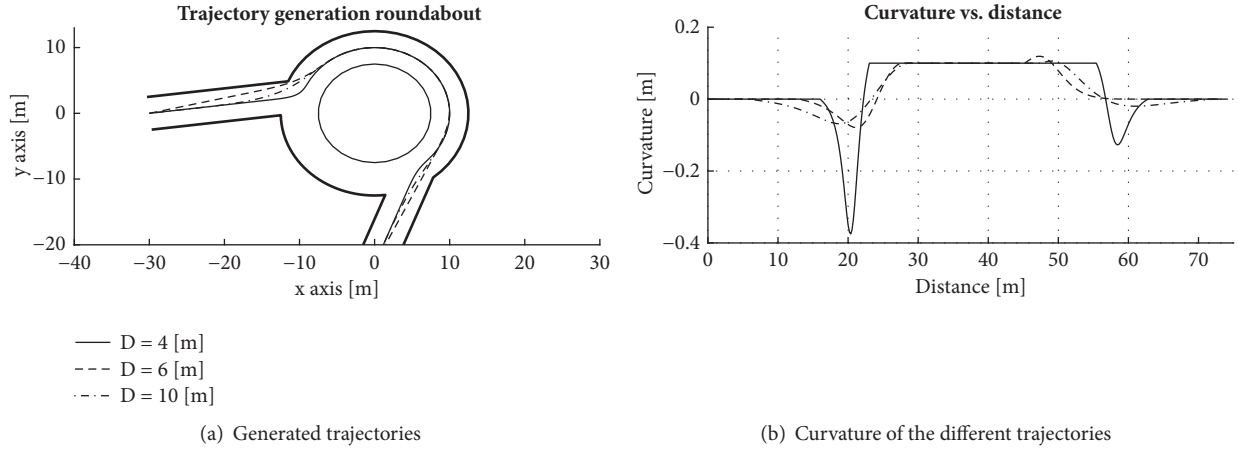
(b) Curvature of the different trajectories

FIGURE 5: Examples of roundabout trajectories for different D values.

The point $\mathbf{P}_3$, in entrance trajectory, is separated of point $\mathbf{P}_4$, a distance given by

$$D_{P_3} = \sqrt{\frac{3}{4} \frac{\left\| \overrightarrow{u_{P_4}} \times (\mathbf{P}_2 - \mathbf{P}_4) \right\|}{K_r}} \quad (12)$$

where $\overrightarrow{u_{P_4}}$ is the tangent vector (with the circle) in the point $\mathbf{P}_4$ and K_r is the roundabout curvature. In the case of exit, the point $\mathbf{P}_4$ is substitute by $\mathbf{P}_0$ and $\mathbf{P}_3$ by $\mathbf{P}_1$.

Figure 5 shows the behavior of trajectory generation and its curvature using the specifications given in the planning method. Figure 5(a) depicts 3 different trajectories generated for different distances D and Figure 5(b) shows the trajectories curvature fitting perfectly the curvature radius $0.1 [m^{-1}]$.

2.3.3. Lane Change.

The approach is done using similar criteria as intersections, but control points are aligned with lane axis and equidistant by a distance D (Figure 2). Where the unitary vectors u_b and u_a are explained in (7), w is the width of the road and D is the separation in u_a axis between each pair of control points $\{D \in \mathbb{R}, D = \|P_{n-1} - P_n\|_{u_a}\}$.

The location of control points is given in Table 2 (LC). The minimum value of D is set to w in our design; these criteria yield to a maximum curvature in $t \approx 0.20$ and $t \approx 0.80$ in the curve definition. If a vehicle is capable of dealing with this curvature considering dynamic limitations in steering wheel angle and lateral acceleration, it will be also capable of handling any trajectory with $D > W$.

The overtaking is considered as a special case composed by two lane changes; a first lane change is using the proposed method and when the first lane change is finished, this lane will be kept until the overtaking process is done. The returning will be done applying symmetry criteria and same propositions used in first lane change.

2.4. Speed Planning Based on Comfort and Vehicle Constraints.

The speed control is directly affected by sudden changes in reference speed, and if these changes are smooth and continuous the reference speed tracking will be done with

a better performance. In such a way a speed planner is proposed based on Bézier curves that permits:

(i) Anticipate future conditions in the speed of the road.

(ii) Applying physical constraints in vehicle acceleration and deceleration.

(iii) Keeping safely the vehicle velocity under speed limits.

(iv) Incorporating comfort of passengers.

The speed planner approach uses 5th order Bézier curve to keep advantages of a higher degree and symmetry. Figure 7 depicts the location of control points for a speed profile curve that is function of distance in the path. The formula related to each control point is presented in Table 2.

Define the separation between consecutive control points P_{i-1} and P_i as $\{D \in \mathbb{R}, D = distance_x(P_{i-1}, P_i) \; \forall i = 1, 2, 3, 4, 5\}$. These conditions generate Bézier curve x-coordinates proportional to the parameter t given by the equation

$$B_x(t) = 5Dt = s \quad (13)$$

with this equation is seeing that the distance in x-axis and the parameter $t \in [0, 1]$ have a proportional relationship. It is introduced $\{s \in [s_0, s_0 + 5D]\}$ to make the calculation easier (total distance of the speed curve).

The physical constraints of the vehicle (acceleration and deceleration process) will have a direct relation with the generated curve. In this case, it is considered the general equation that relates speed to acceleration and doing a variable change $v_l = ds/dt$, the resulting equation will be

$$a_l(t) = \frac{dv_l(t)}{dt} \implies a_l(s) = v_l(s) \frac{dv_l(s)}{ds} \quad (14)$$

where the variable a_l is longitudinal acceleration, v_l is longitudinal speed, t is time, and s position. Doing a nomenclature change from $v_l = B_y$ and $ds = dB_x = 5Ddt$ will result in the equation

$$a_l(s) = B_y \frac{dB_y}{dB_x} = B_y \frac{dB_y}{ds}, \quad s \in [s_0, s_0 + 5D] \quad (15)$$

(a) Speed planning with overlapped intersections

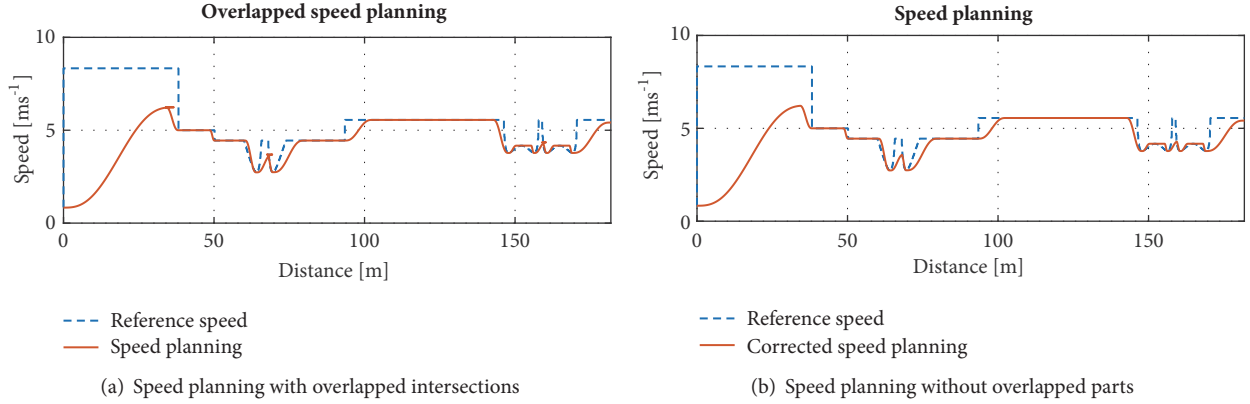(b) Speed planning without overlapped parts

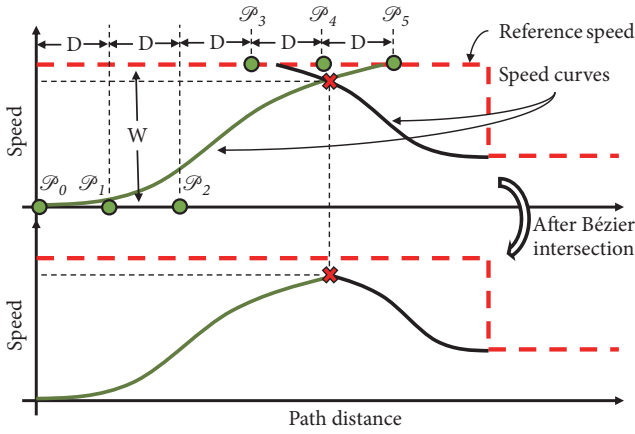FIGURE 6: Stages for speed planning approach.

FIGURE 7: Speed planning designing method.

Applying derivative to (15) maximum points of acceleration can be found. The resulting equation is

$$\frac{da_l}{ds} = \left(\frac{dB_y}{ds}\right)^2 + B_y \frac{d^2B_y}{ds^2} \qquad (16)$$

From (16), introducing the 5th order Bézier equation and doing some approximations, the following roots can be obtained:

$$s_{a_{max}} = 5D \begin{cases} \dfrac{0.49\,(v_o/W) + 0.88}{v_o/W + 1.41}, & \text{if } \dfrac{v_0}{W} > 0 \\[2mm] \dfrac{0.52\,(v_o/W) - 0.03}{v_o/W - 0.46}, & \text{if } \dfrac{v_0}{W} < -1 \end{cases} \qquad (17)$$

providing a direct solution for the maximum acceleration in a speed curve.

The first step in the speed planning method is applying the comfort speed limitation (reference speed) presented in [32] with the equation

$$a_\omega = \sqrt{(1.4a_x)^2 + (1.4v_l^2 K)^2 + a_z^2} \qquad (18)$$

where a_ω is the total acceleration felt by passengers (comfort criteria given by ISO2631-1); longitudinal acceleration a_x and vertical acceleration a_z contributions are approximated to zero (small changes ≈ 0), v_l is longitudinal speed, and K is curvature in each point of the path.

Figure 6(a) depicts speed planning approach with some segments overlapped one with the other. In this stage Bézier curves will be generated using the maximum acceleration criteria for each upward and downward (ensured to be under the speed limit) reference speed step. The intersections between curves will be calculated. In the example, these intersections appeared three times. Calculating the Bézier curve for each speed step (current segment is independent of the segment before) will ensure that numerical instabilities (accumulation of numerical errors by concatenated curves) will not be present a long time.

Finally, Figure 6(b) depicts the last stage in the speed planning calculation that will regenerate all the Bézier curves considering the intersections in speed profile, generating a smoother profile. This behavior can be easily understood looking at Figure 7. The profile will be constrained to the acceleration limits of the vehicle, considering comfort during driving process and keeping speed safely under road limits.

3. Integration on Automated Vehicle Architecture

The architecture presented in [22] is a versatile and modular framework composed by six abstraction blocks which defines the major areas of influence in automated driving applications: acquisition, perception, communication, decision, control, and actuation. This section gives an introduction to the aforementioned architecture combined with details of simulated and experimental platforms used in this approach. For further general details refer to [33].

Figure 8 shows a brief summary of each block that is contained within the architecture. Acquisition is in charge of gathering raw input data coming from real or simulated sensors in the vehicle and obtaining information such as position, velocity, acceleration, obstacles around, driver status, actuators position, and others. Perception has the goal
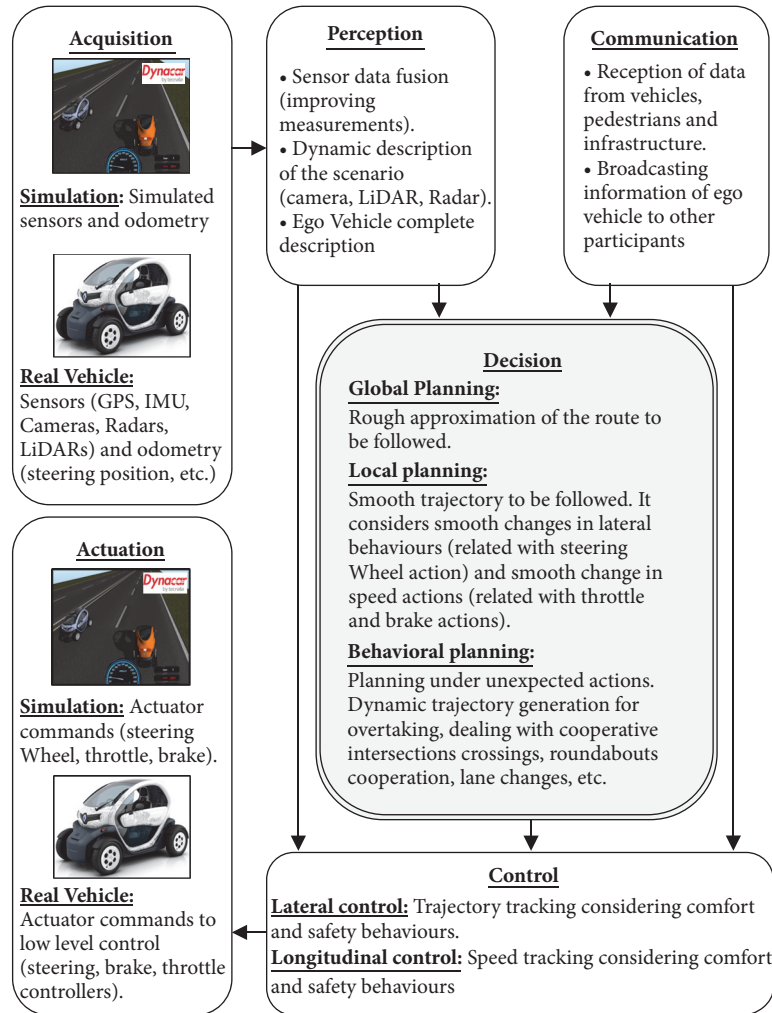
FIGURE 8: Control architecture of automated vehicles.

of postprocessing the information coming from acquisition generating descriptions on physical unit of the environment and the ego-vehicle. Communication refers to the capacities of exchanging information with other participants during driving (infrastructure, pedestrians, or other vehicles) to cooperate or knowing current states of other participants. Control is constituted for the lateral (steering) and longitudinal (throttle and brake) tracking controllers of the vehicle, and actuation contains the low level controllers of each actuator.

The decision module is the main target of the current work (grey coloured module in Figure 8) and it is divided into 3 main subtasks: those are as follows: (i) the global planning is in charge of doing a first approximation of the route; in the current work one general simple point for each roundabout, intersection, or lane change will be used; (ii) the local planning generates smooth and continues trajectories to be tracked by the vehicle; the major contributions of this work are done in this block with the Bézier trajectory designing conditions and the speed profile based on the same type of curves; finally, (iii) the

behavioral planning deals with all the unexpected conditions occurring while driving, e.g., obstacle avoidance, overtaking, etc.

4. Simulation Test Case

The current section explains the approach with a numerical example using the simulation tool Dynacar [34]. The test location corresponds with an urban scenario of the Basque Country in Spain. This is depicted in Figure 9(a) and it is constituted by 2 roundabouts, 3 right turns, and 6 left turns.

The total amount of points used in the map definition will be divided among: 1 starting point, 1 ending point, 9 intersections, and 2 roundabouts, resulting in 13 points defining all the route. Table 3 shows the x-y coordinates in meters (simulator absolute coordinate system), the reference speed in [m/s], and the type of point (1 for intersections and 2 for roundabouts). For roundabout global planning, additional information for its description is required: the radius (meters) and the angles of entrance and exit (radians).

(a) Trajectory generated with the approach

(b) Comparison of the longitudinal acceleration

(c) Comparison of the path curvature and simulated vehicle one
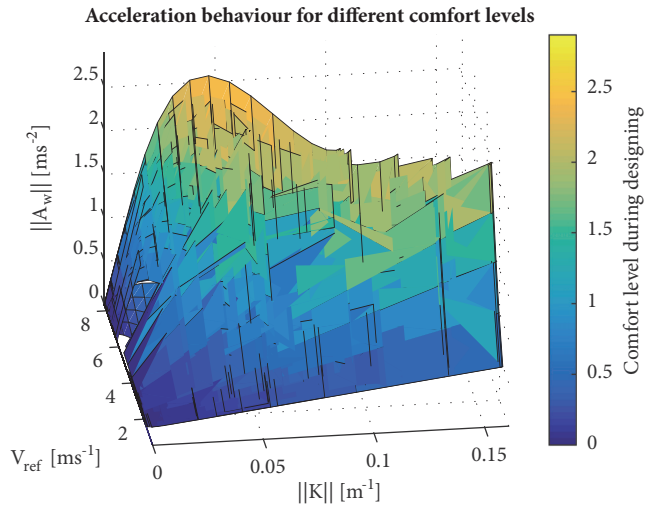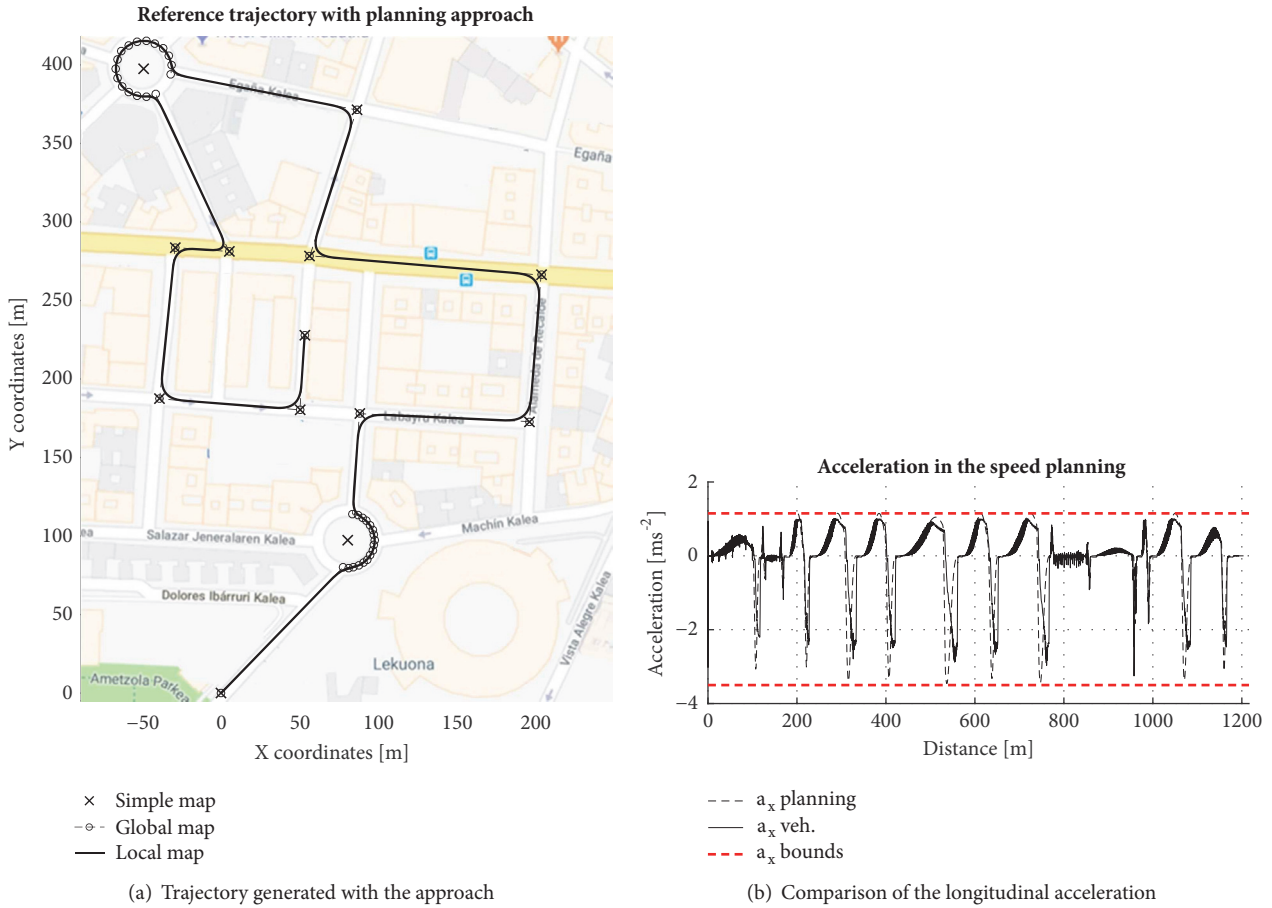
FIGURE 9: Simulated results based on real urban scenario.

The previously described points are shown in Figure 9(a) with a cross marker.

From this map a global plan is generated, which gives a better description of roundabouts in the bend segment (completion of the circle arc). In case of intersections, points in global planner coincide with those used to define the route

in the scenario. All the global planner points are depicted as circles in Figure 9(a).

The soft and continuous black line represents the trajectory generated using the Bézier approach. The values of D (designing parameter of the approach) are set by hand but they can be selected using optimization algorithm as in [31, 35].

TABLE 3: Point description of the map used for global planning.

X	Y	V	Type	R	a_i	a_o
[m]	[m]	[m/s]	[]	[1/m]	[rad]	[rad]
0.00	0.00	11.11	1	–	–	–
80.48	97.09	11.11	2	17.29	0.52	0.09
88.04	177.90	11.11	1	–	–	–
196.21	172.89	11.11	1	–	–	–
203.72	266.16	11.11	1	–	–	–
56.55	278.46	11.11	1	–	–	–
86.24	371.34	11.11	1	–	–	–
−49.30	397.61	11.11	2	17.76	0.00	0.00
5.08	281.16	11.11	1	–	–	–
−29.37	283.73	11.11	1	–	–	–
−39.17	187.34	11.11	1	–	–	–
50.16	180.36	11.11	1	–	–	–
53.19	227.94	11.11	1	–	–	–

An interesting example of the entrance/exit angle in the roundabouts is the one located in the absolute coordinates [80.48; 97.09]. This point is an entrance of a roundabout and it uses the definition of the entrance angle for its description (see (9)):

$$P_e = \begin{bmatrix} 80.48 \\ 97.09 \end{bmatrix} + 17.29 \begin{bmatrix} \cos(-2.26) \\ \sin(-2.26) \end{bmatrix} = \begin{bmatrix} 69.4 \\ 83.8 \end{bmatrix} \qquad (19)$$

The entrance point to present a numerical example is shown, but the exit point can be calculated using the same data and (9).

The speed planning defined for that trajectory is shown in Figure 9(b). The continuous line is the reference acceleration given by the speed profile of the urban scenario and the application of a comfort parameter $a_w = 0.5[m/s^2]$; based on [32] this amount of acceleration a_w corresponds with a value between "not uncomfortable" and "a little uncomfortable" for vehicle passengers. Results show that vehicle succeed on tracking the generated speed profile (by tracking the acceleration profile shown in dashed line). One major cause was the consideration of the maximum acceleration and deceleration (red bounds of Figure 9(b)).

Figure 9(c) shows a surface plot representing the different values of acceleration a_w with respect to the speed profile generated and the curvature of the path. Five different values of a_w were used: 0.5, 1.0, 1.5, 2.0, and 2.5[m/s^2] to generate the surface. Its objective is verifying the smooth and continued relationship with the Bézier speed profile and the level of comfort of the passenger.

5. Real Circuit Tests

The current section shows the trajectory planning approach used with the real vehicle. In this sense, two possible definitions of the route were implemented (Figure 10(a)). For both the center of the lane is used (taken from a manual driving record using GPS) as guide for the implementation of trajectories.

The first case is shown in the left side of Figure 10(a), where the trajectory described by the manual driving is modeled using intersection points in the 180[°] turn (roundabout). In this case, the error in the turning points (top and bottom of the circuit) is greater than using roundabout for the definition of the curve (right side Figure 10(a)).

The trajectory in the right side was tested with 5 different speed profiles and the behavior of the vehicle was analyzed with the curvature. Figure 10(b) depicts the results for these tests. Curvature of the vehicle in the trajectory is represented with a grey line and calculated according to the formula:

$$K(t) = \frac{\omega(t)\cos(\Phi(t))}{V_l(t)} \qquad (20)$$

where K is the curvature, ω is the rate of change of yaw, Φ is the roll angle of the vehicle, and V_l is the longitudinal speed. Curvature of the path is depicted in black and the vehicle is able to replicate the behavior of the planned curvature (the overshoots in curvature are caused by controllers).

Figure 10(c) shows vehicle lateral acceleration (as function of the vehicle speed and the curvature of the circuit) using different speed profiles, generated with a_w equal to 0.5, 1.0, 1.5, 2.0, and 2.5[m/s^2]. Values of total acceleration slightly overpass the limit of 2.5 at some points because the actuators delay is not considered for longitudinal control and the consideration of $a_x \approx 0$ in speed planning. Additionally, this figure shows the lateral acceleration in relationship with the curvature and the speed but without considering the total acceleration because in the speed planner those are assumed as zero. The lack of data taken, considerations over longitudinal acceleration, and controllers delay during tracking generate some surface holes without data. Table 4 shows the maximum acceleration obtained with the approach after filtering all the values $a_x > 0.005[m/s^2]$ (the approach considers $a_x \approx 0$). It is relevant to understand that those values must be filtered because actions like control behavior, delay of the controllers, or even the longitudinal acceleration are not considered and the magnitudes can differ. In general,
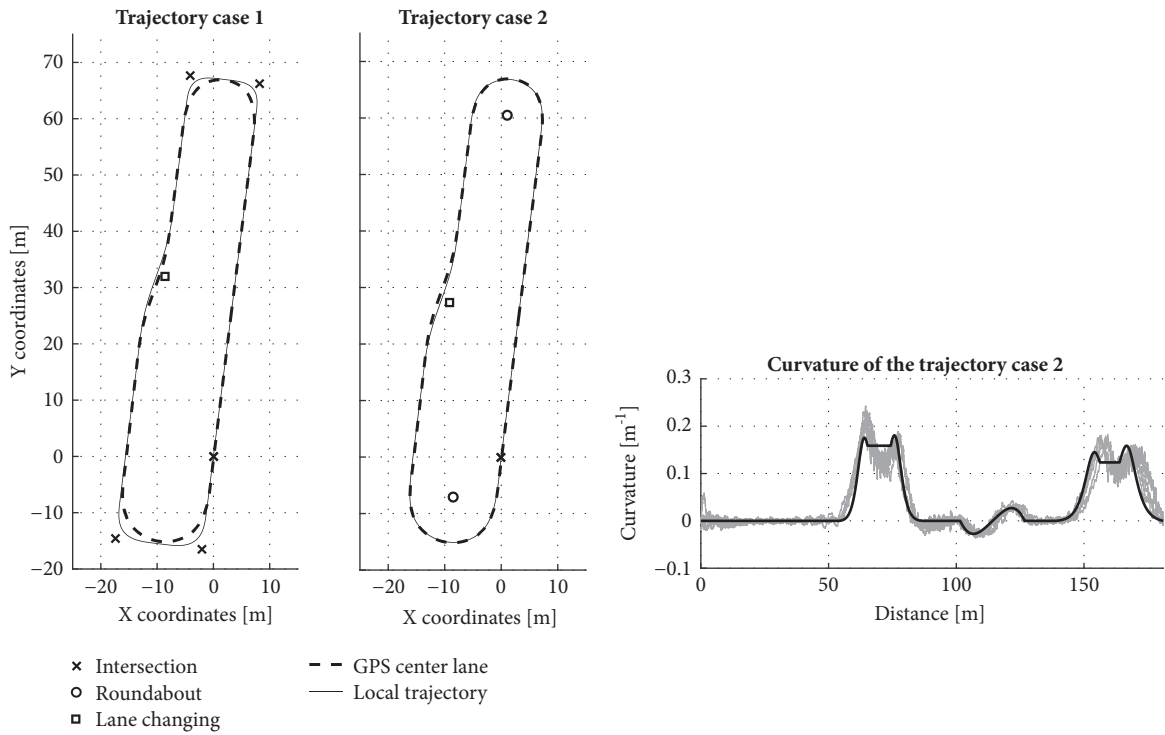
(a) Comparison in trajectory definition

(b) Comparison in trajectory definition
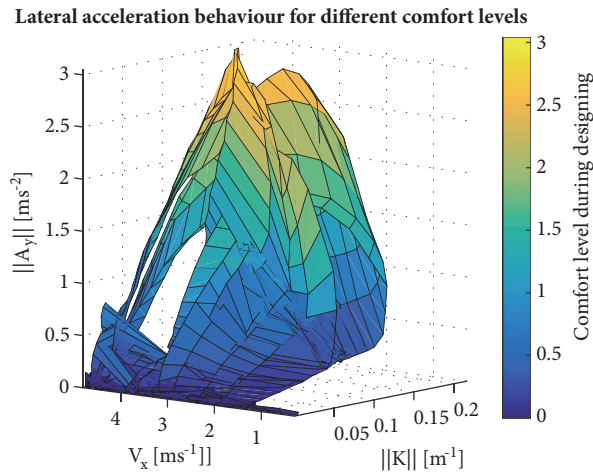
(c) Comparison in curvature for the trajectory definition case 2

FIGURE 10: Real life validation of the Bézier planning approach.

the results obtained are close to proposed values with parameter a_ω (designing).

6. Conclusion and Future Works

This work presents a trajectory and speed planning approach based on Bézier curves used in the decision module of an automated vehicle control architecture. The approach considers urban scenarios with intersections, roundabouts, and lane changes but it is not limited to those; the approach could also be used in scenarios such as highways. In the case of the speed planner, a parametric curve approach to adapt future changes in the speed limit considering physical constraints of the vehicle and traffic rules is presented (i.e., considering the maximum speed limit of the road).

Simplified mathematical models for trajectory planning using Bézier curves on intersections, roundabouts, and lane changes are presented reducing the time of calculation and allowing the use of these definitions for other applications, i.e., trajectory optimization process with computational efficiency. Additionally, the approach is evaluated using a simulated urban scenario based on a location of Basque Country showing that a great variety of urban scenario can be managed using this approach.

TABLE 4: Maximum lateral acceleration obtained in the real experiment using speed profile.

Uncomfortable levels	Not	A little	Fairly	Very	Extreme
Uncomfortable magnitudes $a_\omega [m/s^2]$	0.5	1.0	1.5	2.0	2.5
Filtered max. values $[m/s^2]$	0.45	1.03	1.54	2.00	3.02

The trajectory planner was tested for automated driving, using a comparison of the trajectory with the Bézier curves and the one generated using a manual GPS recording in manual driving. Additionally the generated curvature in the vehicle for different conditions (variations in the speed profile) was compared with the curvature of the trajectory planned showing that it is feasible to be tracked by the vehicle.

The speed planning approach shows the capability of using parametric curves to generate a profile to be tracked correctly by the vehicle, giving a prediction of future behaviors. Consideration of longitudinal acceleration in curve segments is one of the future improvements related to the speed planner of this work.

This approach is considered better than others due to the fact that it includes comfort and safety criteria during trajectory and speed planning. For comfort the ISO2631-1 standard to generate speed profiles based on geometric information given by the trajectory planning was considered. Comfortable speed profiles are related to trajectories and this can be associated with safety during driving (vehicle lateral forces are related to possible dangerous situations), and additionally a continuous curvature of the trajectory planned can reduce possible unexpected situations given by vehicle' automatic control (increasing safety).

Some of the future works are related to using the presented method to generate possible optimal solutions in terms of the parameter D, road geometry, and vehicle dynamics and in such way, substituting the definition by hand of parameter D during trajectory planning.

Data Availability

The datasets generated during and/or analyzed during the current study are available from the corresponding author on reasonable request.

Conflicts of Interest

The authors declare that they have no conflicts of interest.

Acknowledgments

References

[1] J.-w. Choi, R. E. Curry, and G. H. Elkaim, "Path planning based on Bézier curve for autonomous ground vehicles," in *Proceedings of the IEEE Advances in Electrical and Electronics Engineering—IAENG Special Edition of the World Congress on Engineering and Computer Science 2008, WCECS 08*, pp. 158–166, October 2008.

[2] L. Han, H. Yashiro, H. T. N. Nejad, Q. H. Do, and S. Mita, "Bézier curve based path planning for autonomous vehicle in urban environment," in *Proceedings of the 2010 IEEE Intelligent Vehicles Symposium, IV 2010*, pp. 1036–1042, USA, June 2010.

[3] L. Labakhua, U. Nunes, R. Rodrigues, and F. S. Leite, "Smooth trajectory planning for fully automated passengers vehicles: Spline and clothoid based methods and its simulation," *Informatics in control automation and robotics*, pp. 169–182, 2008.

[4] R. Lattarulo, J. Pérez, and M. Dendaluce, "A complete framework for developing and testing automated driving controllers," *IFAC-PapersOnLine*, vol. 50, no. 1, pp. 258–263, 2017.

[5] R. Lattarulo, M. Marcano, and J. Pérez, "Overtaking maneuver for automated driving using virtual environments," in *Proceedings of the Springer International Conference on Computer Aided Systems Theory*, pp. 446–453, 2018.

[6] J. P. Rastelli, R. Lattarulo, and F. Nashashibi, "Dynamic trajectory generation using continuous-curvature algorithms for door to door assistance vehicles," in *Proceedings of the 25th IEEE Intelligent Vehicles Symposium, IV 2014*, pp. 510–515, IEEE, June 2014.

[7] D. González, J. Pérez, R. Lattarulo, V. Milanés, and F. Nashashibi, "Continuous curvature planning with obstacle avoidance capabilities in urban scenarios," in *Proceedings of the 2014 17th IEEE International Conference on Intelligent Transportation Systems, ITSC 2014*, pp. 1430–1435, China, October 2014.

[8] R. Lattarulo, E. Marti, M. Marcano, J. Matute, and J. Perez, "A Speed Planner Approach Based On Bézier Curves Using Vehicle Dynamic Constrains and Passengers Comfort," in *Proceedings of the 2018 IEEE International Symposium on Circuits and Systems (ISCAS)*, pp. 1–5, Florence, Italy, May 2018.

[9] D. González, J. Pérez, V. Milanés, and F. Nashashibi, "A Review of Motion Planning Techniques for Automated Vehicles," *IEEE Transactions on Intelligent Transportation Systems*, vol. 17, no. 4, pp. 1135–1145, 2016.

[10] US Department of Transportation, *Critical Reasons for Crashes Investigated in the National Motor Vehicle Crash Causation Survey*, NHTSA Traffic Safety Facts Crash Stats, February 2015.

[11] J. Dokic, B. Müller, and G. Meyer, "European roadmap smart systems for automated driving," *European Technology Platform on Smart Systems Integration*, January 2015.

[12] G. Meyer and S. Deix, "Research and innovation for automated driving in germany and europe," pp. 71–81, Springer Road Vehicle Automation, 2014.

[13] E. Adell, A. Várhelyi, and M. D. Fontana, "The effects of a driver assistance system for safe speed and safe distance - A real-life field study," *Transportation Research Part C: Emerging Technologies*, vol. 19, no. 1, pp. 145–155, 2011.

[14] J. Ni and J. Hu, "Dynamics control of autonomous vehicle at driving limits and experiment on an autonomous formula racing car," *Mechanical Systems and Signal Processing*, vol. 90, pp. 154–174, 2017.

[15] M. Zhu, H. Chen, and G. Xiong, "A model predictive speed tracking control approach for autonomous ground vehicles," *Mechanical Systems and Signal Processing*, vol. 87, pp. 138–152, 2017.

[16] R. Domínguez, E. Onieva, J. Alonso, J. Villagra, and C. González, "LIDAR based perception solution for autonomous vehicles," in *Proceedings of the 2011 11th International Conference on Intelligent Systems Design and Applications, ISDA'11*, pp. 790–795, Spain, November 2011.

[17] J.-P. Jodoin, G.-A. Bilodeau, and N. Saunier, "Urban Tracker: Multiple object tracking in urban mixed traffic," in *Proceedings of the 2014 IEEE Winter Conference on Applications of Computer Vision, WACV 2014*, pp. 885–892, USA, March 2014.

[18] L. Li, D. Wen, and D. Yao, "A survey of traffic control with vehicular communications," *IEEE Transactions on Intelligent Transportation Systems*, vol. 15, no. 1, pp. 425–432, 2014.

[19] D. J. Fagnant and K. Kockelman, "Preparing a nation for autonomous vehicles: Opportunities, barriers and policy recommendations," *Transportation Research Part A: Policy and Practice*, vol. 77, pp. 167–181, 2015.

[20] N. Wan, A. Vahidi, and A. Luckow, "Optimal speed advisory for connected vehicles in arterial roads and the impact on mixed traffic," *Transportation Research Part C: Emerging Technologies*, vol. 69, pp. 548–563, 2016.

[21] W. Cao, M. Mukai, T. Kawabe, H. Nishira, and N. Fujiki, "Cooperative vehicle path generation during merging using model predictive control with real-time optimization," *Control Engineering Practice*, vol. 34, pp. 98–105, 2015.

[22] T. Shim, G. Adireddy, and H. Yuan, "Autonomous vehicle collision avoidance system using path planning and model-predictive-control-based active front steering and wheel torque control," *Proceedings of the Institution of Mechanical Engineers, Part D: Journal of Automobile Engineering*, vol. 226, no. 6, pp. 767–778, 2012.

[23] T. Gu, J. Snider, J. M. Dolan, and J.-W. Lee, "Focused Trajectory Planning for autonomous on-road driving," in *Proceedings of the 2013 IEEE Intelligent Vehicles Symposium, IEEE IV 2013*, pp. 547–552, Australia, June 2013.

[24] A. Best, S. Narang, D. Barber, and D. Manocha, "AutonoVi: Autonomous vehicle planning with dynamic maneuvers and traffic constraints," in *Proceedings of the 2017 IEEE/RSJ International Conference on Intelligent Robots and Systems (IROS)*, pp. 2629–2636, Vancouver, BC, September 2017.

[25] H. Mouhagir, R. Talj, V. Cherfaoui, F. Guillemard, and F. Aioun, "A Markov Decision Process-based approach for trajectory planning with clothoid tentacles," in *Proceedings of the 2016 IEEE Intelligent Vehicles Symposium, IV 2016*, pp. 1254–1259, Sweden, June 2016.

[26] M. Du, T. Mei, H. Liang, J. Chen, R. Huang, and P. Zhao, "Drivers' Visual Behavior-Guided RRT Motion Planner for Autonomous On-Road Driving," *Sensors*, vol. 16, no. 1, p. 102, 2016.

[27] US Department of Transportation, *A Brief Statistical Summary: Drowsy Driving*, NHTSA: Traffic Safety Facts Crash Stats, March 2011.

[28] A. G. Cunningham, E. Galceran, R. M. Eustice, and E. Olson, "MPDM: multipolicy decision-making in dynamic, uncertain environments for autonomous driving," in *Proceedings of the IEEE International Conference on Robotics and Automation (ICRA '15)*, pp. 1670–1677, Seattle, Wash, USA, May 2015.

[29] K. Zhou, L. Yu, Z. Long, and S. Mo, "Local path planning of driverless car navigation based on jump point search method under urban environment," *Future Internet*, vol. 9, no. 3, 2017.

[30] C. Hubmann, M. Aeberhard, and C. Stiller, "A generic driving strategy for urban environments," in *Proceedings of the 19th IEEE International Conference on Intelligent Transportation Systems, ITSC 2016*, pp. 1010–1016, Brazil, November 2016.

[31] X. Qian, I. Navarro, A. De La Fortelle, and F. Moutarde, "Motion planning for urban autonomous driving using bezier curves and MPC," in *Proceedings of the 19th IEEE International Conference on Intelligent Transportation Systems, ITSC 2016*, pp. 826–833, Brazil, November 2016.

[32] V. Desaraju, H. C. Ro, M. Yang, E. Tay, S. Roth, and D. Del Vecchio, "Partial order techniques for vehicle collision avoidance: Application to an autonomous roundabout test-bed," in *Proceedings of the 2009 IEEE International Conference on Robotics and Automation, ICRA '09*, pp. 82–87, Japan, May 2009.

[33] S. Glaser, B. Vanholme, S. Mammar, D. Gruyer, and L. Nouvelière, "Maneuver-based trajectory planning for highly autonomous vehicles on real road with traffic and driver interaction," *IEEE Transactions on Intelligent Transportation Systems*, vol. 11, no. 3, pp. 589–606, 2010.

[34] H. Delingette, M. Herbert, and K. Ikeluchi, "Trajectory generation with curvature constraint based on energy minimization," in *Proceedings of the IEEE/RSJ International Workshop on Intelligent Robots and Systems (IROS '91)*, vol. 1, pp. 206–211, Osaka, Japan, November 1991.

[35] J. Cuadrado, D. Vilela, I. Iglesias, A. Martín, and A. Peña, "A multibody model to assess the effect of automotive motor in-wheel configuration on vehicle stability and comfort," in *Proceedings of the ECCOMAS Thematic Conference on Multibody Dynamics*, pp. 1083–1092, 2013.

Research Article

Evaluation of the Rain Effects on Gap Acceptance Behavior at Roundabouts by a Logit Model

Dongmin Lee,[1] Sooncheon Hwang,[2] Eunhan Ka,[3] and Chungwon Lee (iD) [4]

[1]*Associate Professor, Department of Transportation Engineering, University of Seoul, 163 Seoulsiripdae-ro,*
Dongdaemun-gu, Seoul 02504, Republic of Korea
[2]*Graduate Student, Department of Transportation Engineering, The University of Seoul, Korea Seoulsiripdaero 163,*
Dongdaemun-gu, Seoul 02504, Republic of Korea
[3]*Researcher, Institute of Construction and Environmental Engineering, Seoul National University, 1 Gwanak-ro, Gwanak-gu,*
Seoul 08826, Republic of Korea
[4]*Associate Professor, Department of Civil and Environmental Engineering, Seoul National University, Korea 1 Gwanak-ro,*
Gwanak-gu, Seoul 151-744, Republic of Korea

Correspondence should be addressed to Chungwon Lee; chungwon@snu.ac.kr

A roundabout is generally known as an efficient, safe, and environmentally friendly intersection. Since 2010, the Korea government has taken the lead in constructing roundabouts as part of a special project. During that time, many ideas have been put forward to improve the safety, operation, and design of such roundabouts. In terms of improvements, it is particularly important to understand roundabout gap acceptance behavior. As such, we investigated gap acceptance behaviors at four roundabouts based on field observation during both good weather and rainy conditions. Based on the observed data, roundabout critical gaps were estimated, and a logit model for gap acceptance using various roundabout variables was developed to investigate gap acceptance maneuvering at roundabouts. A total of 2,421 data events for gap acceptance were collected from the field observation. Out of these events, 64.6% of drivers (1,564 drivers) accepted the given gaps and 35.4% of drivers (857 drivers) rejected them. The values for critical gaps were estimated using several different estimation methods and ranged from 3.3 to 4.7 seconds. The model was developed using four variables including gap size, type of circulating vehicle, traffic volume at the circulating lane, and weather conditions. The developed model shows that a longer gap results in a 3.669 times higher probability of entering roundabouts when the gap is sufficiently great for acceptance than when the gap is smaller. The effects of other variables, such as circulating vehicle types, circulating traffic volume, and weather conditions, are relatively lower than that of a gap size. Rain conditions influenced gap acceptance maneuvering around a roundabout. Drivers need about a 10 percent longer gap to accept entry into roundabouts during rainy conditions, and gap acceptance probabilities are 10 to 20 percent lower for the same given gap time during rainy conditions compared to good weather conditions.

1. Introduction

A roundabout is generally defined as a form of a circular intersection in which traffic travels counterclockwise around a central island and in which entering traffic must yield to circulating traffic [1]. Roundabouts are generally considered an efficient intersection system to reduce intersection travel time, a safe intersection design to decrease the number of accidents and damage from accidents, and environmentally friendly. As such, many countries have incorporated roundabouts in their road designs, including Korea. Since 2010, roundabouts have been constructed in Korea as part of a special government-led project. After 87 roundabouts were constructed in 2010, about 20 to 100 roundabouts are constructed every year. There have been improvements in safety and efficiency benefits due to such construction. However, there have also been many issues and ideas put forward to improve those roundabouts in terms of safety, operation, and

TABLE 1: Mean crash reductions of conversion to roundabouts.

Country	Mean Reductions (%)	
	All Crashes	Injury Crashes
Australia	41-61%	45-87%
Frances	-	57-78%
Germany	36%	-
Netherlands	47%	-
United Kingdom	-	25-39%
United States	35%	76%

Source: [1].

design. Of particular importance for design considerations is an understanding of roundabout gap acceptance behavior.

Although many studies regarding safety and efficiency effects have investigated roundabouts, there were few empirical studies investigating driver behavior at roundabouts. In roundabouts, traffic flows move based on a yield mechanism of the right-of-way principle that circulating traffic has a right-of-way compared to entering traffic. Entering traffic have to yield to circulating traffic inside roundabouts. Due to this roundabout operation principle, the availability of entering into roundabouts, which is a critical element that influences capacity, is determined by considering the gap size of circulating traffic inside the roundabouts. As such, gap acceptance is very significant in roundabouts. In the US Highway Capacity Manual (HCM), the most important elements are the critical gap in circulating traffic and follow-up time of entering traffic [2].

Therefore, our study investigated gap acceptance behaviors at roundabouts based on field observation. The purpose of this study is to estimate the critical gap for roundabouts by using various estimation methods. We also develop a logit model for gap acceptance using various influencing factors at roundabouts to investigate gap acceptance maneuvers. The gap acceptance maneuver at roundabouts is generally affected by weather conditions including rain and snow. Thus, we developed a logit model for gap acceptance at roundabouts that included weather variables.

2. Literature Review

2.1. Roundabouts. The first roundabout was a circle-shaped intersection built in 1905 at Columbus Circle in New York City [1]. This circle shape intersection was called a traffic circle and was designed to enable high-speed entry with priority and slow circulation that yielded to entering traffic. Before traffic volumes significantly increased, traffic circles worked well. However, as traffic volumes increased, traffic circles started to have safety and efficiency problems. Rectifying these problems led to the development of the modern roundabout in the 1960s. The United Kingdom imposed a new rule that required entering traffic to yield and give way to circulating traffic. This rule prohibited vehicles from entering the intersection as incoming traffic until there were sufficient gaps in the circulating traffic. This approach improved the

safety and efficiency of circular intersections. Due to the advantages of roundabouts, many countries adopted modern roundabouts as a common circular intersection and have developed extensive design guides and methods to evaluate operational performance. Many studies have evaluated the effects of roundabout adaptation, typically accident reduction effects. In the United States, conversion to a roundabout results in a reduction of 35% and 76% in total and injury crashes, respectively. These accident reduction effects are similar to results from studies in other countries, as shown in Table 1.

Meanwhile, there have been recently many studies to overcome disadvantages of standard roundabouts in particular actual circumstance. And they suggested to implicate some alternative types of roundabouts such as a Turbo-roundabout, an Assembly roundabout, a traffic signal controlled roundabout, a Dog-bone roundabout, and other new types of roundabouts [3]. Out of these alternative types of roundabouts, a Turbo-roundabout was developed and installed at the end of the 1990s in The Netherlands. The Turbo-roundabout is a type of roundabouts to improve two-lane roundabouts in safety and capacity through eliminating the necessity of weaving and conflicts by the divided curbs [4–6].

2.2. Critical Gap and Follow-Up Time in Roundabouts. The capacity of a roundabout is determined by three traffic flows around the roundabouts: entering traffic, circulating traffic, and exiting traffic. The capacity of a roundabout decreases as the circulating traffic flow increases. Maneuvering is similar to the effect of a right-turning stream [2]. In the process of estimating capacity, there are two main measures: critical gap in circulating traffic and follow-up time for entry traffic. The critical gap from circulating traffic is the minimum time gap that an entering driver would accept to merge into the circulating lane of the roundabout. A driver rejects any gaps less than the critical gap and accepts any gap that is greater. In US studies, critical gap and follow-up time were 4.5 to 5.1 seconds and 3.2 to 3.4 seconds, respectively, in single roundabouts [7]. In Korea, a field experiment was also conducted to estimate critical gap and follow-up time in roundabouts and found them, estimated using Wu's method, to be 5.6 seconds and 2.3 seconds, respectively [8]. The critical gap and the follow-up time measured from the experiment

were relatively greater and smaller than the results in other countries.

2.3. Previous Studies of Gap Acceptance Behavior. Due to the importance of gap acceptance maneuvers in unsignalized intersections and roundabouts, methods have been developed to estimate critical gap, including the Raff method, the Ashworth method, the Troubeck method, and the Wu method. The Raff method is a critical gap estimation method using two cumulative distributions of accepted and rejected gaps [9], and the Ashworth method is based on the hypothesis that average critical gap may be evaluated from the mean of accepted gaps [10]. Meanwhile, the Troubeck method estimates critical gap estimation using a maximum likelihood estimation [11] and is applied with an assumption that the distribution of critical gaps follows a log-normal distribution and calculates the probability that the critical gap would be between the largest rejected and accepted gaps. The Wu method was developed recently and estimates critical gaps based on an equilibrium of a probability concept [12].

These critical gap estimation methods assume, however, that drivers' behavior remains consistent and all drivers are homogeneous in a deterministic approach. As is well known, a deterministic gap acceptance estimation can estimate only the mean critical gap acceptance from the population, and careful drivers may be overrepresented as a result of information loss [13]. To overcome these limitations, a discrete choice model is used to estimate gap acceptance as probability and only the mean value of gap acceptance based on the probability function for success in accepting a gap. Originally in 1981, Daganzo developed a discrete choice model to estimate gap acceptance based on this probability function. This discrete choice model produces the probability function for success in accepting a gap [14]. This discrete choice model to estimate gap acceptance can be formularized based on the distribution of the mean and variance of the gap acceptance function parameter [15]. Mahmassani and Sheffi used a probit model to investigate gap acceptance behavior. They found that the critical gap decreases as long as drivers are waiting for an acceptable gap [16]. The effects of waiting time on gap acceptance were explained by Polus and his research team [17]. A logit model is one of the currently more popular models to explain gap acceptance behavior [18–25].

Weather conditions generally influence driver behaviors such as for speeding, braking maneuvers, gap acceptance behaviors, and other driving behaviors. A FHWA study showed that inclement weather influences such microscopic traffic behavior [26]. This study investigated changes in driver gap acceptance behavior on intersections during rainy weather conditions. They found that there is a more careful driving behavior for left-turn gap acceptance in the rain, and drivers need greater critical gaps. Zohdy and colleagues found that a larger value for the critical gap for a left turn is needed as the intensity of rain increases [18].

2.4. Studies of Gap Acceptance Maneuver in Roundabouts. Investigation of gap acceptance behavior in roundabouts has been conducted thru two approaches. Most of studies estimated critical gap and follow-up time, which are the two key parameters for gap acceptance. Other studies developed roundabout gap acceptance behavior models and there are many different values for critical and follow-up time for roundabouts, which are summarized in Table 2. Xu and Tian investigated gap acceptance characteristics at roundabouts in California, US [27], and the critical gaps were estimated in the range of 4.5 to 5.3 seconds at eight single roundabouts. They found that circulating flow rate and speed are two major influencing factors for critical gap and follow-up time.

Polus and his colleagues developed a disaggregate logit model to evaluate the waiting time effect on critical gaps at a roundabout [17] and included only two variables: waiting time and gap size. In their study, critical gaps at roundabouts were calculated in the range of 2 to 5 seconds and the waiting time may affect gaps in those ranges. However, gaps lower than 2 seconds were not likely to be accepted because the risk was considered too high.

2.5. Effects of Roundabout Construction in Korea. In Korea, roundabout construction has been led by federal agencies, typically the Presidential Council on National Competitiveness, the Ministry of Land, Transport and Maritime Affairs, the Ministry of Public Administration and Security, National Police Agency, and some research institutes. Currently, there are more than 500 roundabouts that have been constructed with federal government subsidies and with only local government funding. The roundabouts have been considered successful, and the construction of roundabouts continues to accelerate. Half of the roundabouts were constructed in urban areas and the others in rural areas. In most of these roundabouts, the number of crashes and the damage from the crashes were significantly reduced, and intersection traffic operational performance improved. Most residents were also satisfied with the conversion from signalized and unsignalized intersections to roundabouts. Overall, there has been an observed reduction of 46.1% in total crashes and 66.7% in fatality as shown in Table 3.

3. Methodology

3.1. Data Collection. Field observations for this study were conducted in Seoul, South Korea, at four typical roundabouts designed using the Korean roundabout design guide [15]. Preliminary observations were conducted at 19 roundabouts, and then four roundabouts were selected for study sites after a final consideration of final design layouts and traffic volume. The field observations were conducted via video recording on both sunny and rainy days. Rainy days selected for data collection were days with more than 5 mm of rainfall. Videos were recorded at time periods from 7:00 A.M. to 9:00 A.M. for morning peak time, from 12:00 P.M. to 2:00 P.M. for afternoon nonpeak time, and from 6:00 P.M. to 8:00 P.M. during evening peak time. Basic characteristics of the four intersections are summarized in Table 4. Data for gap acceptance behaviors were extracted from the recorded video images using video editing equipment to measure more detailed values of gaps.

TABLE 2: Critical and follow-up headways values in previous studies.

Study name	Country	Critical Gap (Sec.)	Follow-up headway (Sec.)
Abdullah Ahmad	India	2.5 ~ 3.0	-
Abrams et al.	US	2.20	-
Brilon	Germany	4.07 ~ 4.45	2.89 ~ 2.99
Cheng Jie	China	4.1 ~ 5.4	-
Dahl & Lee	Canada	3.90 ~ 5.30	2.10 ~ 4.20
Feng Xu	US	4.5 ~ 5.3	-
Fortuijn	The Netherlands	3.16 ~ 3.28	2.10
Gazzarri et al.	Italy	3.54 ~ 4.10	2.52 ~ 2.76
Guo Ruijun	China	2.7	-
HCM (2010)	US	4.1	-
Iraj Bargego	Iran	2.52 ~ 4.03	-
KHCM (2013)	South Korea	3.21	-
Kim, T	South Korea	2.42 ~ 2.7	-
Liang Ren	Australia	4.6 ~ 4.8	-
Mensah S. el al.	US	2.50 ~ 2.60	-
NCHRP (3-65)	US	4.2 ~ 5.9	-
Nicolosi et al.	Italy	3.19 ~ 3.99	3.15 ~ 2.11
Park, S	South Korea	3.7 ~ 4.1	-
Qu X et al.	Australia	-	-
Rodegerdts et al.	US	3.90 ~ 5.90	2.60 ~ 4.30
Shweta Rao	India	1.36 ~ 2.52	-
Vasconcelos et al.	Portugal	3.23 ~ 4.50	-
Vasconcelos et al.	Portugal	3.37 ~ 4.28	2.08 ~ 2.20
Wu	Germany	4.12	2.88
Xu & Tian	US	4.50 ~ 5.30	2.30 ~ 2.80
Zheng et al.	US	3.80 ~ 5.50	2.30 ~ 3.80

Sources: [27–37].

TABLE 3: Accident reduction effects of roundabout in Korea.

Before/After Roundabouts	Average Annual Crashes				
	Total	Fatality	Severe Injury	Injury	Minor Injury
Before	571	15	258	274	24
After	308	5	118	171	14
%	-46.1%	-66.7%	-54.3%	-37.6%	-41.7%

Source: Korean Roundabout Research Center (http://www.roundabout.or.kr/).

Figure 1 shows the maneuvering of gap acceptance at roundabouts according to the sequence of arriving vehicles at the entry lane and circulating vehicles in the circulatory lane. As shown in Figure 1, the difference in the times when circulating vehicles are passing the gap acceptance decision line can be explained as a gap. This decision line is an imaginary line that drivers at the entry lane use to decide whether to enter or not a circulatory lane while looking at oncoming circulatory vehicle traffic. The gap acceptance maneuver is preceded by the decision to accept or decline the circulating vehicle gap as adequate for entry.

This maneuver is illustrated in Figure 1. When entering vehicle #1 arrives at the yield line ① in the middle of the gap of the conflicting vehicles (#1 and #2), the entering vehicle using gap (a) is rejected because the gap (a) is insufficient to safely enter the roundabout as shown in Figure 1(a). In comparison, the gap between circulating vehicles #2 and #3 is sufficiently large that entering vehicle #1 accepts the gap and leaves the yield line on the entry lane to enter the roundabout. At this time, entering vehicle #2 is waiting behind vehicle #1 before vehicle #1 accepts the gap, and then it might leave immediately after the first vehicle starts to enter a roundabout using

TABLE 4: Data collection sites.

#	Intersection Name	Location	# of circulation lanes	# of legs	Diameter of inscribed circle (m)	Volume (v/h/lane) On circulation	On entrance
#1	Jongro Roubdabout	Seoul	1	4	25	315	135
#2	Mansu-dong Roundabout	Incheon	1	3	22	195	75
#3	Dongducheon Roundabout	Dongducheon	1	4	28	425	210
#4	Pyongtaek Roundabout	Pyongtaek	1	4	28	370	180

(a) An illustration of sequential gap acceptance maneuvers

I. Time Interval

A~D: Gap

a: Lag

2. A Vehicle Arriving at Decision Lines (①, ②)

| I | Circulating-Vehicle |

⟨ I ⟩ Entering-Vehicle

3. Times for Vehicle Arriving and Leaving

↓ Time when circulating-vehicle passes the line ② on circulating lane

• Time when entering-vehicle arrives at the yield line ①

○ Time when entering-vehicle leaves from the yield line ① for entering

⋮ Arrival at the end of queue on approaching lane

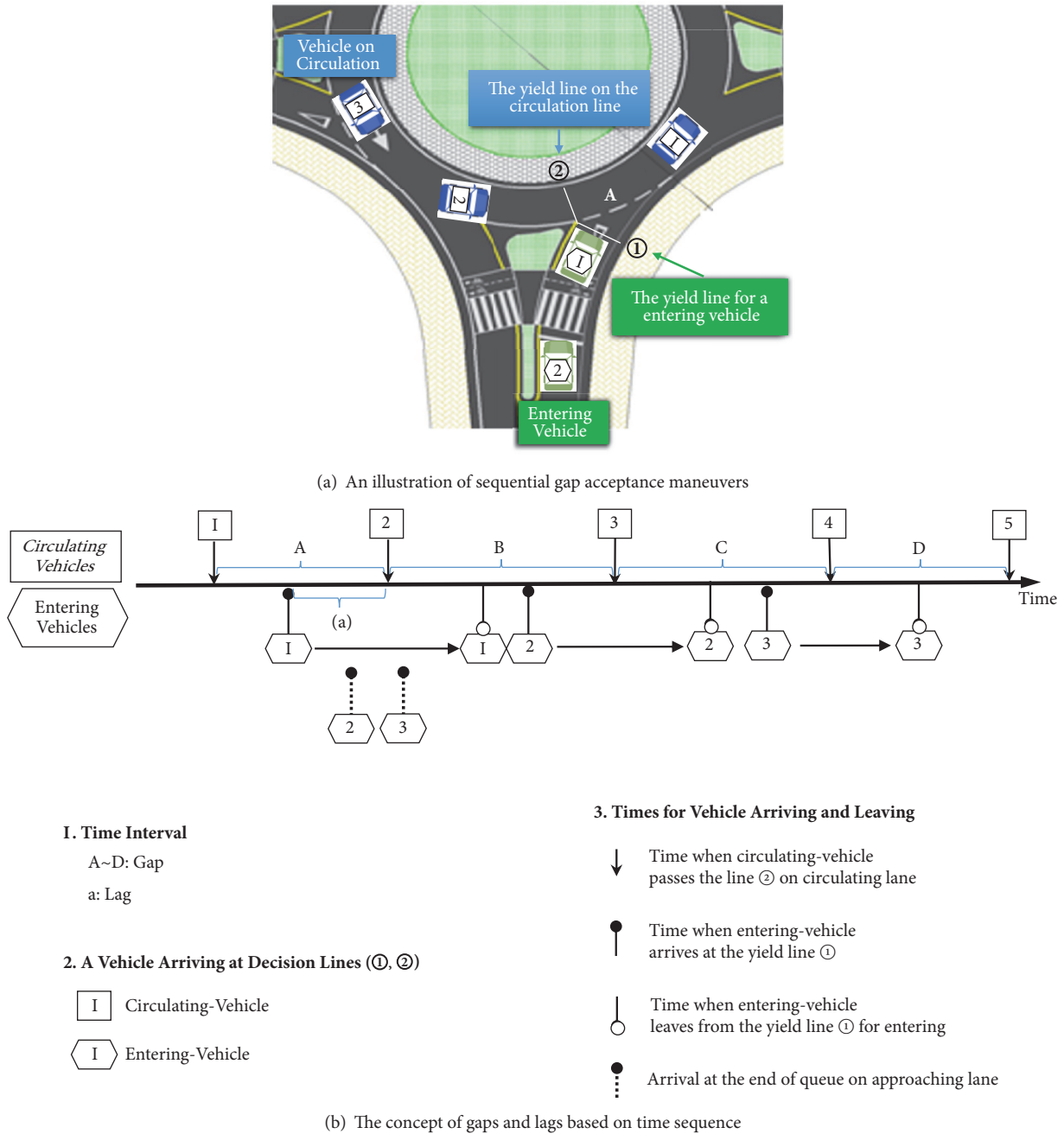(b) The concept of gaps and lags based on time sequence

FIGURE 1: The concept of gap acceptance data extraction from time series maneuvers of roundabouts.

the gap between circulating vehicles #2 and #3. Figure 1(b) illustrates the concept of measured gaps and lags based on a time sequence.

3.2. Model Estimation. A gap acceptance maneuver is a binary problem having only two events: success or failure. A driver waiting at the entrance to a roundabout faces a series of binary choices. For each gap at the circulatory lane, the driver has to decide whether to accept it and enter the roundabout or reject it and wait for the next gap. This process continues until a sufficiently large-enough gap occurs, and the driver accepts

the gap to enter the roundabout. Therefore, the probability of gap acceptance occurrence under given conditions has to be estimated as dependent variables, which can change due to driving environments instead of the event itself. Since this assists in analysis of the gap acceptance decision-making process and for simplicity and wide applicability, a logit model was selected to model estimation of acceptance probability. This study assumes that all gap acceptance decisions are made independently. For every moment, the driver has a utility from accepting or rejecting a confronting gap. The utility from accepting a gap results from avoiding having to wait

TABLE 5: Data summary and variable descriptive statistics.

Category		Normal	Rainy	Total
# of data		1,681	740	2,421
Gap (sec)	Mean	5.12	5.25	5.16
	S.D	2.81	2.97	2.86
	Acceptance (%)	1,135 (67.5%)	429 (58.0%)	1,564 (64.6%)
	Reject (%)	546 (32.5%)	311 (42.0%)	857 (35.4%)
Waiting Time (sec)	Mean	4.06	6.73	4.88
	S.D	5.59	8.99	6.92
Follow-up time (sec)	Mean	17.30	15.78	16.83
	S.D	18.62	15.90	17.84
# vehicles observed on Entrance	Mean	265.1	323.5	282.9
	S.D	84.50	102.05	94.13
	Passenger Car (%)	1,498 (89.1%)	678 (91.6%)	2,176 (89.9%)
	Heavy Vehicle (%)	183 (10.9%)	62 (8.4%)	245 (10.1%)
# vehicles observed on Circulation	Mean	374.5	502.6	413.6
	S.D	143.01	152.45	157.41
	Passenger Car (%)	1,466 (87.2%)	670 (90.5%)	2,136 (88.2%)
	Heavy Vehicle (%)	215 (12.8%)	70 (9.5%)	285 (11.8%)
Weather (%)		1,681 (69.4 %)	740 (30.6%)	-

longer to enter the roundabout, whereas the utility from rejecting a gap is the added safety from not accepting a short and dangerous gap. The traffic situation variables that affect these utilities and the decision whether to accept or reject a gap includes traffic volume, waiting time, types of circulating and entering vehicles, and other attributes.

Probability that a driver n accepts a gap:

$$P_n \left(accept \right) = P_n \left(U_{an} \geq U_{rn} \right) = \frac{1}{1 + e^{-(V_{an} - V_{rn})}} \quad (1)$$

$$U_{an} = V_{an} + \varepsilon_{an} \quad (2)$$

$$U_{rn} = V_{rn} + \varepsilon_{rn} \quad (3)$$

where U_{an} and U_{rn} are utility function of accept and reject, respectively; V_{an} and V_{rn} are the systematic components of the utility of accept and reject, respectively, and are assumed linear in their parameters; ε_{an} and ε_{rn} are the independent and identically Gumbel distributed random components of the utility of accept and reject, respectively.

3.3. Model Validation. Because the logit model in this study produces two outcomes, either "accept" or "reject" for each gap, two different errors type can occur: Type 1 and Type 2. A Type I error is committed if the model predicts that a driver rejects the gap when the driver actually accepts it. Meanwhile, a Type II error is committed if the model predicts that a driver accepts the gap when the driver actually rejects it. The validation for a logit model is generally conducted using the receiver operating characteristics (ROC) curve to test for these two types of errors. ROC curves can show model performance in predicting gap acceptance decisions [15, 38]. The ROC graph is a 2D graph having two axes that include a False Positive Rate (FPR) and True Positive Rate (TPR). If the

ROC graph deducted from a model is closer to the point (FDR = 0, TPR = 1), it can be concluded that the developed model is more accurate and is validated. Statistical significance by a numerical value in the ROC graph method can be evaluated thru a C-statistic value. This C-statistic value means the area under the curve (AUC). If the C-statistic value is closer to 1, it means the ROC curve is close to the point (FPR = 0. TPR = 1), and means that it is a better model.

4. Results

4.1. Data Collection Results. The 2,421 events for gap acceptance were collected from the field observation. Out the total, 64.6% of drivers (1,564 drivers) accepted the given gaps and 35.4% of drivers (857 drivers) rejected it as shown in Table 5. The percentage of events for accepted gaps in rainy conditions was relatively smaller than that in good weather conditions at 58.0% and 67.5%, respectively. Data for 1,681 vehicles were observed under good weather conditions, with 740 vehicles during rainy conditions. About 90% of cars were classified as a passenger car under good and rain weather conditions. The traffic flow was not congested for the observation, and the average volumes for entering roundabouts and for circulating were 283 vehicles/hour and 414 vehicles/hour, respectively.

To test statistical significance of the difference of gap acceptance between good weather and rain weather conditions, K-S tests were conducted as can be seen in Table 6. This K-S test results show that there is statistical difference of gap distributions related weather conditions for both the accepted gap and rejected gap. From these results, it was found that the data analyzed in this study can explain sufficiently the weather's influence on gap acceptance behavior for both gap acceptance and rejection on roundabouts.

TABLE 6: K-S test results for effects of weather conditions (Rain).

Statistics	K-S test for accepted gaps	K-S test for rejected gaps
Z	2.091	1.911
p	< 0.001	0.001

TABLE 7: Critical gaps using various methods.

Location/Time		Raff (Sec.)		Wu (Sec.)	
		Normal	Rainy	Normal	Rainy
	Total	3.75	4.25	3.84	4.23
	RB #1	4.05	4.05	4.14	4.11
Location	RB #2	3.80	3.75	3.76	3.59
	RB #3	3.70	4.05	3.80	4.12
	RB #4	3.85	4.65	3.33	4.69
	Morning Peak	3.55	-	3.77	-
Time	PM Non-peak	4.00	-	4.03	-
	Evening Peak	3.75	4.30	3.82	4.23

TABLE 8: A Logit model development.

Variables	β	S.E,	P	Exp (β)
X1 (Gap, Seconds)	1.300	0.059	< 0.001	3.669
X2 (Type of Circulating Vehicles, 0: Passenger Car, 1: Heavy Vehicle)	-0.437	0.217	0.045	0.646
X3 (Traffic Volume at the Circulating lane)	-0.003	0.000	< 0.001	0.997
X4 (Weather Condition, 0: Good weather, 1: Rainy Condition)	-0.815	0.170	< 0.001	0.443
Constant	-3.158	0.274	< 0.001	0.043
Number of Observations		2,181		
Log-likelihood Function		-635.530		
Restricted Log-likelihood Function		-1417.961		

4.2. Critical Gap Estimation. This study estimated the values of critical gaps using two different estimation methods, the Raff method and Wu method, as shown in Table 7. Critical gap estimation was conducted under normal weather and rainy conditions, as well as for specific data collection times, such as morning peak, P.M. nonpeak, and evening peak time. Critical gaps under rainy conditions were higher than during good weather. As such, rain conditions influenced gap acceptance maneuvering in a roundabout, and drivers needed about an 8 to 13 percent longer gap to accept entry into a roundabout under rainy conditions. These critical gap estimation results are similar to the critical gap times from previous studies in many different countries (Table 2).

4.3. Development of a Logit Model for Gap Acceptance at Roundabouts. A logit model with various independent variables investigates the effects of the factors on gap acceptance at roundabouts. The model parameter coefficients were estimated using the maximum likelihood method. Before

developing the model, the dataset was separated into two groups, one for model development and the other for model validation through a random selection process. Out of the total data, about 90 percent of data (2,181 data) were used for the model development and other data (240 data) were used for the model validation.

In order to develop the gap acceptance model using a logit model formula, eight variables were originally reviewed, and the variables that are significantly correlated with gap acceptance at a 95% significance level were selected. The model was finally developed using four variables including a gap size, a type of circulating vehicle, traffic volume at the circulating lane, and weather conditions, and the model development results are shown in Table 8. The results were as expected, where the utility from accepting a gap increases as the gap increases due to a decrease of the risk in entering roundabouts. The developed model shows that a longer gap results in a 3.669 times higher probability of entering roundabouts when the gap is sufficiently great for acceptance than

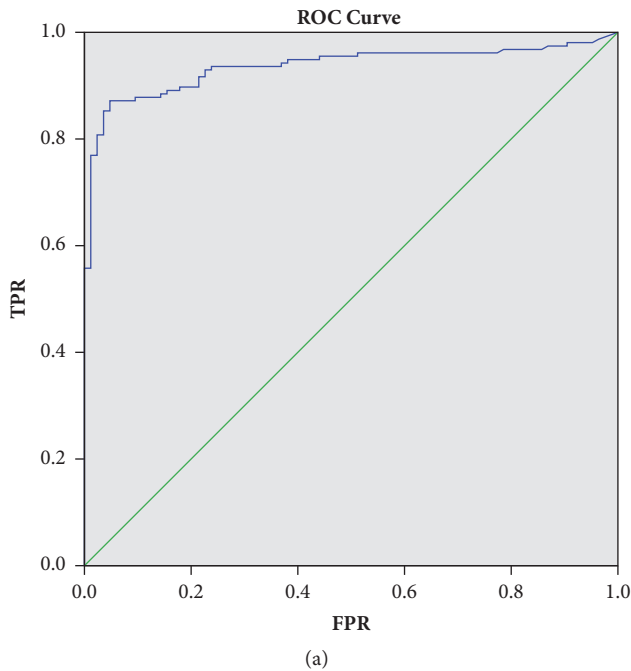| C-Statistic	S.D.	P	95% Confidence Interval	
			Min	Max
0.936	0.016	< 0.001	0.904	0.968

(a)

FIGURE 2: Deduced ROC graph from the model.

when the gap is smaller. When heavy vehicles are circulated inside roundabouts, drivers have a 0.646 times more difficult time accepting gaps to enter the roundabout compared to when there were only passenger cars inside the roundabouts. When the circulating traffic volume is lower, the probability of gap acceptance increases. Lastly, drivers need a longer gap time to accept when it is raining due to a more conservative driving behavior. In the developed model, there was a 0.443 times lower probability of entering roundabouts when it is raining compared to good weather conditions. Through this model development, the limitation of critical gap estimation that the estimation assumes homogenous driving behaviors for all drivers which is unlikely in real situations can be overcome.

This research used 240 data events out of a total 2,421 data events to validate the developed model. The deduced ROC graph is closer to the point (FPR = 0. TPR = 1) as shown in Figure 2 and Table 9. The C-statistic value is 0.936 and validates that the results from the developed model are statistically significant and accurate.

Figure 3 shows the estimated probabilities and elasticity of accepting a gap as a function of the gap size for good weather and rain conditions. Figure 3(a) shows the effects of rain conditions on drivers' gap acceptance probabilities. Drivers need about a 10 percent longer gap to accept entry into roundabouts under rainy conditions, and their probabilities

of gap acceptance are 10 to 20 percent lower with the same given gap time under rainy conditions than good weather conditions. In the case of three-second gaps, there was a 20% lower probability in a rainy condition compared to good weather conditions. The elasticity of the logit model represents the responsiveness of an individual's choice probability in regard to a change in the value of some attribute [17]. As Figure 3(b) explains, when the given gaps are less than five seconds, drivers' gap acceptance probabilities in rain conditions did not change more than the change of gap time in good weather conditions because drivers are not willing to enter roundabouts due to riskier conditions during rain. Meanwhile, when the given gaps are greater than five seconds, drivers' acceptance probabilities in rain conditions changed more with a change in gap time.

5. Conclusions

A roundabout is generally defined as a form of a circular intersection in which traffic travels counterclockwise around a central island and in which entering traffic must yield to circulating traffic. This roundabout is generally known as an efficient, safe, and environmentally friendly intersection. In Korea, roundabouts have been constructed as a government-led special project since 2010, and many issues and improvements for roundabouts have been suggested in terms of safety, operation, and design. Of particular importance is understanding gap acceptance behavior in roundabouts.

Gap acceptance behaviors at a roundabout were investigated based on field observations at four roundabouts during both good weather and rainy conditions. Based on the observed data, roundabout critical gaps were estimated, and a logit model for gap acceptance was developed using various variables to investigate gap acceptance maneuvering at roundabouts. Data for 2,421 gap acceptance events were collected from the field observation. Out these events, 64.6% of drivers (1,564 drivers) accepted the given gaps and 35.4% of drivers (857 drivers) rejected them. Critical gap values were estimated using the different estimation methods and ranged from 3.3 to 4.7. These critical gap estimation results are similar to the critical gap times from previous studies in many different countries (Table 3). The model was developed using four variables: gap size, type of circulating vehicle, traffic volume at the circulating lane, and weather conditions. Model validation was conducted using 240 events out of the 2,421 events, which were not used in the model development. For this model validation, the receiver operating characteristics (ROC) curve was tested for two types of errors that occur in binary choice models. This validation process found that the results from the developed model are statistically significant and accurate. This gap acceptance probability model enables overcoming weakness of critical gap estimation that the critical gap estimation assumes homogenous driving behaviors for all drivers unlikely in real situations.

The developed model showed that a longer gap results in a 3.669 times higher probability of entering roundabouts when the gap is sufficiently great for acceptance than when the gap is smaller. The effects of other variables, such as circulating vehicle types, circulating traffic volume, and weather

(a) Comparison of gap acceptance probabilities between good weather and rain conditions

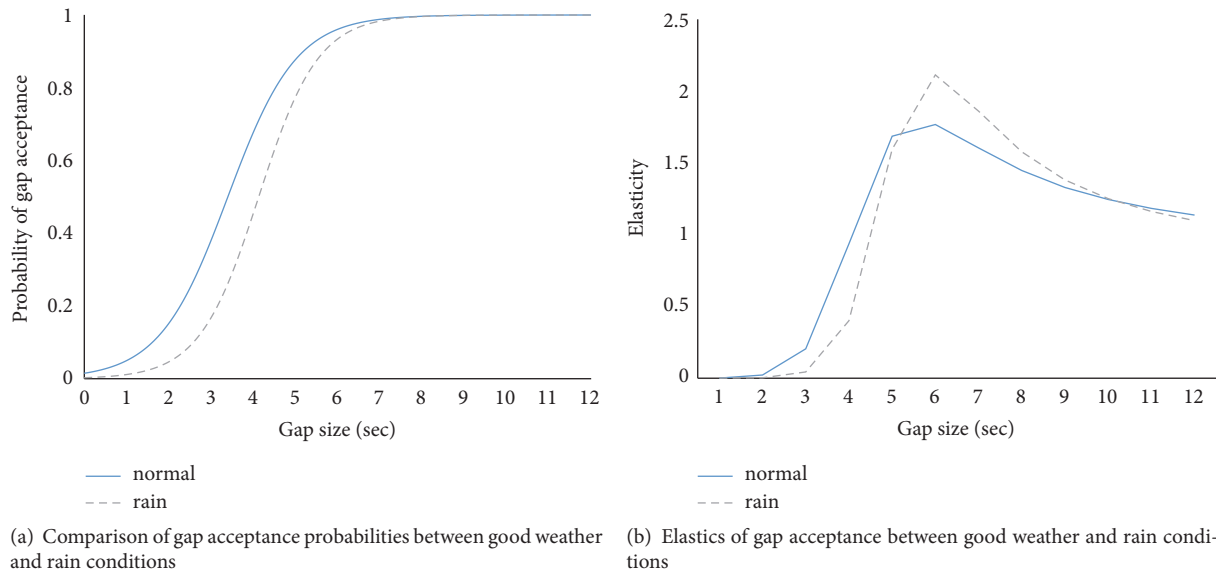(b) Elastics of gap acceptance between good weather and rain conditions

FIGURE 3: Evaluation of the rain condition effects on gap acceptance behavior.

conditions, are relatively lower than that of a gap size. When heavy vehicles are circulated inside roundabouts, drivers had difficulties reflected in a 0.646 times higher value for accepting gaps for entering roundabouts compared to when there were only passenger cars inside the roundabouts. When there is less circulating traffic, the probability of gap acceptance increases. Lastly, drivers need a longer gap acceptance time when it is raining due to a more conservative driving pattern. The developed model gave a 0.443 times lower probability of entering roundabouts when it is raining compared to good weather conditions. Thus, rain conditions influenced gap acceptance maneuvering into a roundabout. Drivers need about a 10 percent longer gap to accept entering into roundabouts under rainy conditions, and the probabilities of gap acceptance are 10 to 20 percent lower given the same given gap time under rainy conditions than good weather conditions.

This study investigated gap acceptance behaviors at roundabouts by analyzing and estimating critical gaps and the developed a gap acceptance logit model for good weather and rainy conditions. Waiting time was not considered as a statistically significant influence factor based on the analysis results in this study, even though previous studies indicated that waiting time affected gap acceptance behaviors.

There are some limitations to this study, and more field data should be collected as roundabout driving behavior and attitudes mature in Korean. There are still many problems when driving thru roundabouts in Korea due to violations of the right-of-way rule. For more sophisticated weather effect analysis, other types of severe weather conditions such as snow and heavy fog should be considered. Lastly, precipitation may also be an interesting influence factor for gap acceptance behavior analysis.

Data Availability

The data used to support the findings of this study are available from the corresponding author upon request.

Conflicts of Interest

The authors declare that they have no conflicts of interest.

Acknowledgments

References

[1] Transportation Research Board, *NCHRP Report 672, Roundabouts: An Informational Guide*, 2nd edition, 2010.

[2] Transportation Research Board, *Highway Capacity Manual*, National Research Council, Washington, DC, USA, 2010.

[3] T. Tollazzi, *Alternative Types of Roundabouts: An Informational Guide*, Springer International Publishing, 2015.

[4] W. Brilon, L. Bondzio, and F. Weiser, "Experiences with turbo roundabouts in Germany," in *Proceedings of the National Roundabout Conference*, pp. 546–580, Kansas City, MO, USA, 2008.

[5] M. Guerrieri, R. Mauro et al., "Analysis of kinematic parameters and driver behaviour at turbo-roundabouts," *Journal of transportation engineering, Part A. Systems*, vol. 144, no. 6, 2018.

[6] E. Macioszek, "Analysis of significance of differences between psychotechnical parameters for drivers at the entries to one-lane and turbo roundabouts in Poland," in *Proceedings of the*

International Conference Transport System Theory and Practice, vol. 505 of *Intelligent Transport Systems and Travel Behaviour,* Springer International Publishing, Katowice, Poland, 2017.

[7] L. Rodegerdts, M. Blogg et al., "Roundabout in the United States," Tech. Rep. NCHRP Report 572, Transportation Research Board of the National Academics, Washington, DC, USA, 2007.

[8] D. Lee and J. You, "A study on appropriate traffic volume calculation for revitalizing roundabout installation," *Journal of Korean Society of Transportation,* vol. 31, no. 6, pp. 43–52, 2013.

[9] M. S. Raff and J. W. Hart, "A Volume Warrant for Urban Stop Signs," The Eno Foundation for Highway Traffic Control, 1950.

[10] R. Ashworth, "The capacity of priority-type intersections with a non-uniform distribution of critical acceptance gaps," *Transportation Research,* vol. 3, no. 2, pp. 273–278, 1969.

[11] R. J. Troutbeck, "Evaluating the performance of a roundabout," *Australian Road Research Board, ARRB Group Limited,* SR no. 45, 1989.

[12] N. Wu, "Equilibrium of probabilities for estimating distribution function of critical gaps at unsignalized intersections," *Transportation Research Record, Journal of the Transportation Research Board,* no. 2286, pp. 49–55, 2012.

[13] A. J. Miller, "Nine estimators of gap acceptance parameters," in *Proceedings of the International Symposium on the Theory of Traffic Flow and Transportation,* G. Newell, Ed., American Elsevier Publishing, Berkeley, Calif, USA, 1972.

[14] C. F. Daganzo, "Estimation of gap acceptance parameters within and across the population from direct roadside observation," *Transportation Research Part B: Methodological,* vol. 15, no. 1, pp. 1–15, 1981.

[15] X. Chen, Y. Qi, and G. Liu, "Empirical study of gap-acceptance behavior of right-turn-on-red drivers on dual right-turn lanes," *Journal of Transportation Engineering,* vol. 139, no. 2, pp. 173–180, 2013.

[16] H. Mahmassani and Y. Sheffi, "Using gap sequences to estimate gap acceptance functions," *Transportation Research Part B: Methodological,* vol. 3, no. 15, pp. 143–148, 1981.

[17] A. Polus, Y. Shiftan, and S. Shmueli-Lazar, "Evaluation of the waiting-time effect on critical gaps at roundabouts by a logit model," *European Journal of Transport and Infrastructure Research,* vol. 5, no. 1, pp. 1–12, 2005.

[18] I. Zohdy, S. Sadek, and H. A. Rakha, "Empirical analysis of effects of wait time and rain intensity on driver left-turn gap acceptance behavior," *Transportation Research Board: Transportation Research Record,* no. 2173, pp. 1–10, 2010.

[19] T. H. Maze, "A probabilistic model of gap acceptance behavior," *Transportation Research Board: Transportation Research Record,* no. 795, pp. 8–13, 1981.

[20] S. M. Madanat, M. J. Cassidy, and M.-H. Wang, "Probabilistic delay model at stop controlled intersection," *Journal of Transportation Engineering,* vol. 120, no. 1, pp. 21–36, 1994.

[21] J. L. Gattis and S. T. Low, "Gap acceptance at atypical stop-controlled intersections," *Journal of Transportation Engineering,* vol. 125, no. 3, pp. 201–207, 1999.

[22] P. Liu, X. Wang, J. Lu, and G. Sokolow, "Headway acceptance characteristics of U-turning vehicles at unsignalized intersections," *Transportation Research Board: Transportation Research Record,* no. 2027, pp. 52–57, 2007.

[23] P. C. Devarasetty, Y. Zhang, and K. Fitzpatrick, "Differentiating between left-turn gap and lag acceptance at unsignalized intersections as a function of the site characteristics," *Journal of*

Transportation Engineering, ASCE, vol. 138, no. 5, pp. 580–588, 2012.

[24] S. Teply, M. I. Abou-Henidy, and J. D. Hunt, "Gap acceptance behavior-aggregate and logit perspectives: part 1," *Traffic Engineering and Control,* vol. 38, no. 9, pp. 474–482, 1997.

[25] S. Teply, M. I. Abou-Henidy, and J. D. Hunt, "Gap acceptance behavior-aggregate and logit perspectives: part 2," *Traffic Engineering and Control,* vol. 38, no. 10, pp. 540–544, 1997.

[26] H. Rakha, K. Daniel, C. Gustave et al., *Microscopic Analysis of Traffic Flow in Inclement Weather,* FHWA-JPO-09-066, U.S. Department of Transportation, Research and Innovative Technology Administration, 2009.

[27] F. Xu and Z. Z. Tian, "Driver behavior and gap-acceptance characteristics at roundabouts in California," *Transportation Research Record: Journal of the Transportation Research Board,* vol. 2071, no. 1, pp. 117–124, 2008.

[28] T. Kim, M. Park, and B. Park, "A critical gap model for roundabouts in Korea," *Journal of Korean Society of Transportation,* vol. 30, no. 2, pp. 93–100, 2012.

[29] S. Park, D. Kim, and J. Jeong, "Evaluation of multi-legged roundabout using surveyed critical gap acceptance," *The Journal of the Korea Contents Association,* vol. 13, no. 9, pp. 400–409, 2013.

[30] A. Ahmad, R. Rastogi, and S. Chandra, "Estimation of critical gap on a roundabout by minimizing the sum of absolute difference in accepted gap data," *Canadian Journal of Civil Engineering,* vol. 42, no. 12, pp. 1011–1018, 2015.

[31] J. Cheng, X. Yang, W. Deng, and X. Huang, "Driver's critical gap calibration at urban roundabouts: a case study in China," *Tsinghua Science and Technology,* vol. 13, no. 2, pp. 237–242, 2008.

[32] R. Guo and B. Lin, "Traffic operation performances at roundabout weaving sections," *Journal of Transportation Systems Engineering and Information Technology,* vol. 10, no. 3, pp. 29–34, 2010.

[33] I. Bargegol, S. H. Hosseini, and M. J. Samet, "Determining the capacity model of urban roundabouts, considering the drivers' behaviour in accepting and rejecting of gaps," in *Proceedings of the IOP Conference Series: Materials Science and Engineering,* vol. 254, June 2017.

[34] L. Ren, X. Qu, H. Guan et al., "Evaluation of roundabout capacity models: an empirical case study," *American Society of Civil Engineers: Journal of Transportation Engineering,* vol. 142, no. 12, 2016.

[35] S. Rao, Y. Krishna, P. Atmakuri et al., "Calibration of performance of roundabouts based on gap acceptance parameters using simulation for indian scenario," in *Proceedings of the 12th International Conference on Transportation Planning and Implementation Methodologies for Developing Countries (TPMDC '16),* pp. 19–21, IIT Bombay, Mumbai, India, 2016.

[36] X. Shi and J. Zhu, "Modification of a gap acceptance theory model of roundabouts' capacities," in *Proceedings of the 16th COTA International Conference of Transportation Professionals,* pp. 1655–1662, Shanghai, China, July 2016.

[37] O. Giuffrè, A. Granà, and M. L. Tumminello, "Gap-acceptance parameters for roundabouts: a systematic review," *European Transport Research Review,* vol. 8, no. 2, pp. 1–20, 2016.

[38] T. Fawcett, "An introduction to ROC analysis," *Pattern Recognition Letters,* vol. 27, no. 8, pp. 861–874, 2006.

Research Article

Group Gap Acceptance: A New Method to Analyze Driver Behavior and Estimate the Critical Gap at Multilane Roundabouts

Khaled Shaaban (iD) **and Hassan Hamad**

Department of Civil Engineering, Qatar University, P.O. Box 2713, Doha, Qatar

Correspondence should be addressed to Khaled Shaaban; kshaaban@qu.edu.qa

The operations of multilane roundabouts, especially three-lane roundabouts, are unique and more complicated than any other type of roundabouts. This study aims to analyze driver behavior and estimate the critical gap at three-lane roundabouts. Video data were collected at two roundabouts. The analysis identified a pattern of group gap acceptance, where vehicles entering the roundabout from different lanes moved in groups during the same gap. In this case, the decision of vehicles entering from outside lanes greatly depended on the gap acceptance decision of vehicles in the inside lane. Analysis showed that the vast majority of the vehicles accept the gap in groups and the critical gap was estimated accordingly. The study provides a new explanation for the operation at multilane roundabouts. The use of this simple method is recommended when estimating critical gaps for multilane roundabouts.

1. Introduction

Roundabouts are popular in many countries, especially in the case of lower volumes when compared to signalized intersections as they reduce queuing and delays at the approaches. Yield-controlled entries of roundabouts oblige vehicles to decide to either reject or accept a gap in the circulating flow. The decision making in most cases depends on the driver's behavior. Roundabout capacity is greatly affected by the gap acceptance behavior of drivers. The Highway Capacity Manual (HCM) provides a method to calculate the capacity of roundabouts, and it involves a number of inputs. One of the main inputs is the critical gap [1]. This value is used in the capacity model to estimate the capacity of existing facilities without the need to perform field measurements, assess the level of service, and predict the capacity at future locations. Furthermore, this value is needed in simulation and traffic modeling of roundabouts for design and research projects.

A gap is an opening in the circulating flow that circulates around the island of the roundabout. As illustrated in Figure 1, gap vehicles are the vehicles that travel in the circulating lanes and create the gaps. The decision vehicle is the vehicle at

the entry of the roundabout that takes the decision, whether rejecting or accepting a gap. The gap closes on the left side and reopens on the right side as shown in Figure 1. Rejecting a gap happens when the driver of the decision vehicle finds the gap small enough that s/he refuses to merge with the circulating flow and remains stopped at the entry point. Accepting a gap is when the driver of the decision vehicle merges with the circulating flow from the vehicle's position at the entry of the roundabout as soon as the gap is large enough not to cause crashes or severe conflicts.

The critical gap is the smallest gap that a driver is assumed to accept [2]. The critical gap is an important parameter that affects the capacity and delay of roundabouts. Monitoring and evaluating of capacity values at roundabouts are a difficult matter due to the high dependence of these parameters on the drivers' behavior [1]. This study aims to investigate the gap acceptance behavior and to determine the critical gap for high-volume three-lane roundabouts. These types of roundabouts are unique, and their operation is more complicated than other types of roundabouts. Furthermore, previous studies have not thoroughly addressed these types of roundabouts to the best of our knowledge.
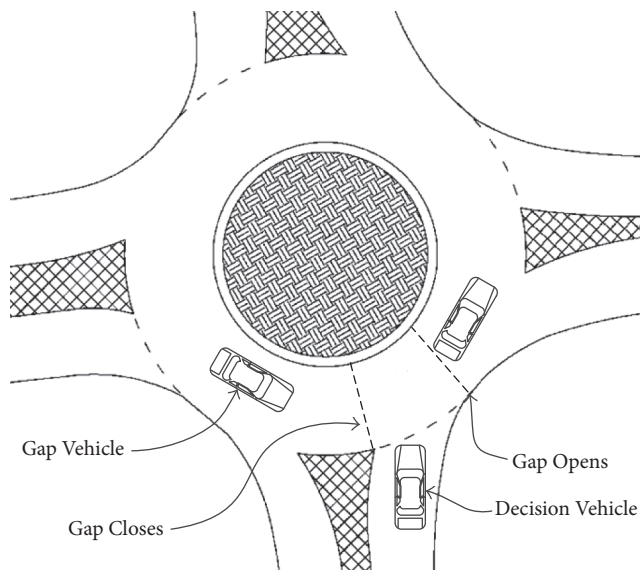
FIGURE 1: Gap acceptance definition.

FIGURE 2: Critical gap based on Raff's method.

2. Literature Review

Numerous studies have investigated critical gaps. Raff [9] developed the earliest and the most popular method of evaluating the critical lag. He defined the critical lag as the lag for which the number of accepted lags shorter than it is similar to the number of rejected lags longer than it. A graphical model was developed in which two cumulative distribution curves related to the number of accepted and rejected gaps intersect to provide the critical lag value. The original Raff's procedure estimated critical lags on the basis of lags accepted and rejected. Miller corrected the Raff's method by including the entire gap data instead of lags only [10]. This new method is known as the modified Raff method. As shown in Figure 2, the modified Raff method determines the critical gap value (t_c), graphically, by finding the intersection point between the two functions:

$$1 - F\left(t_r\right), F\left(t_a\right), \tag{1}$$

where t_a and t_r are accepted and rejected gap times and $F(t_a)$ and $F(t_r)$ are cumulative distribution functions (CDFs) of accepted and rejected gaps.

The intersection point between the cumulative distribution curves corresponds to the critical gap value on the horizontal axis. This value is called the critical gap because most vehicles will more likely to accept a gap of a value larger than them and reject a gap of a value smaller than them. Previous studies showed that the value of t_c is affected by the existing traffic volumes at which this value has been evaluated [11, 12].

Different studies estimated the critical gap values obtained from different analysis methods and then compared them to different international standards or other studies. A summary of the critical gap values determined by previous studies is shown in Table 1. The table contains the analysis methods, location, and types of roundabouts. In summary,
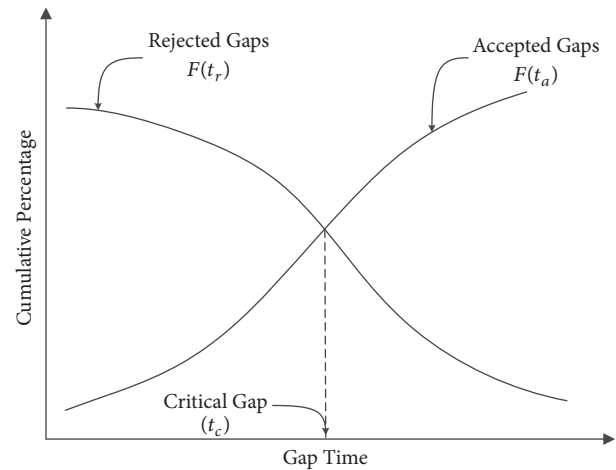
most studies addressed only one- and two-lane roundabouts. In summary, to our knowledge, limited studies investigated or developed a methodology to study the critical gap value for three-lane roundabouts.

Guo [7] compared three methods for the estimation of the critical gap for roundabouts, including Ashworth's method, Raff's method, and the maximum likelihood method to calculate the critical gap at roundabouts. He provided justification for recommending some of the methods over the others in practical applications. As per Guo, the modified Raff's method and the maximum likelihood method are considered easy to use and practical. On the other hand, Ashworth's method will result in a larger result because it only uses values of the accepted gap. Tupper et al. [13] compared four methods of calculating the critical gap for unsignalized T-intersections in terms of the ease of use and the use of data. Raff and the cumulative acceptance methods were identified as the most computationally simple followed closely by the fit maximization method. The equilibrium of probabilities method was the most computationally demanding. The Raff, equilibrium of probabilities, and fit maximization methods utilized both the accepted and rejected gap data, requiring a smaller sample size. The cumulative acceptance method utilized only the accepted gap data requiring a larger sample size for meaningful results. It was therefore decided to use the modified Raff's method in this study because it is easy to use, requires a small sample size, and produces reasonably accurate results.

3. Methods

3.1. Group Gap Acceptance. Vehicle interactions at the round-abouts vary depending on the number of circulating lanes. As the number of lanes increases, the complexity of the vehicular interactions increases. Three-lane roundabouts have complicated interaction patterns. Any two-gap vehicles in the circulating lanes regardless of the lane they are occupying can create an acceptable gap. Therefore, there should be 14 interaction cases as illustrated in Figure 3. If the decision

TABLE 1: Summary of past studies.

Author(s)	Year	Analysis method	Critical gap (s)	Type of roundabout	City, country
Flannery and Datta [3]	2007	Maximum likelihood method	3.94		Florida and Maryland, USA
Xu and Tian [4]	2008	Maximum likelihood method	4.8	1-lane	California, USA
Mensah et al. [5]	2010	Raff's method	2.55		Maryland, USA
Fitzpatrick et al. [6]	2013	Raff's method	2.2		Massachusetts, USA
Xu and Tian [4]	2008	Maximum likelihood method	L: 4.70/ R: 4.40		California, USA
Guo [7]	2010	Raff's method	2.91	2-lane	Dalian, China
		Revised Raff's method	2.78		
		Maximum likelihood method	2.65		
		Ashworth method	3.2		
Kusuma and Koutsopoulos [8]	2011	Maximum likelihood method	3.58		Stockholm, Sweden

Case	Vehicle Interactions
1	Vehicle I with Vehicles F1 & F2
2	Vehicle I with Vehicles F1 & C2
3	Vehicle I with Vehicles F1 & N2
4	Vehicle I with Vehicles C1 & F2
5	Vehicle I with Vehicles C1 & C2
6	Vehicle I with Vehicles C1 & N2
7	Vehicle I with Vehicles N1 & F2
8	Vehicle I with Vehicles N1 & C2
9	Vehicle I with Vehicles N1 & N2
10	Vehicle M with Vehicles C1 & C2
11	Vehicle M with Vehicles C1 & N2
12	Vehicle M with Vehicles N1 & C2
13	Vehicle M with Vehicles N1 & N2
14	Vehicle O with Vehicles N1 & N2

F: Far
C: Center
N: Near

I: Inside
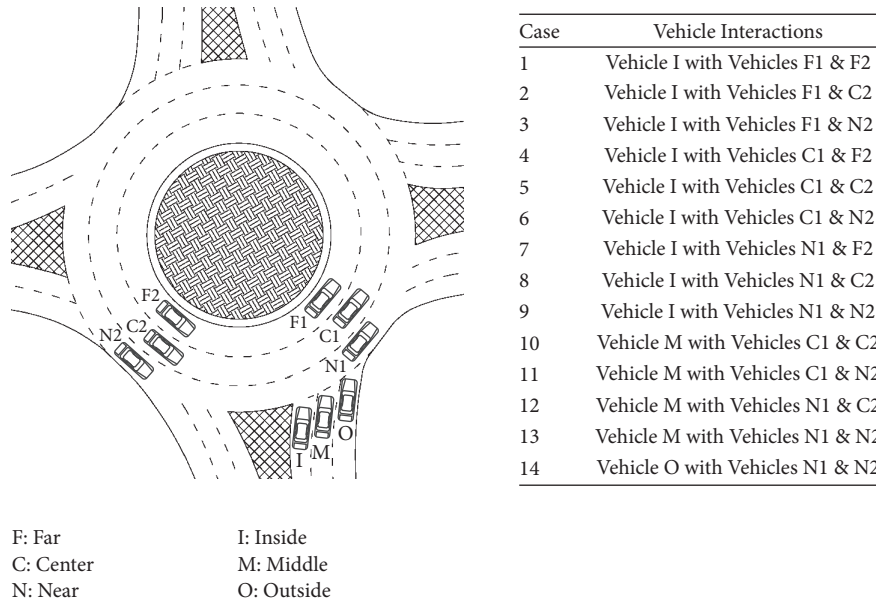M: Middle
O: Outside

FIGURE 3: Traditional interaction cases.

vehicle is in the inside lane, cases 1 through 9 are applicable covering the path of the decision vehicle and all the possible paths vehicles combinations in the circulating lanes. If the gap vehicle is in the middle lane of the approach, cases 10 through 13 are applicable. For the outside lane, only one case is applicable.

Vehicles were observed to accept gaps in groups. The group gap acceptance behavior is based on the actual mechanics of accepting or rejecting gaps observed in the field at the two study locations. Vehicles in the middle and outside lanes, follow vehicles, take advantage of the gap for the inside vehicle to enter the roundabout. As shown in Figure 4, seven cases were observed (A to G) in the field. Cases A, B, and C are based on the vehicle in the inside lane accepting a gap. Case A occurs when all lanes are occupied. In this case, the vehicle in the inside lane accepts the gap. At the same time, the follow vehicles in middle and outside lanes accept the same gap by following the vehicle in the inside lane. Case B occurs if the

vehicle in the outside lane does not accept the gap with the follow vehicle in the middle lane. Case C occurs when the vehicle in the middle lane rejects a gap whereas the vehicles in the inside and outside lanes accept it. Case D occurs in case of no vehicles in the inside lane. In this case, the vehicle in the middle lane accepts a gap, and the follow vehicle in the outside lane accepts the same gap. The remaining cases involve only one decision vehicle. Cases E, F, and G occur if the decision vehicles accept the gap individually.

3.2. Data Collection. Video footage was used to collect the data at two high-volume three-lane roundabouts in the city of Doha, Qatar. The first roundabout is located at the intersection of Al Gharrafa Road and Al Maszhabiya Street. The second roundabout is located at the intersection of Haloul Street and Mesaimeer Road. The two selected roundabouts are similar in geometry. Both represent the typical configuration of three-lane roundabouts in the city of Doha. The circulation

Case A

Case B

Case C

Case D

Case E

Case F

Case G

■ Decision vehicle accepting the gap with follow vehicles
■ Follow vehicle accepting the same gap of the decision vehicle
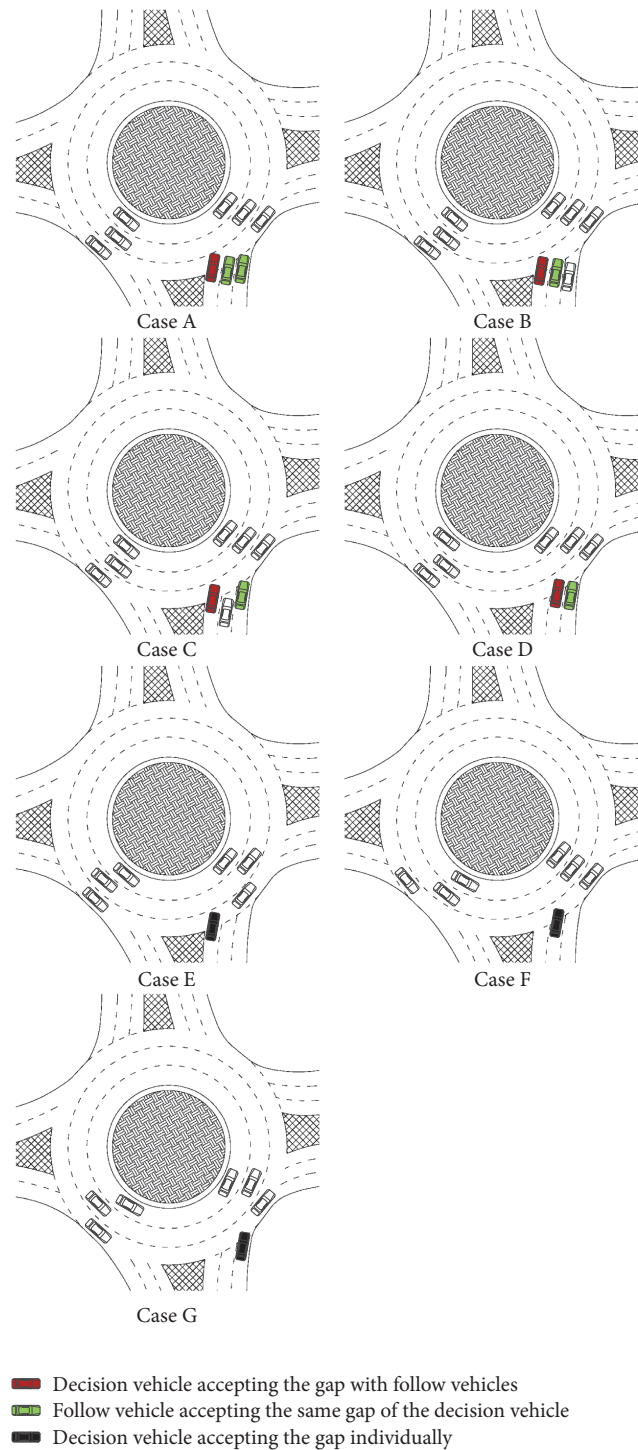■ Decision vehicle accepting the gap individually

FIGURE 4: Interaction cases based on group gap acceptance.

inside the roundabouts is counterclockwise in Qatar. Vehicles traveling in the circulating lanes around the middle circular island have the right-of-way, where the vehicles at the yield-controlled entrances have to find a gap in order to merge with the circulating flow. Both roundabouts were selected because of the heavy traffic volumes and consistent entry flow to ensure a large sample size. Cameras were installed strategically at different angles at the studied approach to ensure a clear view without the obstruction of large-sized vehicles. Data were collected for the northbound approaches at both intersections as shown in Figure 5. A total of 15 hours of footage was captured covering the peak and off-peak hours. Data collection was performed from 6:00 a.m. to 9:00 p.m. in clear weather conditions.

FIGURE 5: Aerial photo for roundabouts and camera locations.

3.3. Gap Measurement. The video data were analyzed frame by frame with an accuracy of 0.03 s based on a frame rate of 30 frames per second using Forevid analysis software to determine the time of each accepted and rejected gap. In Raff's method, the critical gap is estimated by either considering only gaps [12] or by combining gaps and lags together [14, 15]. This study considered only gaps and did not consider any lags similar to Brilon et al. [15]. In this study, only decision vehicles that come to a full stop at the yield line were considered. This condition was not a problem because of the relatively large circulating volumes. The majority of the vehicles entering the roundabout stopped first before proceeding. A gap is formed in the circulating lanes by having two-gap vehicles following each other in the same or a different lane with enough gap that can fit a decision vehicle. The gap is considered accepted when the decision vehicle's driver takes the decision to proceed into a gap in the circulating flow moving from the state of full stop at the approach. On the other hand, a gap is considered rejected when the driver of the decision vehicle decides not to proceed in the case of a gap in the circulation flow regardless of its size. For the vehicles entering the roundabout, direction, vehicle type, and departure time were recorded. For the vehicles circulating in the roundabout, the passing time at specified lines across the road and direction were recorded. This information was used to identify the different interaction cases and to determine the accepted and rejected gaps for the vehicles.

3.4. Vehicle Types. In this study, vehicles were classified under three categories: passenger vehicles, medium vehicles, and heavy vehicles. Each of the used classes is basically a group of vehicles that are approximately similar in dimensions and performance. The passenger vehicles group includes sedans, sport-utility vehicles, pickup trucks, and vans. Medium vehicles group includes single-unit two-axle trucks, small recreational vehicles, minibuses, and ambulances. Heavy vehicles group includes large buses, trailers of all sizes, and dump trucks. The summary of the collected data is presented in Table 2. Most of the vehicles in the sample (95.47%) were passenger vehicles.

3.5. Interaction Cases. The vehicular interaction cases are not similar amongst the different types of roundabouts because the number of lanes in each type of the roundabouts dictates the complexity of the interaction cases. Three-lane roundabouts have complex interaction cases, as explained earlier, and, due to that, new interaction cases were developed in a way that reflects the driver decision-taking more accurately. Some of the cases rarely occurred such that there are not enough data points to perform the analysis. Only the cases that have an abundance of data points have been analyzed. The total number of observed interactions exceeded 4,500 interactions over the duration of the data collection for both locations. As indicated in Table 2, case A was the most occurring case with 74.98% of all cases.

4. Results

4.1. Overall Critical Gap. Using the modified Raff's method, the overall critical gap, defined as the intersection between the CDFs of the rejected and accepted gaps at which the probability of rejecting or accepting, was estimated for all the data points. This value was estimated by equalizing the sigmodal functions of the cumulative distribution plots. The overall critical gap for the two roundabouts was 2.40 seconds. Figure 6 shows the CDFs that yielded the critical gap value of the two three-lane roundabouts.

4.2. Critical Gap for the Interaction Cases. Most of the interaction cases observed were case A, where the vehicles at the roundabout entry proceed together. The critical gap value for case A was 2.45 s, which is close to the overall critical gap value. A summary of the overall critical gap, the critical gaps of the different interaction cases, and vehicle types are listed in Table 3. Figure 7 shows the graphical representation of the data based on the modified Raff's definition to obtain the critical gap for each vehicular interaction case.

4.3. Critical Gap for the Vehicle Types. It was found that the critical gap values for passenger, medium, and heavy vehicles are in an ascending order. The passenger vehicles had a critical gap value of 2.39 s compared to 2.53 s and 3.03 s for medium and heavy vehicles, respectively. The number of data points for medium and heavy vehicles shows that more data points are required to obtain more accurate results. Figure 7 shows the graphical representation of modified Raff's method for the different vehicle types.

TABLE 2: Summary of data collected.

| Location		Al Gharrafa St. roundabout		Haloul St. roundabout		Combined	
Classification	Type	Count	Percentage	Count	Percentage	Count	Percentage
Gap	Accepted	1025	44.55%	1112	46.66%	2137	45.62%
	Rejected	1276	55.45%	1271	53.34%	2547	54.38%
Vehicle type	Passenger vehicle	2210	96.05%	2262	94.92%	4472	95.47%
	Medium vehicle	62	2.69%	63	2.64%	125	2.67%
	Heavy vehicle	29	1.26%	58	2.43%	87	1.86%
Group gap	A	1860	80.83%	1652	69.32%	3512	74.98%
	B	118	5.13%	302	12.67%	420	8.97%
	C	205	8.91%	180	7.55%	385	8.22%
	D	23	1.00%	4	0.17%	27	0.58%
Individual gap	E	87	3.78%	239	10.03%	326	6.96%
	F	6	0.26%	5	0.21%	11	0.23%
	G	2	0.09%	1	0.04%	3	0.06%
Total		2301	100%	2383	100%	4684	100%
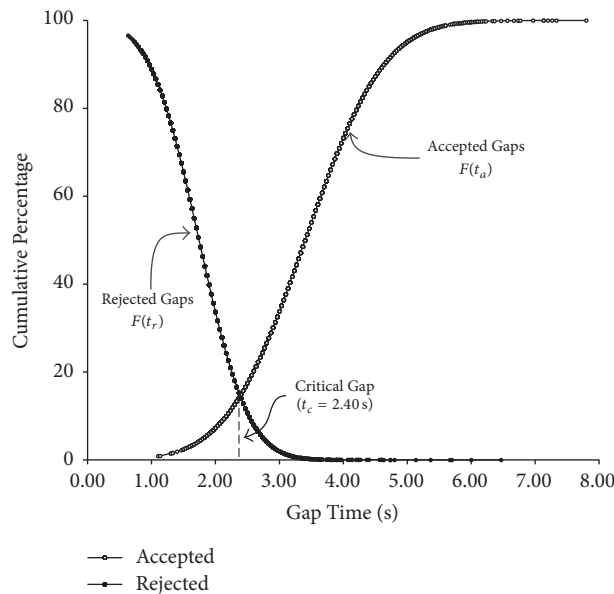
FIGURE 6: Overall critical gap.

5. Conclusions

The presented method, group gap acceptance, was used to analyze driver behavior and estimate the critical gap for three-lane roundabouts. Data were collected at two roundabouts in the city of Doha, Qatar. More than 4,500 interactions were recorded. Data were classified based on the vehicle type and interaction between vehicles. Field results indicated that the gap acceptance decision for vehicles entering from the inside lane affects the decision of vehicles entering from the outside lanes. In this behavior, named group gap acceptance, the vehicles in the outside lanes follow the vehicle in the inside lane and enter the roundabout during the same gap.

The overall critical gap value was 2.40 s. The critical gap for passenger vehicles was the lowest (2.39 s) compared to medium (2.53 s) and heavy vehicles (3.03 s). Nine driver interaction cases were identified (A–G). Most of the interactions (92.75%) involved more than one vehicle entering the roundabout and moving together in groups. Case A, three vehicles in a group, was the dominant interaction case, accounting for more than 74.98% of the data points collected from two locations, with a critical gap value of 2.45 s.

The presented method, group gap acceptance, was used to analyze driver behavior and estimate the critical gap for three-lane roundabouts. The critical gap for three-lane roundabouts, but the value of the overall critical gap, seems to be much lower than that obtained for one- and two-lane roundabouts [3–8]. Considering that driver behavior is a major contributor to the operational performance of round-abouts, the results may be an indication of aggressive driver behavior, which was identified in prior studies conducted
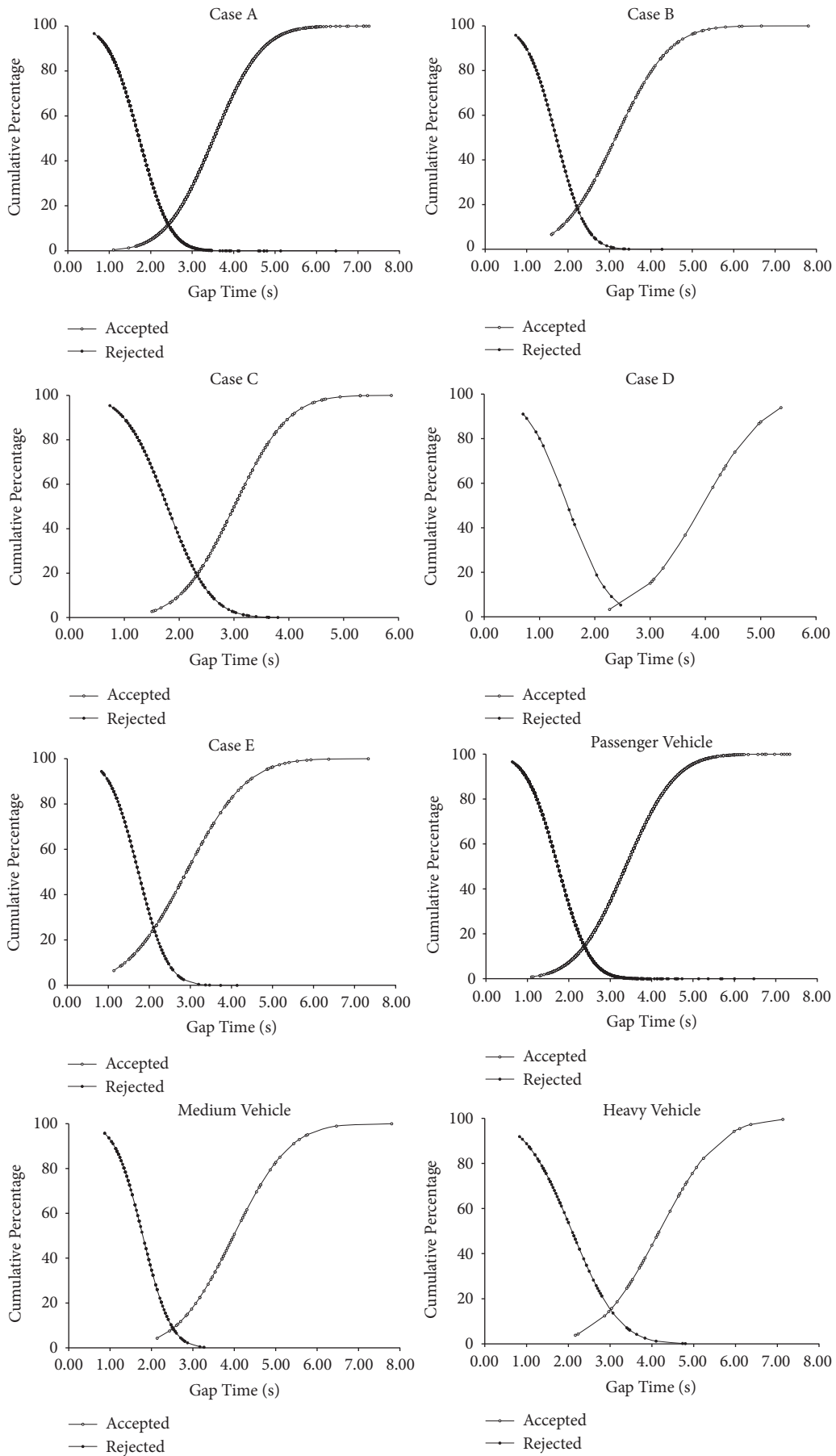
FIGURE 7: Critical gap for different cases.

Table 3: Summary of critical gap values.

Classification	Type	Critical gap (s)
Overall		2.40
Vehicle types	Passenger vehicle	2.39
	Medium vehicle	2.53
	Heavy vehicle	3.03
Interaction cases	A	2.45
	B	2.22
	C	2.33
	D	2.47
	E	2.11
	F	Not enough data
	G	Not enough data

in Qatar [16–18]. Such behavior may be caused by drivers becoming frustrated at heavily congested roundabouts and entering the roundabout when there is an insufficient gap.

The values obtained in this study can be used as a baseline for critical gap values of three-lane roundabouts in Qatar and other countries in the region, such as Saudi Arabia, United Arab Emirates, Bahrain, Kuwait, and Oman. These values can be used in numerous applications. For example, they can be input in capacity-prediction models and used in the simulation of traffic flow at multilane roundabouts to replicate real-life conditions. The method developed in this study can also be employed to estimate critical gap values for different types of multilane roundabouts in other regions.

The current study has a number of limitations. It did not consider the effect of pedestrians or cyclists on critical gap values because no pedestrians or cyclists were observed at the study locations, as expected throughout this region [19]. Furthermore, this study did not consider the effects of the geometry of the roundabout. Some roundabouts have an elliptical shape, whereas others have a steep slope, with circulating lanes, three legs, or slip ramps. In the current study, both roundabouts were circular, flat, and had four legs. Furthermore, the approaches to the roundabout did not feature slip ramps. In addition, the vehicular interaction cases in the study were based on allowable legal movements. Driving behaviors considered illegal, such as a vehicle entering the far circulating lane from the outside lane, were not included, as such behaviors, besides being careless, high-risk maneuvers, are in violation of traffic law and do not depict acceptable gap acceptance maneuvers.

Disclosure

The statements made herein are solely the responsibility of the authors.

Conflicts of Interest

The authors declare that there are no conflicts of interest regarding the publication of this paper.

References

[1] C: National Research and B: Transportation Research, *HCM 2010 : highway capacity manual*, Transportation Research Board, Washington, Wash, USA, 2010.

[2] R. J. Troutbeck, "Estimating the mean critical gap," *Transportation Research Record*, vol. 2461, pp. 76–84, 2014.

[3] A. Flannery and T. Datta, "Operational performance measures of American roundabouts," *Transportation Research Record*, vol. 1572, pp. 68–75, 1997.

[4] F. Xu and Z. Z. Tian, "Driver behavior and gap-acceptance characteristics at roundabouts in California," *Transportation Research Record*, vol. 2071, no. 1, pp. 117–124, 2008.

[5] S. Mensah, S. Eshragh, and A. Faghri, "A critical gap analysis of modern roundabouts," in *Proceedings of the 89th Annual Meeting of the Transportation Research Board*, Washington, Wash, USA, January 2010.

[6] C. Fitzpatrick, D. Abrams, Y. Tang, and M. Knodler, "Spatial and temporal analysis of driver gap acceptance behavior at modern roundabouts," *Transportation Research Record*, no. 2388, pp. 14–20, 2013.

[7] R. Guo, "Estimating critical gap of roundabouts by different methods," in *Proceedings of the 6th Advanced Forum on Transportation of China (AFTC 2010)*, pp. 84–89, Beijing, China, 2010.

[8] A. Kusuma and H. N. Koutsopoulos, "Critical gap analysis of dual lane roundabouts," pp. 709–717.

[9] M. S. Raff, "A volume warrant for urban stop signs," 1950.

[10] A. J. Miller, "A note on the analysis of gap—acceptance in traffic," *Journal of the Royal Statistical Society*, vol. 23, no. 1, pp. 66–73, 1974.

[11] A. Miller, "Nine estimators of gap-acceptance parameters," in *Bulletin Transport Section, Civil Engineering*, vol. 5, 1971.

[12] W. Brilon, R. Koenig, and R. J. Troutbeck, "Useful estimation procedures for critical gaps," *Transportation Research Part A: Policy and Practice*, vol. 33, no. 3-4, pp. 161–186, 1999.

[13] S. Tupper, M. A. Knodler Jr, C. Fitzpatrick, and D. S. Hurwitz, "Estimating Critical Gap–A Comparison of Methodologies Using a Robust, Real-World Data Set," in *Proceedings of the Transportation Research Board 92nd Annual Meeting*, 5019, 13 pages, 2013.

[14] R. Ashalatha and S. Chandra, "Critical gap through clearing behavior of drivers at unsignalised intersections," *KSCE Journal of Civil Engineering*, vol. 15, no. 8, pp. 1427–1434, 2011.

[15] W. Brilon, R. Koenig, and R. J. Troutbeck, "Useful estimation procedures for critical gaps," *Transportation Research Part A: Policy and Practice*, vol. 33, no. 3, pp. 161–186, 1999.

[16] K. Shaaban, J. S. Wood, and V. V. Gayah, "Investigating driver behavior at minor-street stop-controlled intersections in Qatar," *Transportation Research Record*, vol. 2663, pp. 109–116, 2017.

[17] A. Tageldin, T. Sayed, and K. Shaaban, "Comparison of time-proximity and evasive action conflict measures case studies from five cities," *Transportation Research Record*, vol. 2661, pp. 19–29, 2017.

[18] K. Shaaban and A. Pande, "Evaluation of red-light camera enforcement using traffic violations," *Journal of Traffic and*

Transportation Engineering (English Edition), vol. 5, no. 1, pp. 66–72, 2018.

[19] K. Shaaban, D. Muley, and A. Mohammed, "Analysis of illegal pedestrian crossing behavior on a major divided arterial road," *Transportation Research Part F: Traffic Psychology and Behaviour*, vol. 54, pp. 124–137, 2018.